CENTRE FOR RESEARCH & TECHNOLOGY HELLAS
INSTITUTE OF APPLIED BIOSCIENCES

UNIVERSITY OF IOANNINA
SCHOOL OF HEALTH SCIENCES
DEPARTMENT OF BIOLOGICAL APPLICATIONS AND TECHNOLOGY

PhD Thesis

Functional studies of the neoplastic B cells In Chronic Lymphocytic Leukemia; intrinsic and extrinsic mechanisms

Elisavet Chartomatsidou
Biologist

November, 2018

3 members committee

1st supervisor: Kostas Stamatopoulos, M.D., Ph.D., Director of Institute of Applied Biosciences, Center for Research and Technology Hellas, Thessaloniki, Greece

2nd supervisor: Theoni Trangas, Ph.D., Head and Professor of the Department of Biological Applications and Technology, University of Ioannina, Ioannina, Greece

3rd supervisor: Georgios Thifronitis, Ph.D., Professor of the Department of Biological Applications and Technology, University of Ioannina, Ioannina, Greece

7 members committee

1. Kostas Stamatopoulos, M.D., Ph.D., Director of Institute of Applied Biosciences, Center for Research and Technology Hellas, Thessaloniki, Greece
2. Theoni Trangas, Ph.D., Head and Professor of the Department of Biological Applications and Technology, University of Ioannina, Ioannina, Greece
3. Georgios Thifronitis, Ph.D., Professor of the Department of Biological Applications and Technology, University of Ioannina, Ioannina, Greece
4. Maria Papaioannou, Associate Professor of the Department of Medicine, Aristotle University, Thessaloniki, Greece
5. Theologos Michaelides, Associate Professor of the Department of Biological Applications and Technology, University of Ioannina, Ioannina, Greece
6. Ourania Tsitsiloni, Associate Professor of the Department of Biology, National and Kapodistrian University of Athens, Athens, Greece
7. Eleftheria Chatzimichael, Assistant Professor of the Department of Medicine, University of Ioannina, Ioannina, Greece

Εθνικό Κέντρο Έρευνας και Τεχνολογικής Ανάπτυξης (ΕΚΕΤΑ)
Ινστιτούτο Εφαρμοσμένων Βιοεπιστημών (ΙΝΕΒ)

Πανεπιστήμιο Ιωαννίνων
Σχολή Επιστημών Υγείας
Τμήμα Βιολογικών Εφαρμογών και Τεχνολογιών

Τίτλος διδακτορικής διατριβής

"Λειτουργική ανάλυση των νεοπλασματικών Β λεμφοκυττάρων στη Χρόνια Λεμφοκυτταρική Λευχαιμία: ενδογενείς και εξωγενείς μηχανισμοί "

Χαρτοματσίδου Ελισάβετ
Βιολόγος

Νοέμβριος, 2018

Τριμελής Συμβουλευτική Επιτροπή

1. Σταματόπουλος Κωνσταντίνος, Αιματολόγος, Διευθυντής του Ινστιτούτου Εφαρμοσμένων Βιοεπιστημών, ΕΚΕΤΑ
2. Τράγκα Θεώνη, Ομότιμη Καθηγήτρια Βιοχημείας, Τμήμα Βιολογικών Εφαρμογών και Τεχνολογιών, ΠΙ
3. Θυφρονίτης Γεώργιος, Καθηγητή Μοριακής και Κυτταρικής Ανοσολογίας, Τμήμα Βιολογικών Εφαρμογών και Τεχνολογιών, ΠΙ

Επταμελής Εξεταστική Επιτροπή

1. Θυφρονίτης Γεώργιος, Καθηγητή Μοριακής και Κυτταρικής Ανοσολογίας, Τμήμα Βιολογικών Εφαρμογών και Τεχνολογιών, ΠΙ
2. Παπαϊωάννου Μαρία, Αναπληρώτρια Καθηγήτρια Αιματολογίας, Ιατρική Σχολή, ΑΠΘ
3. Σταματόπουλος Κωνσταντίνος, Αιματολόγος, Διευθυντής του Ινστιτούτου Εφαρμοσμένων Βιοεπιστημών, ΕΚΕΤΑ
4. Τράγκα Θεώνη, Ομότιμη Καθηγήτρια Βιοχημείας, Τμήμα Βιολογικών Εφαρμογών και Τεχνολογιών, ΠΙ
5. Μιχαηλίδης Θεολόγος, Αναπληρωτής Καθηγητής Μοριακής Γενετικής, Τμήμα Βιολογικών Εφαρμογών και Τεχνολόγων, ΠΙ
6. Τσιτσιλώνη Ουρανία, Αναπληρώτρια Καθηγήτρια Ανοσολογίας, Τμήμα Βιολογίας, ΕΚΠΑ
7. Χατζημιχαήλ Ελευθερία, Επίκουρη Καθηγήτρια Αιματολογίας, Τμήμα Ιατρικής, ΠΙ

Contents

1 Prologue

The present PhD thesis was conducted at the Institute of Applied Biosciences (INAB) in the Centre for Research and Technology Hellas (CERTH) in Thessaloniki, Greece under the guidance of Dr. Kostas Stamatopoulos, Director of the Institute. His support and knowledge are only a few of the elements of his influence on growing my inspiration for research.I warmly thank him for giving me the opportunity to conduct this PhD thesisat the Institute. Furthermore, I would like to express my sincere gratitude to my University supervisors Drs Theoni Tranga and George Thyphronitis, both Professors at the Department of Biological Applications and Technology in the University of Ioannina, Greece, who introduced me to the field of Immunology, as I obtained my bachelor degree also in this department and whose motivation has a lasting effect on my studies and future career plans.

Moreover, I would like to thank Drs. Niki Stavroyianni, Director, and Achilles Anagnostopoulos, Director, at the Department of Hematology and HSCT Unit of the “G. Papanikolaou” General Hospital, Thessaloniki, Greece, for their important contribution to the current study through the provision of relevant clinical samples from patients diagnosed with Chronic Lymphocytic Leukemia. Also, I would like to thank Drs.Paolo Ghia, Head of Strategic Research Program on CLL and B-cell Neoplasia Unit, Division of Experimental Oncology, Milan, Italy; and, Richard Rosenquist, Professor in Clinical Genetics at the Karolinska University Hospital, Sweden for their support to this project.

I have been fortunate to have spent my time at CERTH among an extraordinary group of fellow PhD students and Postdocs. They have all enriched my professional life and made the study in this department invaluable. I would foremost like to thank Drs. Stavroula Ntoufa and Nikos Papakonstantinou, both for their assistance over these research years, as well as for their guidance from my bachelor to PhD thesis. The current thesis would not be completed without my co-workers and friends Marianna Akritidou, Alessandra Rovida, Marina Geroussi, Giorgos Gavrielides, Giannis Gkekas, Giorgos Tsiolas, Maria Koutroumani, Maria Tsagiopoulou, Evangelia Migga and importantly, Mata Laidou,whose priceless help, time and companionship created a wonderful lab atmosphere. Moreover, I want to thank Dr Konstantina Kotta for sharing her expertise to flow cytometry which has been an important contribution to this project.

Finally, I must express my very profound gratitude to my family for providing me with unfailing support and continuous encouragement through out my years of study and through the process of researching and writing this thesis. This accomplishment would not have been possible without them.

2 Introduction

2.2 Introduction to the immune system

The term immunity usually refers to the ability of any organism to defend itself against pathogenic agents, both extrinsic (infectious agents, environmental toxins etc) and intrinsic (tumor cells, apoptotic cells etc). The sum of different cell types, tissues and molecules which contribute to maintaining the homeostasis is referred to as the immune system and their coordinate responses as the immune response. Each component of any agent, both intrinsic and extrinsic, capable of eliciting an immune response is termed an antigen.

One of the most important properties of the immune system concerns the ability to distinguish self from non-self antigens. Antigen recognition and immune defense rely on multiple mechanisms, which act in parallel and complementary ways in order to mountan effective immune response. The immune system has evolved from more simple to more complicated organisms and enhances the adaptation to constant environmental pressure[1].

In higher organisms, like humans, there are two parallel and complementary branches of the immune system:

1. **Innate immunity**, also called natural or native immunity, which mediates the initial protection against infections[2].
2. **Adaptive immunity**, also called specific or acquired immunity, which develops more slowly and mediates later, even more effective, defense against infections[3].

Interactions between these two systems lead to specialized and more effective defenses. To effectively protect the host against disease, the immune system must fulfill four main tasks. The first concerns antigen recognition. The second is to contain and, if possible, eliminate the pathogen. At the same time, the immune response has to be controlled so that the host is not damaged. Immune regulation is, therefore, a third and important feature of the immune system and failure at this level may lead to conditions, such as autoimmune disorders or allergy. Finally, the fourth task is to provide protection against recurring disease from the same pathogen. This is possible thanks to the so-called immune memory, a unique feature of the adaptive immune system, whose exact mechanism remains incompletely understood[3].

2.2.1 Structure and function of the human immune system

At the cellular level, the organization of the human immune system is based on the coordinated action of various cell populations with distinct roles. In adults, all immune cells (leukocytes) derive from a common precursor, the hematopoietic stem cell (HSC) of the bone marrow. Various hematopoietic growth factors induce the proliferation and differentiation of the pluripotent HSCs towards different cell types.

The development, differentiation and activation of most leukocytes continue while cells follow a path through different tissues of the body in responseto chemical signals. In general, micro- and macro-environmental stimuli modulate the transcription of lineage-determining genes. The myeloid lineage gives rise to most cells of the innate immune system (monocytes/macrophages, granulocytes, mast cells, dendritic cells). The lymphoid lineage, on the other hand, gives rise to the natural killer (NK) cells of innate immunity and the B and T cells of the adaptive immune system (**Figure 1**).

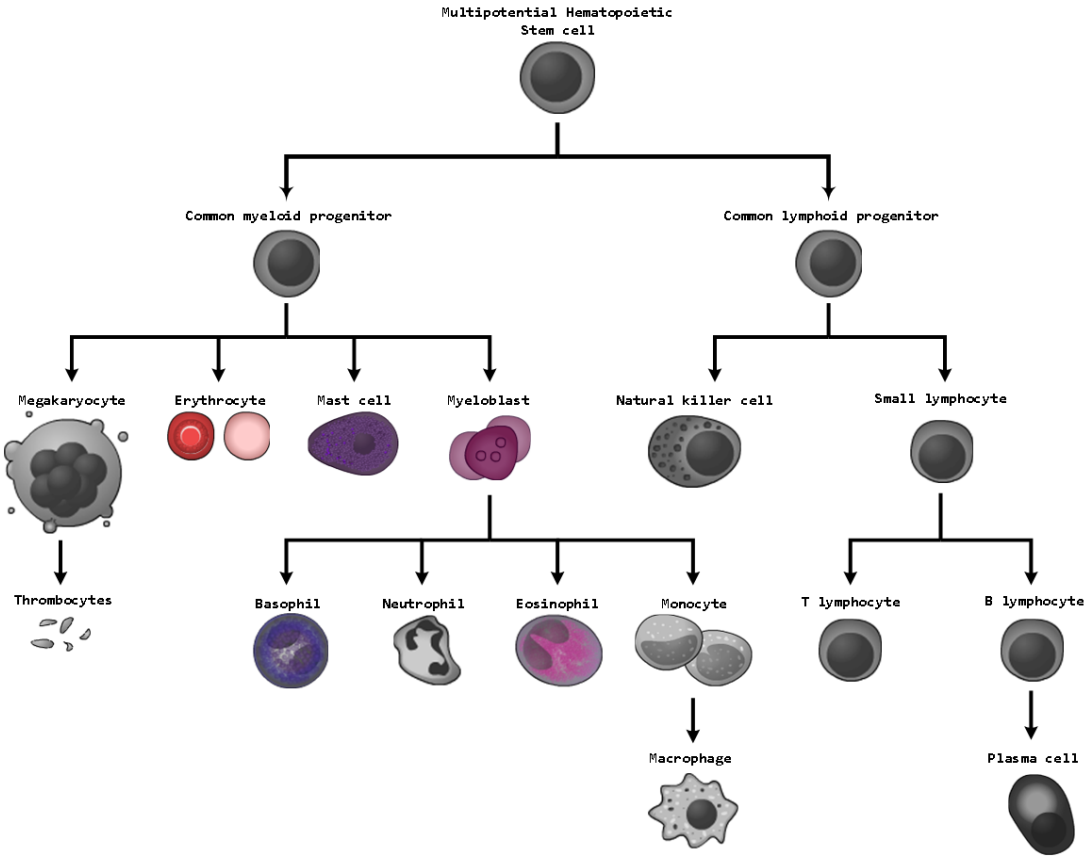

Figure 1: *Development of different mature blood cells are generated from the hematopoietic stem cell.*

The architecture of human immune tissues and organs has evolved in such a way so as to increase the possibility of contact between pathogens and immune cells, hence enabling to mount a quick immune response. Cells that participate in innate immunity either reside in tissues, or circulate in the blood stream and migrate to tissues in sites of inflammation. Concerning the adaptive immunity, lymphocytes circulate in the blood and lymph and are also found in large numbers in lymphoid tissues or lymphoid organs. Lymphoid organs are broadly divided into central or primary, where lymphocytes are generated, and peripheral or secondary, where mature naïve lymphocytes are maintained, antigen is presented and adaptive immune responses are initiated. The bone marrow and the thymus are called primary lymphoid organs, whereas the lymph nodes, the spleen and the mucosa-associated lymphoid tissue (MALT) belong to the secondary lymphoid organs (**Figure 2**).

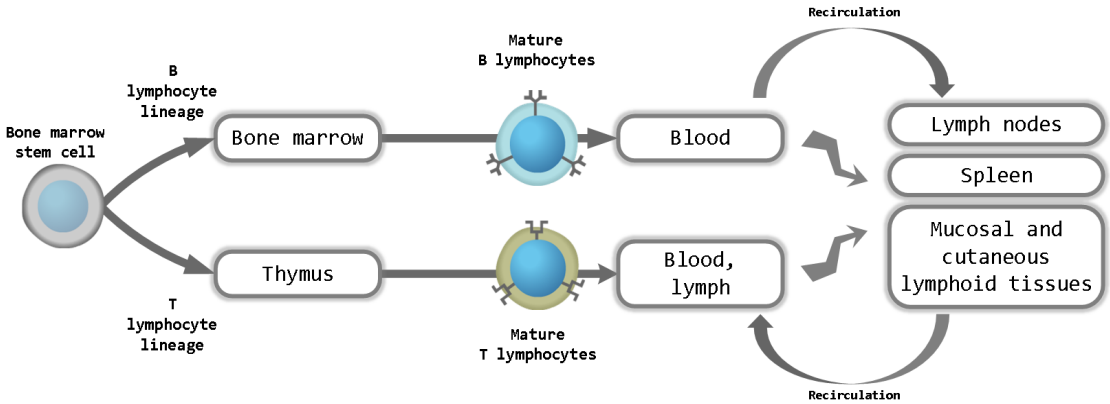

***Figure 2**: Primary and secondary lymphoid organs where different functions and stages of maturation for B and T cells take place.*

2.3 Innate immunity

The microorganisms encountered daily throughout the life of a healthy individual only occasionally cause perceptible disease. Most are detected and eliminated within minutes or hours by innate defense mechanisms that do not rely on the clonal expansion of antigen-specific lymphocytes and, thus, do not require a prolonged period of induction. Only when the innate host defenses are bypassed, evaded or overwhelmed is an adaptive immune response required. In this context, the innate immune system provides an initial

discrimination between self and non-self. However, it is constrained by a rather limited and invariant repertoire of receptors used to recognize invading pathogens. The common pathogen constituents recognized by pattern recognition receptors of the innate immune cells are usually quite different from the pathogen-specific antigens that are recognized by lymphocytes. They are molecular structures that have remained conserved in the microbial taxa, but have disappeared from evolutionarily evolved organisms[2].

2.3.1 Receptors of innate immunity

Pathogen recognition is a difficult task given the heterogeneity and constant evolution of most pathogens. Metazoan species have developed several recognition strategies to deal with this issue. The most common concerns the pattern-recognition strategy, which is based on the recognition of molecules that are broadly conserved among microbial agents, yet absent from the host. Such patterns (pathogen-associated molecular patterns, PAMPs) are sensed in the context of innate immunity by specific receptors, called pattern recognition receptors (PRRs), which serve as a first line of defense against invading microbial agents. The cell walls of Gram-positive and Gram-negative bacteria, for example, are composed of a matrix of proteins, carbohydrates and lipids in a repetitive array. Repetitive structures that are conserved in the microbial taxa but are absent from the host serve as PAMPs and are recognized by the PRRs of the innate immune system[2].

The pattern recognition receptors of the innate immune system may have several different functions. Some are phagocytic receptors which stimulate the ingestion of the pathogens they recognize. The mannose-binding lectin (MBL), for example, which recognizes a particular orientation of sugar residues found only in microbes, once bound to the pathogen, opsonizes it and facilitates its phagocytosis. Other PRRs are chemotactic receptors, which guide cells of the immune system to sites of infection. The fMet-Leu-Phe (fMLP) receptor which recognizes formylated methionine residues of bacterial polypeptides is a typical example. This receptor is found on macrophages and neutrophils and its ligation guides these cells to sites of infection. Another important function of PRRs is to induce the production of effector molecules of the innate immune response and, moreover, to induce the production of proteins which will contribute tothe initiation and

shaping of any subsequent adaptive immune response. Binding of pathogens to some receptors on macrophages or dendritic cells may signal for the upregulation of costimulatory surface molecules and enable them to act as antigen-presenting cells to T lymphocytes, thereby initiating an adaptive immune response. The best-defined activation pathway of this type is triggered through a family of evolutionary conserved transmembrane receptors called Toll-like receptors (TLRs)[4], which will be discussed more extensively below.

2.4 Receptors of adaptive immunity: focus on immunoglobulin molecular structure and function

Immunoglobulins (IG) are the antigen-recognition molecules of B cells. Immunoglobulins are glycoproteins produced by B cells that can be found in two basic forms:

1. Present on the B cell membrane.
2. Secreted in the circulation by plasma cells (antibodies).

Membrane-bound IG on the B cell surface functions as the cell's receptor for antigen and, together with certain accessory signaling molecules, is known as the **B cell receptor**, **BcR**[5].

IGs are heterodimers consisted of four peptide chains as shown in **Figure 3**. The structure of each IG consists of two identical light (L) chains and two larger identical heavy (H) chains. More specifically, two types of light chains exist, termed kappa (κ) and lambda (λ). A given IG has either κ or λ chains, never one of each. The ratio between the two in the repertoire differs among species: in humans, the κ:λ ratio is approximately 2:1. No functional differences have been found between antibodies that carry κ or λ chains.

The heavy chains of an IG molecule can be divided into five general classes: μ, γ, δ, ε, α and according to the class they belong to, there are five IG isotypes (classes) – IgM, IgG, IgD, IgE, and, respectively. Their carboxy-terminal part characterize their distinctive functional propertiesand are not associated with the light chains. IgG is by far the most abundant IG classand has several subclasses (IgG1, 2, 3, and 4 in human).

The amino-terminal sequences of both heavy and light chains vary greatly. The amino-terminal variable domains (V domains) of the heavy and light chains (VH and VK/VL, respectively), comprise the V region of the IG which defines antigenic specificity. In fact, most differences between different IGsare located in the complementarity-determining regions (CDRs) of both light and heavy chain variable domains. C domains, on the other hand, present far fewer differences.

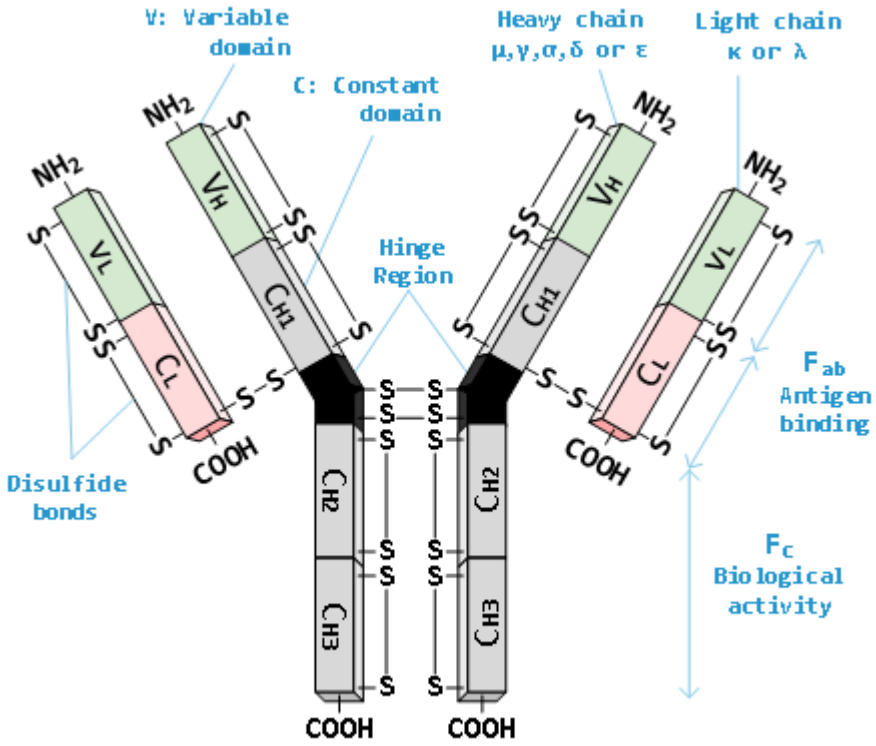

***Figure 3**: Immunoglobulin structure*

2.4.1 Immunoglobulin gene rearrangements

IGs are encoded by gene complexes formed during B cell differentiation through the recombination of distinct genes. B cells failing to express a functional immunoglobulin die by apoptosis. Intact heavy and light chain genes exist in the germ line DNA. Four groups of genes -variable (V), diversity (D), joining (J) and constant (C)- exist in the IGheavy gene locus (IGH), while three (V, J and C) exist in the IG kappa and lambda light chain gene loci (IGK and IGL, respectively). V genes

are located at the 5’ end DNA region followed by (D -->) J--> C to the 3’ end (**Figure 4**).

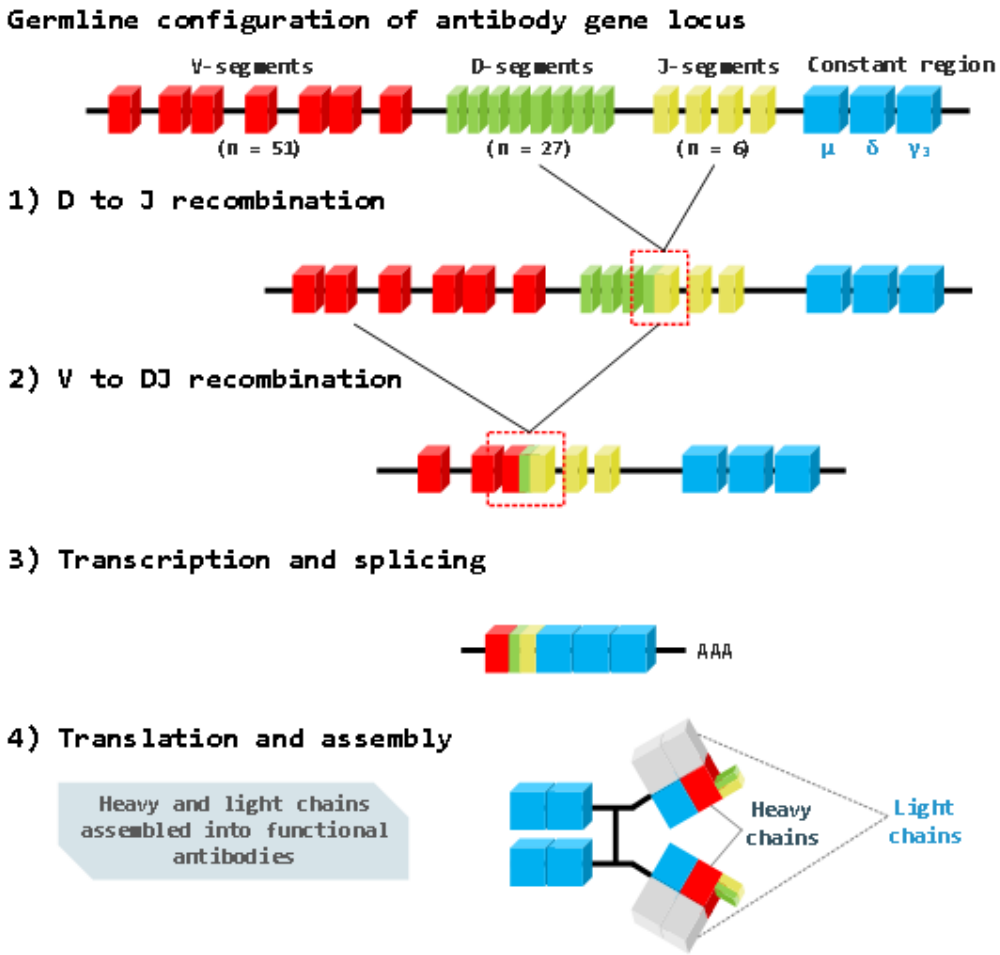

***Figure 4**: Schematic representation of the recombination of V(D)J genesfor the assembly of immunoglobulin molecules.*

The expression of immunoglobulin relies on the somatic recombination of the V, D, J genes that encode for the variable domain. Diversity is generated during this process by the use of different combinations of V, D, and J genes in different clones of lymphocytes, called combinatorial diversity. This kind of diversity is limited by the available number of V, D, J genes in the germline. V(D)J recombination is mediated by a group of enzymes collectively called VDJ recombinases, expressed only in immature B (and T) cells. Diversity is augmented through the modification

of the junctions of V, D and J genes (junctional diversity) by the random addition of non-germline encoded nucleotides (N-nucleotides) catalyzed by the enzyme terminal deoxyribonucleotidyl transferase (Tdt). Thanks to these two processes, humans can recognize different epitopes (more than 10^9) with an equivalent number of distinct clones of B cells, each with a single antigen receptor specificity[4,5].

2.4.2 Development and survival of B cells

B cells mature in the bone marrow (antigen-independent phase) and relocate for activation to the peripheral lymphoid organs (antigen-dependent phase). Generally, all stages of differentiation in the bone marrow are defined by IG gene rearrangements and are depicted graphically in **Figure 5**.

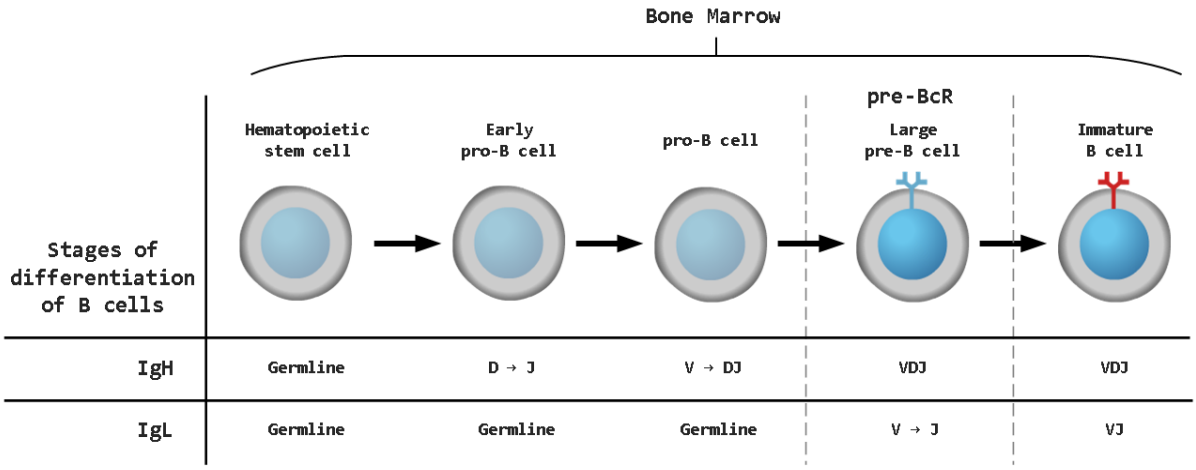

***Figure 5**: Developmental stages of a B lymphocyte in the bone marrow.*

In different stages of development in the bone marrow, there are special checkpoints to ensure normal development. Driven by IL-7 and other cytokines, pro-B cells proliferate and produce a large pool of cells. The first checkpoint operates at the next stage, where pre-B cells express μ heavy chain (heavy chain gene rearrangement completed) together with a surrogate light chain that constitutes the pre-BcR complex. VDJ recombination takes place in only one of the two inherited parental alleles (allelic exclusion), hence each cell can express receptors of a single specificity. A second checkpoint operates when immature B cells express a complete IgM (light chain gene rearrangement completed) that weakly

recognizes self antigen (positive selection). Weak recognition ensures that the B cell will receive signals for further development and survival, but will not be harmful (negative selection) (**Figure 6**).

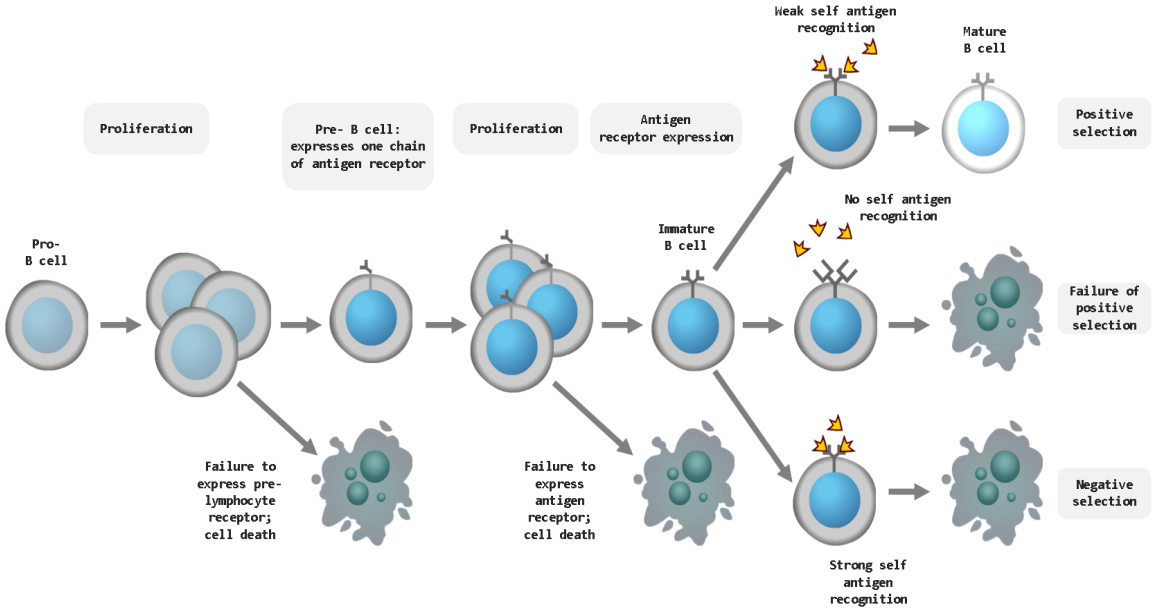

***Figure 6**: Positive and negative selection. Special checkpoints along B cell maturation ensure normal development.*

In order to avoid programmed cell death in the bone marrow, cells have to successfully follow a cellular path for the completion of a functional BcR and the regulation of self-reactivity. When the recombination leads to a non-functional BcR IG complex or to an IG strongly recognizing self antigens, B cells die by apoptosis (**clonal deletion**). Alternatively, they are offered a second opportunity of surviving, by either 1) re-activating the recombination mechanisms of IGgenes and attempting further gene rearrangements to produce a functional IG gene complex or replace the original complex encoding for a potentially harmful receptor by a new one (**receptor editing**); or 2) turning into a state of unresponsiveness or diminished responsiveness to antigen (**anergy**), where they lose membrane IgM (or express low levels of membrane IgM) and express high levels of IgD[4].

B cells leave the bone marrow and move to the secondary lymphoid organs. There, when mature B cells recognize antigen, they proliferate and finally differentiate into plasma and memory B cells. These processes take place in defined structures called **germinal centers**.

During the first stage of germinalcenter formation, activated B cells undergo intense proliferation. These proliferating B cells, known as centroblasts, appear in human germinal centers as a well-defined dark zone. Centroblasts eventually give rise to centrocytes, which are small, non-dividing B cells that express membrane IG. Centrocytes move from the dark zone into the light zone, where they make contact with antigen displayed as antigen-antibody complexes on the surface of follicular dendritic cells.

B cells are located in follicles (B cell zone). If a B cell has reacted to an antigen, a follicle may include a germinal center. T cells are located outside follicles in the parafollicular cortex (T cell zone). This orientation is achieved because cells, such as follicular dendritic cells (FDCs), produce chemokines attracting different lymphocyte populations[4].

Overall, each germinal center derives from one or very few clones of B cells and provides a micro-environment important for the development and maturation of B cells through interactions with other immune cells and cytokines. Germinal centers are the sites of affinity maturation, formation of memory B cells, class switching, and plasma-cell formation. In general, affinity maturation and memorycell formation require germinal centers. However, some class switching and significant plasmacell formation can also occur outside germinal centers[4,6].

Class switch recombination

IgM and IgD are the first antigen receptors expressed by B cells, and IgM is the first antibody produced in the course of an immune response. Class switching enables the same assembled VH exon to be associated with different IGHC genes. This process is stimulated by external signals, such as cytokines released by T cells or mitogenic signals delivered by pathogens, and involves an irreversible non-homologous DNA recombination which is guided by stretches of repetitive DNA known as switch regions (S regions). When a B cell switches from the co-expression of IgM and IgD to the expression of another subtype, DNA recombination occurs between the S_{μ} and the S region upstream of the gene for the other isotype. Switch regions lie right upstream each IGHC gene, with the exception of the IGHD gene whose expression is not dependent on DNA rearrangement. The entire intervening

DNA is deleted and, therefore, the process cannot be reversed. Isotype switch is a result of distinct cytokine expression by other cell types. For instance, IgE isotype is driven by IL-4 whereas IgG2a by IFNγ.

Somatic hypermutation

Somatic hypermutation (SHM) refers to the introduction of changes, most often point mutations and much less frequently insertions/deletions, in the genes encoding the V domain of the IG heavy and light chains. SHM is triggered by encounter with antigen and underlies the so called "affinity maturation" of the antibody. Mutations which result in disrupting or reducing the affinity of the IG receptor for the antigen are selected against. Clones bearing mutations which increase the affinity of the produced receptor for the antigen are preferentially selected to mature into antibody-secreting plasma cells. SHM results in further increasing the diversity of the peripheral B cell repertoire to approximately 10^{12} different specificities. More importantly, it adjusts the existing clones to the specific antigen that is encountered each time.

2.5 Chronic Lymphocytic Leukemia

2.5.1 General

Chronic Lymphocytic Leukemia (CLL) is a malignancy of $CD5^+$ B cells, which are clonally expanding in blood, bone marrow, lymph nodes and spleen. Clonal B cells display increased expression of CD19, CD5 and CD23 B cell antigens, while CD20 and CD79b are expressed at lower levels compared with normal B cells[7,8,9].CLL is one of the most frequent adult leukemias in the western world (~40% of all adult leukemias in the US), affectingmore men than women(2:1), with a median age at diagnosis of around 72 years[10,11]. CLL is less common in Asia with a very low average incidence (<0.01%) and remains rare even among Japanese immigrants in western counties[12].

2.5.2 Hereditary factors

The most consistent risk factor for CLL occurrence is the familial history of lymphoid malignancies such as CLL itself, non-Hodgkin lymphoma (NHL) and/or Hodgkin lymphoma (HL), as relatives of patients facing one of these diseases have a significantly greater probability of developing CLL compared to the general population[13,14]. Additionally, CLL appears to be more frequent among monozygotic than dizygotic twins[15]. To date, single-nucleotide polymorphisms (SNPs) in 30 loci associated with familial CLL have been discovered, providing a genetic background to the observed epidemiological figures[12]. Adults infected with hepatitis C (HCV) are also more prone to develop many lymphoproliferative disorders, CLL included[16].

2.5.3 IGHV gene somatic hypermutation status in CLL

The somatic hypermutation status of the rearranged clonotypic immunoglobulin heavy variable (IGHV) genes helps in distinguishing two subgroups of CLL cases. The "mutated-CLL" (**M-CLL**) subgroup is characterized by the expression of IGHV genes differing from the germline by >2%[17]. The "unmutated CLL" (**U-CLL**) subgroup, on the other hand, is characterized by the expression of IGHV genes differing from the germline by ≤ 2%[17].

Both subgroups display a highly biased repertoire of IG genes, implicating antigen selection in CLL pathogenesis[18]. Moreover, certain immunoglobulin genes (IGHV1-69, IGKV1-33/1D-33, IGLV3-21) are preferentially used in unmutated rearrangements, whereas others (IGHV4-34, IGKV2-30, IGLV2-8) are more frequent in mutated ones[19].

Differences in the SHM status of the IGHV genes are reflected in significantly distinct biological profiles between U-CLL vs M-CLL. In particular, U-CLL clones have been associated with an aggressive disease course and poor prognosis, while M-CLL ones are associated with a favorable disease outcome. This highly variable profile could be attributed to differences in microenvironmental interactions with resultant activation or deactivation of signaling pathways, clonal evolution, differing epigenetic status and differential propensity for acquiring genetic aberrations[20,21].

M-CLL cells more often express oligo-reactive and mono-reactive BcRs, while U-CLL cells tend to express low-affinity, poly-reactive and self-reactive BcRs[22]. M-CLL cases also display decreased signaling capacity, which has been attributed to anergy following chronic antigenic stimulation. On the other hand, U-CLL cases carry BcRs that are more competent

and exhibit less signs of anergy, instead retaining more responsiveness to signaling; this feature may underlie their noted aggressiveness since persistent antigenic stimulation may promote their survival and growth[23].

Additionally, key signaling molecules differentially expressed between U-CLL and M-CLL subtypes significantly define the quality of response after BcR antigen stimulation and signal transduction. These include CD38 and ZAP-70, whose expression is far more frequent in U-CLL vs M-CLL, hence determining cell signaling fate and, consequently, impacting on outcome. CD38 is a transmembrane protein that supports B cell interactions and differentiation through the binding of CD31[24], a cell-adhesion molecule expressed by cells of the CLL microenvironment, including nurse-like cells (NLCs) and T lymphocytes[25]. $CD38^{+}$ CLL B cells display greater BcR signaling capacity, linked to increased Ca^{2+} influx upon IgM stimulation and increased basal phosphorylation levels of BcR downstream signaling molecules[26]. Generally, patients with high CD38 expression experience faster progression and have a shorter life expectancy[27]. ZAP-70 is a key signaling molecule normally found in T and NK cells, structurally homologous to the spleen tyrosine kinase (SYK) of B cells. High ZAP-70 expression in CLL cells enhances BcR signaling[28] and these patients tend to have a more aggressive disease course compared to those with low ZAP-70 levels[29].

2.5.4 Biological and clinical considerations

CLL is clinically very heterogeneous, ranging from very indolent to aggressive and rapidly progressing disease: certain patients may experience stable disease with a nearly normal life expectancy and no need for therapy for many years, while others have very aggressive disease, may require treatment soon after diagnosis and prove resistant to therapy[17,31]. Heterogeneity at the molecular and cellular level underlies this clinical heterogeneity[22]. Indeed, ample evidence suggests that the interplay between cell-intrinsic and cell-extrinsic factors contributes to leukemogenesis and drives the progression of CLL[30].

2.5.5 Diagnosis

Most often, patients with CLL do not display any symptoms at the time of diagnosis,feel well and do not require treatment. However, CLL can have a range of clinical symptoms. A minority of patients can present fatigue, excessive night sweats, weight loss and increased

frequency of infections associated with hypogammaglobulinemia, enlarged, but painless, lymph nodes, enlarged spleen causing pain in the upper left portion of the abdomen and hepatomegalydetected by physical examination. Some patients can also develop autoimmune cytopenia[12,32]. Over time, a small fraction of CLL cases transform to a more aggressive lymphoma, termed Richter's syndrome (RS)[33,34]. RS morphologically most commonly resembles diffuse large B cell lymphoma (DLBCL).

2.5.6 Staging

Various biological and genetic markers contribute to the prognosis of CLL, since the heterogeneity that characterizes the disease extending from genomic abnormalities[35] to distinct immune cell signaling[36] has important implications for the overall patient management and eventual outcome. The clinical stratificationof CLL follows the Rai and Binet staging systems, relying on physical examination and blood counts, which subdivide patients with CLL into distinct prognostic groups[12,32].

2.5.7 Laboratory features

The laboratory assessment for the diagnosis of CLL requires a complete blood cell count and flow cytometry. The initial diagnosis is based on the detection of ≥5,000 clonal CLL B cellsper microliter of peripheral blood. Documentation of the clonality of the circulating B lymphocytes is possibleby flow cytometry. CLL cells typically express a distinct immunophenotype with low levels of surface immunoglobulin with monotypic (either κ-immunoglobulin or λ-immunoglobulin) light chain expression,combined with co-expression of CD19, CD5, and CD23. This phenotypic profile is distictive for CLL B cells and differentiates them from any normal B cell type, hindering the identification of a normal counterpart[37].

2.6 CLL treatment – basic principles

The treatment modalities for CLL include chemotherapy, chemoimmunotherapy and inhibitors that target molecules significant for the proliferation and survival of CLL cells[12]. The standard first-line treatment of medically fit patients with CLL lacking aberrations of the *TP53* gene is chemoimmunotherapy (CIT) with fludarabine (purine analogue),

cyclophosphamide (alkylating agent), and rituximab (anti-CD20 monoclonal antibody) (FCR)[32,38].

However, considering the fact that the median age of CLL diagnosis is 72 years, compromised physical status, including comorbidities, renders a significant number of patients unfit for intensive CIT. Thus, for older patients and patients with a history of infections, bendamustine (a bifunctional alkylating agent) and rituximab are a more suitable option, while for older patients with comorbidities a valid, effective and safe, option includes the combination of chlorambucil (alkylating agent) with an anti-CD20 monoclonal antibody such as rituximab, obinutuzumab or of atumumab [38].

In recent years, inhibitors of BcR signaling and BCL2 have been approved and became available for use. BcR inhibitors include BTK inhibitors, PI3K inhibitors and spleen tyrosine kinase (SYK) inhibitors[12]. **Ibrunitib** is a BTK inhibitor approved in the United States and Europe for use both as initial therapy and in cases with relapsed disease. This drug changed the landscape of CLL treatment with remarkable results in response rate and overall survival[39,40]. A new highly selective BTK inhibitor, under investigation in CLL therapy, is acalabrutinib, which is associated with high overall response rates and durable remission in previously treated cases[41].

PI3K inhibitors include **Idelalisib**, which has been approved in the United States and in Europe, and other drugs such as duvelisib, TGR-1022 and ACP-319 which are under clinical investigation. Idealisib combined with rituximab has shown great efficacy in the relapsed/refractory setting[42].

Venetoclax functions as a BCL2 anti-apoptotic molecule inhibitor and triggers apoptosis in CLL cells[43]. This drug has been approved for use in relapsed cases with deletion of the short arm of chromosome 17 del(17p) showing very promising results[44]. This drug can be safely combined with rituximab or obinutuzumab[12]. (**Figure 7**)

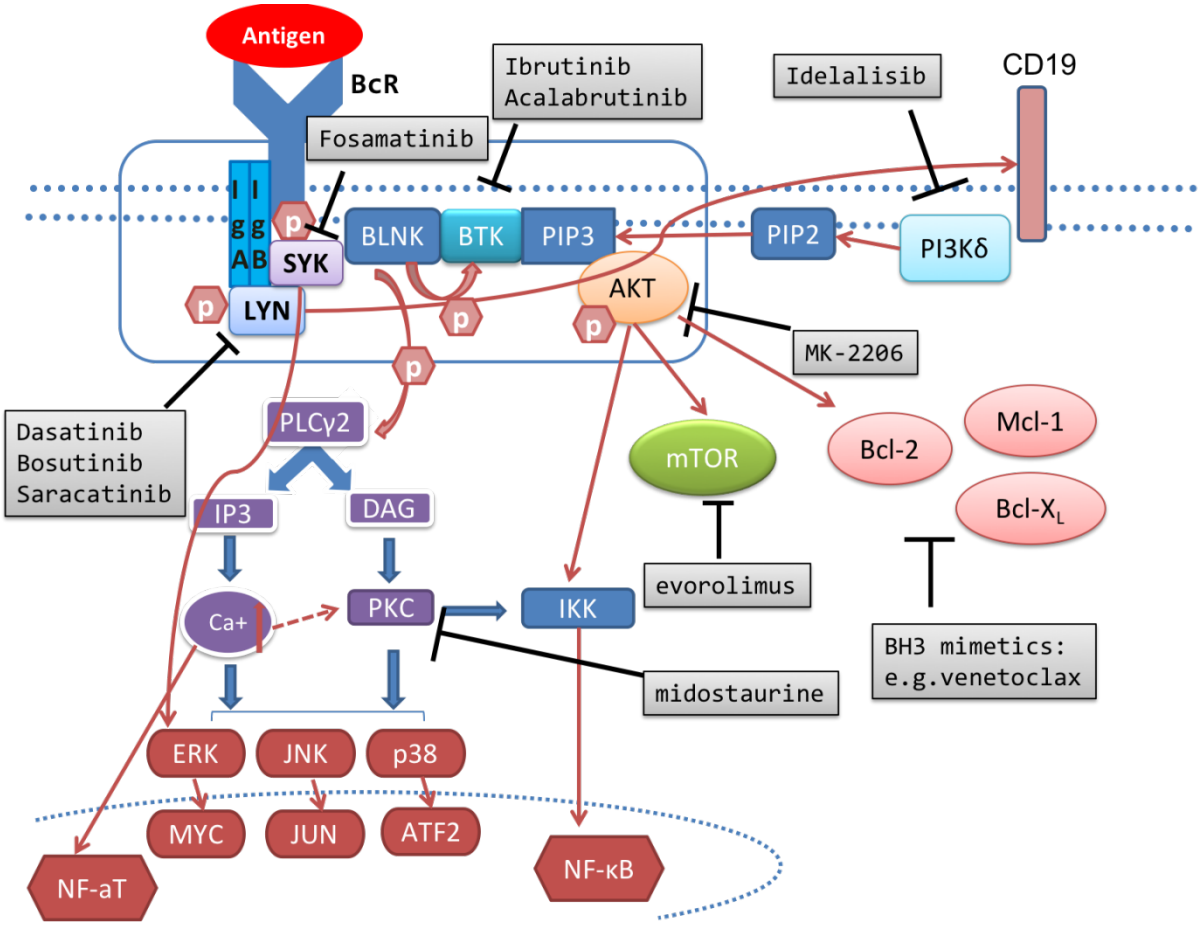

***Figure 7**: Targeted treatment of CLL through inhibition of important signaling molecules.*

2.6.1 Pharmacological agents targeting BcR signaling

Inhibitors targeting key enzymes in the signaling pathway downstream of the BcR represent an important therapeutic advance for the treatment of CLL. Here we will describe the current clinical use of the two approved agents, Ibrutinib and Idelalisib.

Ibrutinib

Ibrutinib is an orally available small molecule that forms an irreversible covalent bond with the Cys481 residue of the BTK kinase. It is highly potent for BTK with an IC_{50} of 0.5 nM[45]. Ibrutinib, has dramatic antitumor effects in CLL and other B cell malignancies[46–49].

BTK is known to promote survival through pathways such as NF-κB and activation of MAP kinases via Src family kinases[50], which are of great importance for the transduction of signals through the BcR in CLL. Several studies have shown that treatment with Ibrutinib inhibits numerous processes, including ERK signaling, NF-κB DNA binding, CpG–mediated

CLL-cell proliferation, and tumor-cell migration[45,50,51]. This agent also inhibits other members of the Tec family of tyrosine kinases, such as IL-2–inducible T-cell kinase (ITK), an important member of the signaling pathway in T cells[45,52,53]. Ibrutinib has a favorable therapeutic index, however in the group of patients with high-risk characteristics, responses are inferior[49].

Idelalisib

Class I phosphatidylinositol 3-kinases (PI3Ks) regulate cellular functions relevant to oncogenesis[54]. More specifically, cells of hematopoietic origin express the PI3K p110 δ isoform (PI3Kδ), playing a key role in B cell proliferation and survival. The PI3K pathway is constitutively activated in CLL and dependent on the expression of the PI3Kδ isoform[55]. Idelalisib is an oral inhibitor that targets PI3Kδ displaying great capacity in inducing apoptosis in primary CLL cells in a time- and dose-dependent manner, yet sparing normal T cells and natural killer cells and also not affecting antibody-dependent cellular cytotoxicity. Moreover, Idelalisib promotes inhibition in CLL cell chemotaxis toward CXCL12 and CXCL13 and migration beneath stromal cells (pseudoemperipolesis). Furthermore, after BcR triggering, Idelalisib reduces the production of chemokines in stromal co-cultures. Idelalisib also diminishes survival signals through the BcR or emanating from nurse-like cells, and reduces the activation of AKT and MAP kinase (ERK) through BcR- or chemokine-receptor signaling[55].

Despite the significant efficacy and tolerability of BcR signaling inhibitors, even in heavily treated patients, they are often characterized by suboptimal responses, reflecting resistance[56–58]. This indicates the need for introducing novel combination strategies in the clinical practice[59].

2.7 Cell-extrinsic pathogenetic mechanisms

Cell-extrinsic mechanisms are critical for the development and progression of CLL[60].The special and unique microenvironment in the bone marrow and secondary lymphoid tissues is critical for B cell differentiation and maturation, while it constitutes the most significant

extrinsic factor underlying heterogeneity in CLL. This CLL microenvironment is critical for the proliferation, survival and tissue homing of CLL cells, as indicated by the spontaneous apoptosis of these cells *ex vivo*[61]. Of note are the microenvironmental interactions of CLL cells with bystander cells and soluble stimuli in the tumor milieu through various receptors e.g. the BcR, TLRs, CD40, cytokine receptors and complement receptors, amongst others, that will be covered in detail in the following paragraphs[36,61–67] (**Figure 8**).

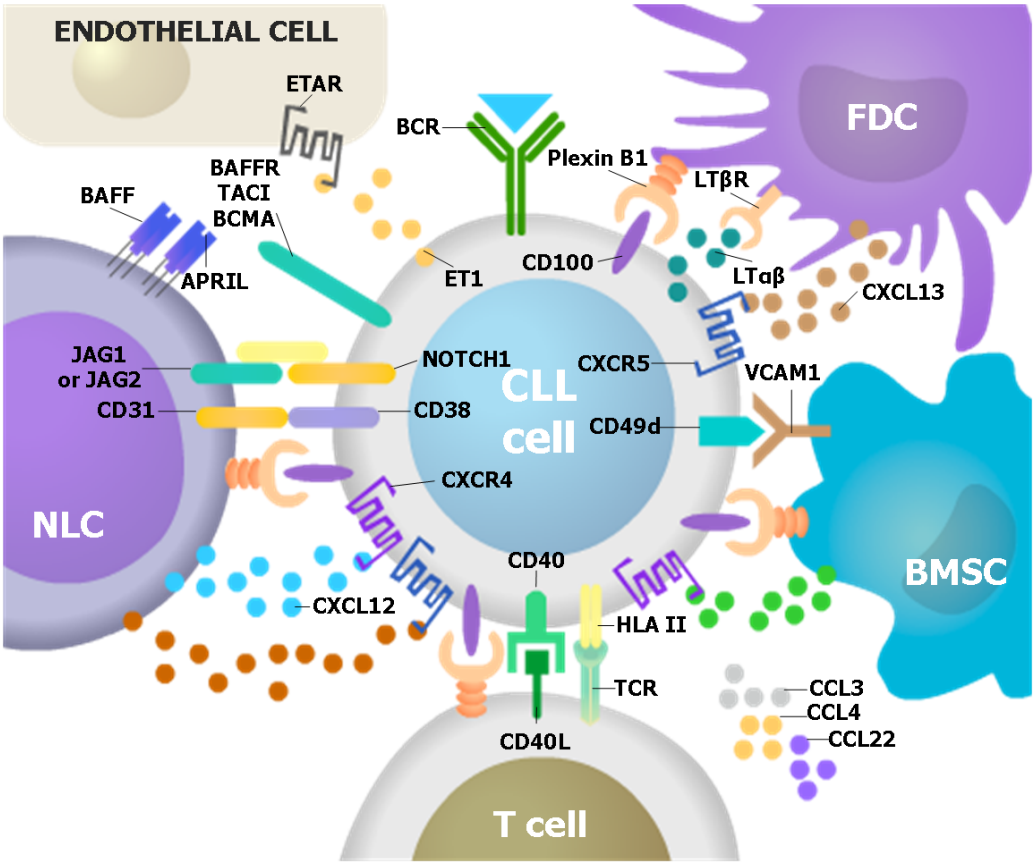

***Figure 8: The chronic lymphocytic leukemia microenvironment**. Schematic overview of the microenvironment of a CLL cell in a pseudofollicle. CLL cells interact through various receptorswith multiple non-malignantbystander cellular types, including bone marrow stromal cells (BMSCs), monocyte-derived nurse-like cells (NLCs), follicular dendritic cells (FDCs), endothelial cells and T cells and microenvironmental chemical triggers.*

2.7.1 The role of the B cell receptor in CLL

CLL cells interact with their microenvironment through multiple receptors, of which the most important is the BcR. When an antigen binds the BcR, upstream kinases like the Spleen Tyrosine Kinase (SYK) and the Tyrosine-Protein Kinase (LYN) become activated and

phosphorylate the ITAMs of the IG-α/IG-β heterodimer (CD79A/CD79B)[68]. Upon ITAM phosphorylation, Phospholipase C gamma 2 (PLC-γ2) becomes activated inducing calcium signaling, while cytoskeleton activators (e.g. VAV1) become triggered. Moreover, this leads to activation of the PI3K (Phosphoinositide 3-kinase) signaling pathway and the BTK (Bruton's Tyrosine Kinase), a non tyrosine kinase receptor of the Tec kinase family, essential for BcR signaling. Phosphorylated Proteinase Protein kinase C (PKC) triggers NF-κB signaling and mitogen-activated protein kinases (MAPKs), which leads to nuclear transcription including that of the CCL3 and CCL4 chemokine genes[68,69] (**Figure 9**).

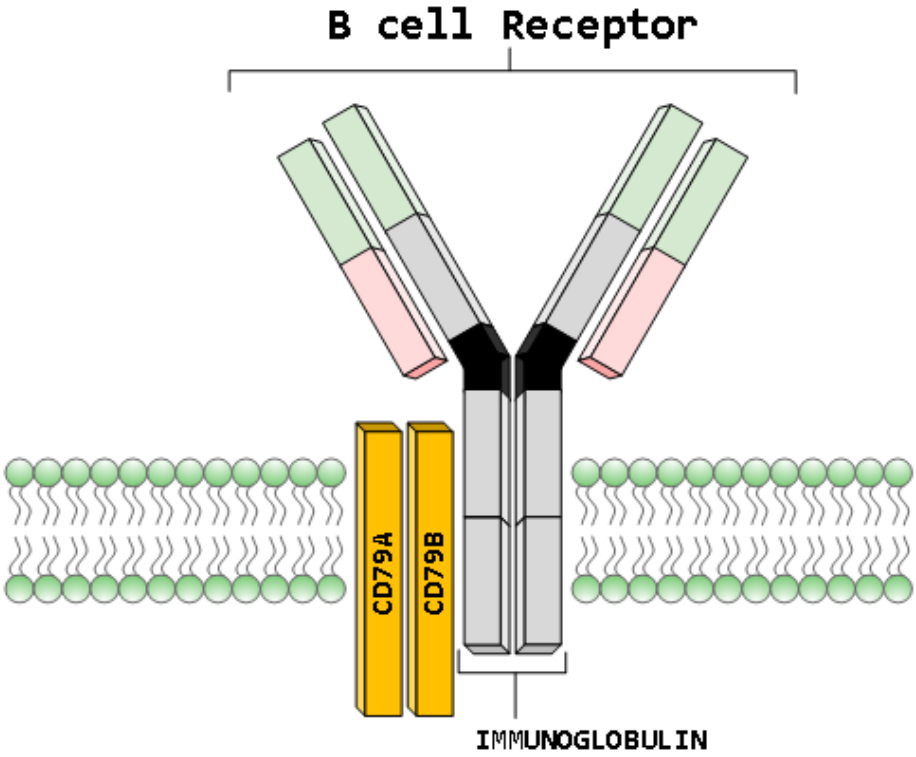

***Figure 9**: BcR complex and co-receptors.*

In CLL, despite low expression of surface IG (sIG), BcR signaling is not defective as indicated by the fact that *in vitro* BcR IG cross-linking causes effective activation in many CLL cases[70,71]. CLL cases that typically respond to BcR stimulation carry unmutated IGHV genes and express ZAP70 and/or CD38. In contrast, cases with mutated IGHV genes, that do not generally express ZAP70 and/or CD38, do not respond to stimulation, resembling the corresponding condition of cells anergized after chronic exposure to antigen[27,72].

A systematic study attempted to correlate the activation of kinases downstream the BcR with the mutational status of the IGHV genes. It was found that Akt and Erk were phosphorylated in all U-CLL cases and in 75% of the M-CLL, suggesting that in most cases the BcR signaling pathway is active. However, JNK was not active in most cases and NF-κB was activated in almost half. Therefore, it appears that CLL cells respond partially to the activation of the BcR[73]. This molecular pattern resembles anergic B cells in murine systems[74]. However, similar responses have also been observed in $CD5^+$ B lymphocytes of mice[75], hence it is unclear whether this pattern is characteristic of leukemic cells or whether it reflects the cell from which they originate.

In addition, a recent study showed that a subset of malignant clones unableto respond to *in vitro* cross-linking of their sIG displayed continuous Erk activation and absence of activation of Akt and the transcription factor NF-AT, suggesting that these cells became anergic after prolonged *in vivo* exposure to antigen. The study, however, failed to correlate the capacity of response to the SHM status of the IGHV genes[70].

2.7.2 The role of CD40 in CLL

CD40L or CD154, ligand of CD40 receptor, is expressed in activated T lymphocytes, macrophages and platelets[76], while the CD40 receptor is expressed in normal B lymphocytes and CLL cells[77,78]. Generally, the interaction between CD40-CD40L leads to proliferation and differentiation of B lymphocytes, dendritic cells and monocytes, as well as overexpression of co-stimulatory molecules and increased antigen presentation[79,80]. More specifically, antigen recognition by the T cell receptor leads to increased expression of CD40L in $CD4^+$ T lymphocytes and of CD80/CD86 co-stimulatory molecules in APCs, as well as enhanced signaling through CD40 in the latter. Activation and differentiation of T lymphocytes is regulated by this way through humoral immunity[81]. The expression of CD80 and CD86, along with the co-stimulatory molecule B7, is important for the proliferation of T lymphocytes. Activation of CLL cells throughthe CD40 receptor induces the expression of B7 molecules, and so these cells present antigen better than non-stimulated CLL cells[82]. A strong survival signal is also given after the recognition of CD40L bythe CD40 receptor of CLL cells[6383]. The interaction of CD40-CD40L in CLL cells is shown to induce the expression

of EZH2 through the activation ofthe alternative NF-κB pathway[84]. EZH2 is responsible for the silencing of pre-apoptotic genes and will be further presented below. The effect of CD40-CD40L interaction on survival differs in normal and leukemic B cells, and this difference may be exploited therapeutically[63].

2.7.3 The role of TLR9 in CLL

TLRs play an important role in CLL[85]. CLL cells are capable of signaling through the TLRs and TLR expression patterns may be related to the development and progression of CLL[86,87].
Studies suggest a pleiotropic effect of TLR9 stimulation with oligonucleotides containing CpG motifs or ODN2006, on leukemic B cell growth and survival [67,88]. This ligand is specifically recognized by TLR9 and its stimulation induces proliferation mainly in CLL cells from patients with unmutated IGHV genes, whereas apoptosis is induced in CLL cases with mutated IGHV genes[62,89]. This distinct response was attributed to increased Akt signaling in the proliferating cases. Actually, introduction of constitutively active Akt in non-proliferating CLL cells was sufficient for induction of cyclin A after CpG stimulation.

2.8 Cell-intrinsic pathogenetic mechanisms in CLL

Cell-intrinsic aberrations are critical in the natural history of CLL. These include recurrent genomic lesions such as chromosomal abnormalities and mutations in critical genes (e.g. *TP53, NOTCH1, SF3B1*)[90] as well as other perturbations, including, amongst others, altered microRNA expression[91] and epigenetic profiles[92] leading to disordered gene expression and function.
Almost 80% of all CLL patients carry at least one of the four most common chromosomal aberrations: trisomy 12, deletion in the 13q14 chromosomal region [del(13q)], del(11q) and del(17p)][93]. Trisomy 12, found in ~15% of total CLL cases, is associated with a higher incidence of Richter's transformation and secondary tumors[94], while when it co-occurs with *NOTCH1* mutations it may be linked to poorer survival[95].
Del(13q) is the most common chromosomal abnormality in CLL (>50% of total patients) and typically associated with a favorable prognosis, although the longer deletions seem to

enhance the aggressiveness of the disease[90]. The minimal deleted region (MDR) of this deletion includes, amongst others, the microRNA cluster *MIR15A–MIR16-1* locus and the deleted in leukemia 2 (*DLEU2*) locus which encodes the long non-coding RNA *DLEU2.* The produced *DLEU2–mir-15-16* cluster regulates the expression of anti-apoptotic proteins or proteins crucial in the regulation of cell cycle progression[96]. Moreover, the *DLEU7* gene, included in the MDR, encodes a putative negative regulator of the NF-κB transcriptional complex[97].

Del(11q) is found in 10-15% of all CLL cases, mostly in the U-CLL subgroup. It results in loss of the encompassed tumor suppressor gene ataxia telangiectasia mutated (*ATM*), which encodes a protein involved in DNA repair[98]. More than 30% of del(11q) cases carry mutationally disactivated remaining *ATM*alleles[99]. These patients display increased genomic instability, tendency of acquiring additional genetic lessions and chemoresistance[100].

Del(17p) is present in ~7% of CLL at diagnosis, predominantly in U-CLL cases[93]. This deletion invariably includes band 17p13, where the tumor suppressor gene *TP53* is located, while the remaining allele of this gene is found mutationally inactivated in around 80% of del(17p)cases. Cases with *TP53* aberrations display high genomic complexityand overall poor prognosis[90].

Besides chromosomal abnormalities, CLL genetic heterogeneity is also driven by recurrent somatic gene mutations e.g. in the *TP53, NOTCH1* and *SF3B1*genes. These mutations appear to not only play a pathogenetic role, but may also represent new biomarkers for the identification of poor-risk CLL[101–104]. Indeed, they are generally enriched in CLL patients that have transformed to Richter's syndrome and/or in progressive/refractory CLL cases[105]. *TP53* mutations (devoid of second-allele 17p deletions) are associated with a short survival and poor response to DNA-damaging chemotherapeutic regimens. For this reason, *TP53* disruptions constitute a significant predictive marker and they should be always tested in a routine clinical setting, especially before the start of chemotherapy[106–108].

Mutations in the coding region of *NOTCH1* (around 10% of all CLL patients) are mainly observed in U-CLL[109–111]. A significant fraction, ~40%, ofpatients with *NOTCH1* mutations also carry trisomy 12 with negative clinical outcome, as previously discussed[109,112]. The *NOTCH1* gene encodes a transmembrane receptor, that when triggered leads to

transcriptional upregulation[113]. *NOTCH1* mutations result in constitutive activation of this pathway with resultant changes in the gene expression signature[114].

SF3B1 is another gene frequently found mutated in CLL (~10% of all CLL cases, mostly U-CLL). This gene encodes a key component of the U2 snRNP that participates in the early stages of RNA splicing[115]. This interaction between *SF3B1* and RNA is the one disrupted by the mutations leading to several transcripts having an abnormal 3' splicing acceptor site[116]. Moreover, *SF3B1* mutations appear to also have a role in DNA damage responses[117]. Thus, *SF3B1* mutations possibly enhance CLL cell proliferation and/or survival[118,119].

2.8.1 Epigenetic deregulation in CLL

Epigenetics is the study of inheritable changes in the genome, which occur without modifying the DNA sequence, thus linking the genotype to the phenotype and ultimately regulating gene expression. Epigenetics, like genetic information, is inherited, but unlike the latter, it is reversible (epigenetic plasticity) and influenced by various stimuli or environmental factors[120].Aberrations in the epigenetic profiles may affect mechanisms such as cell division, apoptosis and response to environmental stimuli.

The three main epigenetic mechanisms, namely DNA methylation, histone modifications and microRNAs (miRNAs), regulate gene transcription by modifying access to gene promoters and regulatory regions.

- **DNA methylation** occurs almost exclusively at CpG dinucleotides and is catalyzed by DNA methyltransferases, which carry a methyl-group from S-adenosyl-methionine to the fifth carbon of cytosine in order to form 5'methyl-cytosine. Usually CpG dinucleotides are concentrated in regions called CpG islands (CGIs) which are defined as areas larger than 200 bases containing at least 50% C and G[121]. Generally, methylation of CpG islands is associated with gene silencing.

- **Histone modification** is any covalent post-translational modification to a histone protein (methylation, phosphorylation, acetylation, ubiquitylation, and

sumoylation). These modifications can impact gene expression by altering chromatin structure or recruiting histone modifiers. Histone modifications act in diverse biological processes such as transcriptional activation/inactivation, chromosome packaging, and DNA damage/repair[122].

- **microRNAs (miRNA)**area large group of small RNA molecules (19-25 nucleotides in length), which negatively regulate the expression of genes, leading to either mRNA degradation or suppression of translation. Functional studies indicate the important role of miRNAs in almost all cellular processes studied, while changes in their expression are implicated in the pathogenesis of cancer[123,124].

As in many cancers, epigenetic modifications appear to be crucial in the transformation, progression and evolution of CLL, while they constitute putative therapeutic targets as they can be modulated by several drugs. Generally, CLL displays methylation heterogeneity as it is characterized by an extensive hypomethylation with some hypermethylated regions[130]. The extent of this heterogeneity is related with the genetic complexity of the disease as locally disordered methylation within the leukemic clone could increase the opportunities for somatic mutations[131,132]. Distinct methylation profiles of prognostic genes have been revealed between M-CLL and U-CLL subgroups[133] and they are reminiscent of these subgroups, revealing the separation capacity of methylation patterns[134].

CLL has also been found to be associated with alterations in microRNA (miRNA) expression profile. A very common miRNA abnormality includes *mir15a* and *mir16a-1* which are deleted, altered or downregulated in around 60% of total CLL cases carrying del(13q) and they both target *BCL2* and *MCL1*[125,126]. Moreover, many other miRNAs have been found deregulated among CLL cases, while a differential expression profiles of miRNAs have been observed among different CLL subgroups[65]. Loss or reduced expression of all or some of *miR-29a/b, miR-29c, miR-34b, miR-181b* and *miR-3676*, which affect the expression of the *TCL1A* gene by targeting its 3‘ untranslated region*,* leads to enhanced expression of this gene, promoting the development of CLL in transgenic mice[127,128]. Additionally, increased expression of the m*ir-155* has linked with augmented B cell proliferation and BcR signaling leading to an aggressive disease outcome[129].

2.8.1.1 Histone trimethylation by EZH2 and its role in cancer

EZH2 (Enhancer of zeste homolog 2, EZH2) is one of the best studied histone methyltransferases (HMTs). EZH2 induces gene repression through trimethylation of histone H3 at lysine 27 (H3K27me3)[135,136].EZH2 is a polycomb group (PcG) protein that functions in concert with other proteins (EED, SUZ12 and RBBP4) in the multi-subunit polycomb repressive complex PRC2. PRC2 exerts methyltransferase activity to H3K27 via the SET domain of the EZH2 subunit. This results in transcriptional repression via various mechanisms, including the recruitment of DNA methyltransferases (DNMT) and PRC1 (another polycomp repressive complex), which acts to maintain the gene repression via ubiquitination of H2AK119[137,138] (**Figure 10**).

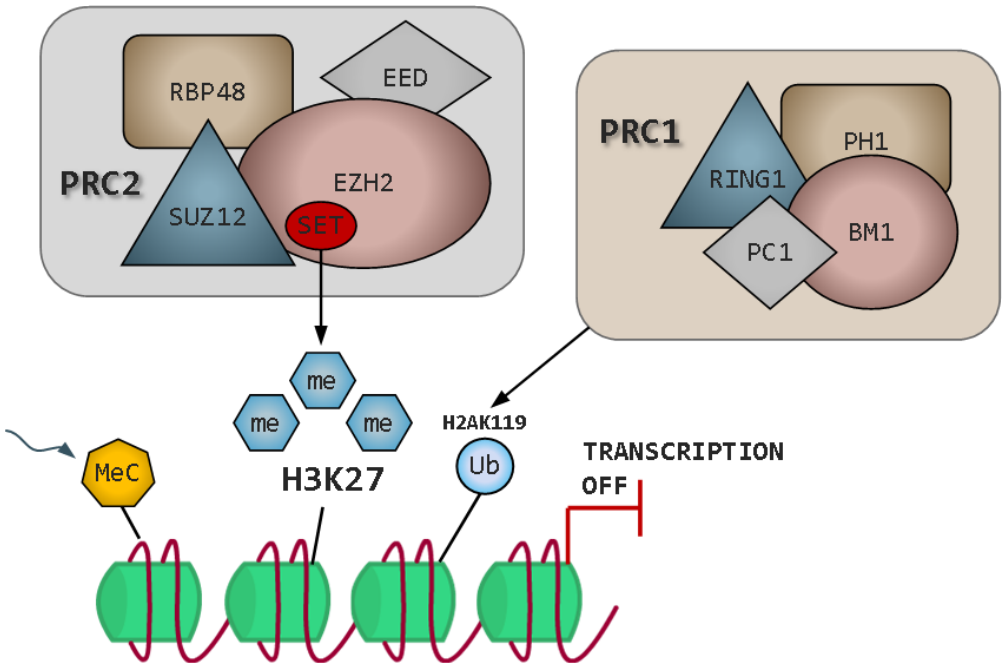

***Figure 10**: PRC complexes and the role of EZH2 in regulation of transcriptional repression.*

The expression of EZH2 is controlled by a complex mechanism and its overexpression is a hallmark of several cancers, especially their more aggressive subtypes, being associated with metastasis, tumor progression, and poor clinical outcome[139,140]. Different mechanisms have been reported as a cause of increased EZH2 levels in tumor cells, including activating gene mutations[141], gene amplification[142], transcriptional dysregulation[143,144], hypoxia[145],

and perturbed microRNA expression[146,147]. Notably, EZH2 is also recurrently mutated in several forms of cancer[136,148,149]. Both gain-of-functionand loss-of-function mutations occur in different cancers.

Under normal conditions, cell growth is induced by a homeostatic balance assured by the interaction of EZH2 and MYC[150].MYC enhances the expression of EZH2 indirectly, by activating PTEN, a PI3K pathway regulator, which then suppresses AKT expression and ultimately induces gene suppression through the function of the methylotransferase EZH2[151]. This interaction between EZH2 and MYC is disrupted in several cancer types[152].

EZH2 is critically implicated in embryonic development[153] and also participates in maintaining the multi-potency of adult stem cells in various contexts, including the long-term self-renewal potential of hematopoietic stem cells, by switching off pro-differentiation genes and promoting a shift toward proliferation by increasing expression of genes which facilitate progression through the cell cycle[150]. EZH2 plays acritical role in B cell ontogeny, with high expression in lymphoid progenitors[154], reduction in resting B cells, and pronounced up-regulationin activated B cells from GCs, wherein B cells undergo rapid proliferation and IG affinity maturation[155]. These observations implicate EZH2 in GC B cell proliferation and, possibly,in the pathogenesis of lymphomas derived from GC B cells. This is supported by the finding of activating mutations in the EZH2 SET domain in both DLBCL of the germinal center subtype and follicular lymphoma, tumors deriving from GC B cells[149].

2.8.1.2 Pharmacological inhibition of EZH2

Considering that aberrant EZH2 expression emerges as a key driver in the development and progression of many cancer types, not paradoxically, development of EZH2-specific inhibitors has been an active area of investigation. Several pharmaceutical companies (e.g.GlaxoSmithKline, Novartis and Epizyme) currently investigate such compounds in phase I/II clinical trials in different cancer types, including B cell lymphomas (including, follicular lymphoma and DBCL).

In the present study we assessed the effects of three EZH2 inhibitors, namely EPZ6438,

GSK126 and GSK343, that have shown preclinical and clinical efficacy in cancer, including several B cell malignancies.

EPZ6438 (tazemetostat) is a highly selective inhibitor of the enzymatic activity of EZH2 with good oral bioavailability[156]. Knutson et al. have shown that treatment with EPZ6438 resulted in decreased levels of H3K27me3 and dose-dependent tumor growth inhibition in mice carrying SMARCB1-mutant malignant rhabdoid tumors and EZH2-mutant NHL xenograft-bearing mice [156,157]. In 2018, a first in human, phase 1 study with tazemetostat was completed and showed a favorable antitumor activity in patients with refractory B-cell non-Hodgkin lymphoma and advanced solid tumors, including epithelioid sarcoma[158].

GSK343 has displayed good selectivity against EZH2 in both enzymatic and cellular assays, demonstrating a selectivity of more that 1000-fold against other methyltransferases and 60-fold against EZH1. GSK343 has been found to efficiently deplete H3K27me3 levels, suppress the growth of DLBCL cell lines and induce the expression of genes regulating the cell cycle[159].

GSK126 is the most potent EZH2 inhibitor developed thus far. GSK126 inhibits both wild-type and mutant EZH2 methyltransferase activity with similar potencies and is also competitive with S-adenosyl-methionine (SAM) and non-competitive with peptide substrates. GSK126 is more than 1000-fold selective for EZH2 versus only 20-fold for other human methyltransferases[160].GSK126 effectively inhibits both the proliferation of EZH2 mutant DLBCL cell lines and the growth of EZH2 mutant DLBCL xenografts in mice[161].In 2016 it was reported that GSK126 inhibits cell migration and angiogenesis in solid tumor cell lines through down-regulation of VEGF-A expression[162]. Moreover, GSK126 was found to exhibit *in vivo* anti multiple-myeloma effects with inhibition of xenografted human multiple myeloma growth in nude mice[163].

2.8.1.3 EZH2 and CLL

In 2013our group implicated for the first time EZH2 in the pathophysiology of CLL[164]. More specifically, we found EZH2 increased expression in a subgroup of U-CLL patients (subset

#1) with aggressive clinical course compared to a different subgroup of patients (subset #4) that belongs to the M-CLL category and is associated with indolent disease course[165,166]. Furthermore, we reported that EZH2 expression is modulated by miR-101, a well known epi-miRNA, which was downregulated in CLL subset #1. We also documented an inverse correlation between EZH2 mRNA and protein levels with miR-101 expression, since changes in miR-101 expression brought about by silencing using a miR-101 inhibitor or overexpression using a miR-101 mimic affected EZH2 protein expression in primary CLL cells. These observations suggested that increased EZH2 expression in clinically aggressive subset #1 is linked to downregulation of miR-101[164].

Subsequently, an independent study reported that EZH2 was overexpressed in CLL patients with poor prognosis and correlated with high white blood cell count, ZAP-70 expression and chromosomal abnormalities[167]. Moreover, an inverse correlation was also observed between miR-26A1 and EZH2 in primary CLL cells, suggesting that targeting this regulatory loop might represent a beneficial therapeutic approach[168].

2.9 Tcl1 *mouse model of CLL*

In order to address the pronouncedheterogeneity of CLL, a series of different genetically engineered murine models have been developed over the years. The landmark murine model for CLL is the TCL-1 transgenic (Tg) mouse that was established in 2002 and resembles the aggressive subtype of the disease[128]. This animal model for CLL has offered new insights into the pathogenesis of the disease and provided a great tool to test new therapeutic agents[172].

The *Tcl1* gene at 14q32.1 is involved in chromosomal translocations and inversions in mature T cell leukemias. In B lymphocytes, *TCL1* expression begins at the pro-Bcell stage, when B cells are still immature and ceases in mature B cells. Nevertheless, overexpression of*TCL1* has been identified in several B cell malignancies, including follicular lymphoma, mantle cell lymphoma, DLBCL, and splenic marginal zone B-cell lymphoma. The majority of patients with CLL expresses *TCL1* and its high expression is associated with progressive disease features, including unmutated IGHV genes, ZAP-70 expression, del(11q), and an

overall aggressive disease outcome[170,171].

The Eμ-TCL-1transgenic mice develop splenomegaly and hepatomegaly, resembling CLL/SLL-like disease in humans. The B cell population in peripheral blood expresses a phenotype characterized of $B220^{low}IgM^{+}CD5^{+}$starting at 6 months of age and mice become visibly ill at 10 to 18 months. Monoclonal or oligoclonal expansions of low proliferative activity that exhibit minimal or absent levels of somatic mutations in the clonotypic IGHV genes is detected, with the elder mice eventually developing a CLL-like disorder similar to the patients with aggressive and treatment-resistant disease[128].

3 Aim of the present study

Despite the significant efficacy and tolerability of BcR signaling inhibitors, i.e. Ibrutinib and Idelalisib, even in heavily treated patients with CLL, responses to these drugs are almost never complete while resistance does occur, indicating the need forintroducing novel combination strategies in clinical practice.

In 2013, we provided for the first time evidence that miR-101 regulates EZH2 expression in CLL and that EZH2 overexpression is a feature of aggressive CLL. Subsequently, we showed that downregulation of EZH2 expression and function affected CLL cell viability, highlightimg EZH2 as a potential novel druggable target in CLL.

On these grounds,the aim of the present study was to investigateEZH2 expression and function in a larger cohort of CLL cases andalso explore its impact on disease progression. Moreover, we were interested in investigating whether EZH2 is implicated in modulating signaling pathway activation in CLL and whether synergism may exist between EZH2 and signaling inhibitors. This is relevant considering that pharmacological inhibitors of the enzymatic activity of EZH2 are tested in phase I/II clinical trials in different cancer types, including B cell lymphomas. Hence, at least in principle, targeting both processes might represent a novel therapeutic strategy for CLL, especially for cases with suboptimal response to signaling inhibitors.

4 Materials and Methods

4.1 Negative selection of B cells

The RosetteSep kit (StemCell Technologies, Vancouver, Canada) was used for negative selection of $CD19^+$ B-cells from peripheral blood patient samples, following the manufacturer's instructions. This kit specifically targets non-B cells for removal, using a cocktail of mouse and rat monoclonal antibodies that recognizespecific cell surface markers on human blood nucleated cells (CD2, CD3, CD16, CD36, CD56, CD66b) and glycophorin on red blood cells (RBCs). This increases the density of the unwanted (rosetted) cells, such that they pellet along with the free RBCs when centrifuged over a density gradient medium such as Ficoll-Paque. Desired cells, thus, are never labeled with antibody and are easily and carefully collected as a highly enriched population at the interface between the plasma and the density gradient medium. Negative selection was preferred, as it ensures that isolated B cells will not be artificially stimulated through positive selection.

4.2 Validation of $CD19^+$ purity by flow cytometry

The purity of all preparations was checked by flow cytometry (BD FACSCalibur) for CD19 and always exceeded 95%.

Procedure:

1. 10 µl of CD3 FITC (fluorescein isothiocyanate) /CD19 PE (phycoerythrin) monoclonal antibodies are added to100 µl of blood (10^6 cells/ml)
2. Samples are mixed by vortex and then incubated for 10 min at room temperature (RT)
3. 2 ml of ammonium chloride solution (NH_4Cl) are added to the mixture, in order to lyse any erythrocytes
4. Samples are mixed by vortex and then incubated for 10 min in room temperature
5. Samples are centrifuged at 2000 rpm for 5 min at RT
6. Supernatant is discarded and 1ml of DPBS 1X is added to the mixture, followed by vortex
7. Data acquisition on a BD FACS CANTO (Becton Dickinson Immunocytometry Systems, San Jose, CA)

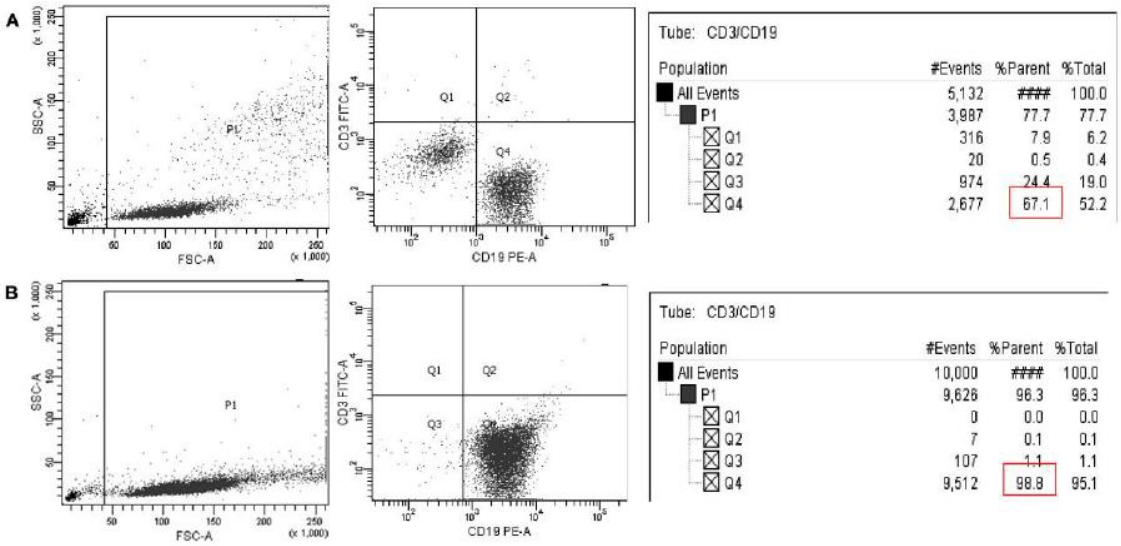

Figure 11: Determination of CD19⁺ purity by flow cytometry. *A) Cell sample before purification. Gating is on viable cells. B) Cell preparation after purification. CD19⁺ cells were always above 95%, in this case 98.8%.*

4.3 RNA extraction

Total RNA was extracted from CLL cells using the QIAamp RNA Blood extraction kit (QIAGEN GmbH, Germany) according to the manufacturer's instructions, including the recommended DNase I digestion step.

Procedure:

1. Cells were defreezed in 37ºCwith gentle agitation
2. Centrifuge for 5 min at 2000 rpm
3. Discard supernatant
4. Wash the cells with 1ml DPBS 1X
5. Repeat centrifuge
6. Discard supernatant
7. Add 600µl RLT buffer and mix by pipetting
8. Pipet lysate directly into a QIAshredder spin column
9. Centrifuge for 2 min at 13000 rpm
10. Discard QIAshredder spin column and save homogenized lysate.
11. Add 600µl 70% ethanol and mix by pipetting
12. Carefully pipet the sample into the QIAamp spin column

13. Centrifuge for 30 sec at 10000 rpm
14. Discard supernatant
15. Add 350µl RW1 buffer
16. Repeat centrifuge
17. Discard supernatant
18. Add the DNase I incubation mix 80 µl (10 µl DNase I stock solution and 70 µl Buffer RDD) directly to the QIAamp spin column membrane, and place on the benchtop (20–30°C) for 20 min
19. Add 350 µl RW1 buffer to the QIAamp spin column.
20. Centrifuge for 30 sec at 10000 rpm
21. Discard supernatant
22. Add 500 µl RPE buffer to the QIAamp spin column.
23. Repeat centrifuge
24. Discard supernatant
25. Add 500 µl RPE buffer to the QIAamp spin column.
26. Centrifuge for 3 min at 13000 rpm
27. Discard supernatant
28. Add 30 µl of RNase-free water directly into the QIAamp membrane and incubate for 10 min at room temperature
29. Centrifuge for 1 min at 10000 rpm
30. Store sample at -80^{o}C

4.3.1 Quantification and quality control of RNA

In order to check the quality of RNA extraction, the samples were electrophoresed on a 2% agarose gel. Extracted RNA samples were quantified with the Qubit^{TM} Quantitation platform using the Qubit RNA BR assay kit (Life technologies) following the manufacturer's instructions.

4.4 cDNA synthesis

RNA samples were used as template for cDNA synthesis via reverse transcription (SuperScript™ II Reverse Transcriptase – Life techonologies) using random hexamers as primers.

Procedure:

1. The appropriate volume for 1 µg of RNA was collected from the RNA extracts and mixed with RNAase-free H_2O up toafinal volume of 9.2 µl
2. RNA was denatured at 70^oC for 5 min and immediately chilled on ice for 10 min
3. The mixture was used as a template for cDNA synthesis
4. 10.8 µl of the following mastermix were added
5. Synthesized cDNA was dissolved in 30 µl RNAase free H_2O

Table 1:*Reagents and volumes used for cDNA synthesis.*

Reagents	**Volume per reaction (µl)**
5X First-Strand Buffer	4
$MgCl_2$ 50mM	0.8
DTT O.1M	2
RNase OUT	0.5
Random hexamer Primers 500Mm	1
dNTPs 10Mm	2
SuperScript II Reverse Transcriptase	0.5

Table 2:*Thermocycler conditions for cDNA synthesis.*

Temperature	**Time**
20^oC	10 min
42^oC	45 min
99^oC	3 min

4.4.1 Assessment of cDNA quality

In order to excludethe possibility of RNA amplification failure, which could lead tofalse negative results, we used as control the retinoic acid receptor a gene (*RARA*), which encodes one of the receptors for retinoic acid. *RARA* cDNA was amplified by PCR using specific primers (RAR6: 5' GGTGCCTCCCTACGCCTTCT 3', RAR8: 5' GGCGCTGACCCCATAGTGGT 3').

Procedure:

1. Preparation of the Mastermix according to **Table 3**

Table 3: *Reagents and volumes ofthe mastermix for PCR amplification of the RARA control gene sequences.*

Reagents	**Volume per reaction (µl)**
cDNA	2
Buffer 10x	2.5
MgCl2	1
dNTPs 10mM	0.5
Primer RAR6	0.75
Primer RAR8	0.75
Taq Polymerase	0.1
H2O	17.5
Final volume	25

2. Transfer 23 µl of the Mastermix to eppendorf tubes
3. Add 2 µl of each cDNA to eppendorf tubes
4. Procced to the PCR according to the cycling conditions on **Table 4**

***Table 4**: Cycling conditions of the PCR*

Temperature	Time	
94°C	5 min	
94°C	1 min	40
53°C	1 min	
72°C	1 min	
72°C	10 min	
18 °C	∞	

5. Gel electrophoresis of PCR products in order to check if the PCR reaction was successful

cDNA samples were also checked for the presence of contamination by genomic DNA by PCR amplification using primers specifically binding to an intron of the β-actin gene. As a positive control, total extracted genomic DNA from Blymphocytes wasused. Samples with a positive PCR product were considered as genomic DNA-contaminated and excluded from qPCR amplification.

Procedure:

1. Preparation of the Mastermix according to **Table 5**

***Table 5:** Reagents and volumes ofthe mastermix for PCR amplification of β-actin gene sequences.*

Reagents	Volume per reaction (µl)
cDNA	3
Buffer 10x	2.5
MgCl2	1.25
dNTPs 10mM	0.75
Primer A2	1.5
Primer A10	1.5
Taq Polymerase	0.1
H2O	14.4
Final volume	25

2. Transfer 22 µl of the Mastermix to eppendorf tubes
3. Add 3 µl of each cDNA to eppendorf tubes
4. Procced to the PCR according to the cycling conditions on **Table 6**

***Table 6**: Cycling conditions of the PCR*

Temperature	**Time**	
94°C	5 min	
94°C	1 min	39 cycles
55°C	1,5 min	
72°C	2 min	
72°C	4 min	
4 °C	∞	

5. Gel electrophoresis of PCR products in order to check if the PCR reaction was successful

4.4.2 Quantification of *EZH2* mRNA levels with RT-qPCR

EZH2 mRNA levels were determinedby real-time quantitative PCR, with commercially available primers for both the *EZH2* and*ABL* genes,the latter used as a housekeeping control (endogenous control) for expression normalization(RT² qPCR Primer Assay, SABiosciences, USA). Samples were measured in triplicate in the automated Real-Time Detector Biorad Chromo4. TheMaxima SYBR Green/Fluorescein qPCR Master Mix (2X) (Thermo Fisher Scientific, USA) was used for amplification.The SYBRGreen dye has the ability to bind to monoclonal or double-stranded DNA and levels of gene expression are detectedby fluorescence. Data analysis was performed using the ΔΔCt algorithm.

Table 7: *Reagents and volumes of Mastermix for theRT-qPCR*

Reagents	**Volume per reaction (μl)**
cDNA	2.5
SYBRGreen MasterMix	12.5
Primer Mix	1
H2O	9
Final volume	25

Table 8*: Cycling conditions of the RT-qPCR*

Temperature	**Time**	
95°C	10 min	
95°C	15 sec	40 cycles
55°C	30 sec	
72°C	30 sec	
72°C	2 min	
95°C	1 min	
65°C	2 min	
Multing curve		
15°C	∞	

4.4.3 Data analysis with the ΔΔCt method

The ΔΔCt method demonstrates how to calculate the relative gene expression by comparing expression between two different data sets. The algorithm uses as initial data the Ct value, which is the point where the product of the reaction passes into the exponential amplification phase.The initial step in the analysis concerns the normalization of the results using housekeeping genes, according to the formula:

$$\Delta Ct = Ct^{AVG\ EZH2} - Ct^{AVG\ ABL}$$

where AVG EZH2 is the average number of Ct values of the three reactions for the gene of interest, *EZH2*, of each case and AVG is the average number of Ct values of the three reactions for the reference gene, ABL, of each case.
Finally, the difference in expression (fold-change) is calculated by the formula:

$$\textbf{Fold change} = 2^{-\Delta\Delta Ct}$$

4.5 Protein expression analysis

4.5.1 Total protein extraction

Cells from each patientat the basal level as well as treated and untreated cultured cells were lysed and total protein extracted using RIPA buffer (Thermo Scientific) and Pierce proteinase and phosphatase inhibitors (Thermo Scientific).

Procedure:

1. Dilute pellet in proper amount (20µl/1x10^6 cells) of Lysis buffer
2. Incubate for 15 min
3. Centrifuge for 15 min at 4°C, at 14000 rpm
4. Transfer supernatant into cold eppendorf tubes
5. Store protein extracts at -20°C (or at -80°C for longer periods of time)

4.5.2 Quantification of protein extracts

Protein quantification was performed using the Pierce BCA Protein Assay kit, (Thermo Scientific), following the manufacturer's instructions. This assay is a detergent-compatible formulation based on bicinchoninic acid (BCA) for the colorimetric detection and quantitation of total protein. The purple-colored reaction product of this assay is formed by the chelation of two molecules of BCA with one cuprous ion. This water-soluble complex exhibits a strong absorbance at 562nm that is nearly linear with increasing protein concentrations over a broad working range (20-2000µg/ml). Protein concentrations are reported with reference to standards of the common protein bovine serum albumin (BSA) and determined through Elisa Reader (ELx800 from BIO-TEK Instruments Inc.).

4.5.3 Western Blotting

Protein blotting, the transfer of proteins to a membrane support, is a technique for the visualization and identification of proteins. When bound to membranes, proteins are readily accessible for immunological analyses, quantitative staining, or demonstration of protein-protein or protein-ligand interactions. The overall procedure involves two phases: protein transfer to a membrane and detection of the membrane-immobilized protein. It uses gel electrophoresis to separate denatured (linear) proteins by the length of the polypeptide (molecular weight). The proteins are then transferred to a membrane (PVDF membrane), where they are stained with antibodies specific to the target protein.

4.5.3.1 SDS-polyacrylamide gel electrophoresis (SDS-PAGE)

Sample preparation

Use **Table 9** as a guide to prepare a set of protein samples. The final protein concentration used was 10 µg.

***Table 9**: Reagents and volumes for each gel depending on the number of wells*

Reagent	**Volume**
NuPAGE LDS sample buffer	¼ of the final volume
NuPAGE reducing	1/10 of the final volume
Protein extract	10 µg

1. Mix samples gently and incubate for 10 min at 70° C
2. Place samples on ice

Procedure:

1. Preparation of running buffer NuPAGE MOPS (1x), total volume TV= 800 ml
2. Set up the electrophoresis system, Invitrogen XCell SureLock (Invitrogen, Paisley, UK) following the manufacturer's instructions
3. Place running buffer in the inner and outer chamber of the device
4. Load the samples carefully in each well of the NuPAGE 10% Bis-Tris Gel (Invitrogen, Paisley, UK)

5. Load 2 ladders (*Seeblue Plus2 Pre-stained standard and MagicMark™ XP Western Protein Standard,ThermoFisher Scientific)
6. Setup system and apply 180 volt for 1 h and 10 min

* The SeeBlue Plus2 Pre-Stained Standard allows to easily visualize protein molecular weight ranges during electrophoresis and quickly evaluate Western transfer efficiency. The MagicMark™ XP Western Protein Standard can then be visualized either using appropriate substrates for enzyme-labeled antibodies or via fluorescent dye-labeled antibodies or is thus used for the detection of the protein of interest.

4.5.3.2 Electrophoretic transfer of proteins to PVDF membrane (Semi-dry system)

The transfer step involves moving the proteins from a gel onto a synthetic membrane support (blot). The proteins are immobilized on the membrane with non-covalent bonds and the transfer to membranes is conducted via electrophoretic transfer. Inelectrophoretic transfer an electric field is used to elute proteins from gel and transfer them to membrane (e.g. PVDF).

The term semi-dry refers to the limited amount of buffer that is confined to the 2 stacks of filter paper. Gel and membrane are sandwiched between buffer wetted filter papers that are in direct contact with flat-plate electrodes (**Figure 23**). In this kind of system the distance between the electrodes is limited only by the thickness of the gel and the membrane sandwich. As a result, high electric field strengths and high-intensity blotting conditions are achieved.

***Figure 12**: The semi-dry system. Gel and membrane are sandwiched between buffer wetted filter papers that are in direct contact with flat-plate electrodes.*

Procedure:

Prepare Transfer buffer (1x) as described at **Table 10.**

***Table 10**: Reagents and volumes for the Transfer Buffer (1Lt)*

Reagent	**Volume**
NuPAGE Transfer Buffer 20x	50 ml
Methanol	100 ml
dH_2O	Until TV=1000 ml

1. Incubation of Polyvinylidene Difluoride (PVDF, 0.45 μm pore size, Invitrogen, Paisley, UK) transfer membrane in cold methanol for 5 min
2. Ingrain all 2 whatman papers, 6 sponges, PVDF membrane and the gel with Transfer buffer 1x
3. Prepare thestack according to **Figure 12**
4. Setup the electrophoresis system,and place Transfer buffer only in the inner chamber (semi-dry transfer)
5. Setup system and apply 40 volts for 2 hrs(running NuPAGE blot programme)
6. After the transfer has been completed, wash PVDF membrane with PBS 1x-Tween 0.1% (PBS-T) for 5 min x 3 by shaking

4.5.3.3 Blocking

Blocking of non-specific binding of the antibodies used for detection of the target protein is achieved by placing the membrane in a dilute solution of protein non-fat dry milk. The protein in the dilute solution attaches to the membrane in all places where the target proteins have not attached. Thus, when the antibody is added, there is no room on the membrane for it to attach other than on the binding sites of the specific target protein. This

reduces "noise" in the final product of the western blot, leading to clearer results while also eliminating false positives.

Procedure:

1. Block membrane for 30-45 min shaking (slowly) in non-fat milk 2,5%/PBS-T at RT
2. Wash membrane with PBS-T 3 x 5min by shaking

4.5.3.4 Immunoblotting

Place the membrane in, either BSA 0,1%/PBS-T or non-fat milk 2,5%/PBS-T with the anti-protein antibody in a specific dilution after optimization of dilution mean, concentration and exposure time (**Table 11**).

***Table 11**: Dilution of primary monoclonal antibodies (mabs), molecular weights, concentrations and exposure times*

mabs	Concentration	Exprosure time	kDa	Provider
EZH2	1/200 2.5% milk	30 min	80	BD Biosciences
p-PLCγ2	1/500 2.5% milk	15 min	150	Cell Signaling Technology
b-actin HRP conjucated	1/30.000 2.5% milk	1 min	40	Sigma-Aldrich
H3K27me3	1/5000 0.1% BSA	10 min	~15-17	Millipore
H3	1/10.000 2.5% milk	10 min	~15-17	Abcam

1. Incubate the membrane "overnight" at 4 ^{o}C or for 2 hrs at RT shaking
2. Wash membrane with PBS-T x 3
3. Incubate membrane with goat anti-mouse or anti-rabbit IgG conjugated with horseradish peroxidase (HRP) for 2 hrs, at RT shaking (**Table 12**)
4. Wash membrane with PBS-T x 3

***Table 12**: Dilution of secondary antibodies (mabs), molecular weights, concentrations and exposure times*

mabs	Concentration	Provider
Anti-mouse IgG HRP conjugated	1/1250 5% milk	R&D systems
Anti-rabbit IgG HRP conjugated	1/1250 5% milk	R&D systems

4.5.3.5 Immunodetection

For the immunodetection of proteins, Scientific SuperSignal Chemiluminescent Substrate (ThermoFisher Scientific) was used, which is enhanced chemiluminescent (ECL) HRP substrate for detection. The images were visualized in GeneGnome from Syngene Bio Imaging by using GeneSnap.

4.5.4 Measurement of protein signals

For each sample, β-actin was used for the normalization of EZH2 and p-PLCγ2 protein expression and total H3 for the normalization of the H3K27me3 levels. Ratios of each protein band intensity relative to the respective housekeeping gene band intensity were calculated for each sample using the Image J software as described on:
http://lukemiller.org/index.php/2010/11/analyzing-gels-and-western-blots- with-image-j/

4.6 Stimulation of CLL cells in liquid cultures

Purified $CD19^+$ B cells were cultured in RPMI medium supplemented with 10% fetal calf serum, and 15 ug/ml gentamicin (RPMI complete) in 24- or 48-well plates in the presence (Stimulated) or absence (Control) of specific ligands. The ligands used were: goat F(ab') anti-human IgM 20 (mg/ml) (ThermoFisher Scientific) for BcR; CD40L (100ng/ml) plus enhancer (1ug/ml) for improved stability and enhanced immune activation (Alexis Biochemicals) for CD40; and, CpG oligonucleotides (2.5 mg/ml) (ODN2006, stimulatory CpG-ODN type B, human specific; Invivogen) for TLR9. Cell cultures were maintained at 37°C in a humidified atmosphere containing 5% CO_2 for certain time points.

Procedure:

1. Dilute $CD19^+$ cells in RPMI complete (at a concentration of $3x10^6$ cells/ml)
2. Set proper amount of diluted sample in the well plate
3. Pipette appropriate volume of ligand in each well

Cells remained in culture for: (i) 10 min with anti-IgM for the determination of p-PLCγ2 levels, (ii) 12h, 48h with anti-IgM for the kinetics analysis of EZH2 mRNA levels (iii) 3h, 6h, 12h, 24h with CpG/CD40L/enhancer for the kinetics analysis of EZH2 mRNA levels, (iv) 12h with CpG and/or CD40L/enhancer for assessing EZH2 mRNA levels, (v) 24hwith CpG and/or CD40L/enhancer for assessing EZH2 protein levels and (vi) 3 days with CpG for assessing viability and H3K27me3 levels.

4.7 Treatment of CLL cells with signaling and EZH2 pharmacologic inhibitors

Purified $CD19^+$ B cells were cultured as described above in the presence of EZH2 inhibitors, GSK126, GSK343 or signaling inhibitors Ibrutinib (IB) and Idelalisib (IDE) (Sellechem). In more detail, cells were treated with DMSO or increasing concentrations of IB or GSK126 for 3 and 6 days.

For selected cases, cells were pre-stimulated as described above in the presence of CpG for 24 hrs and then exposed to either single treatment with EZH2 inhibitors (10 μM GSK343, 10 μM GSK126) or signaling inhibitors (5 μM IB, 10uM IDE), or combined inhibition with IB/GSK343 or IB/GSK126 or IDE/GSK343 and remained in culture for 3 days.

4.7.1 Harvesting

After different time points cells were harvested and prepared for the next procedures.

Procedure:

1. Pipette gently and transfer all the amount of liquid culture in a collection tube
2. Centrifuge for 5 min at 4^{o}C, at 5000 rpm
3. Discard supernatant
4. Wash enriched cells with 1ml DPBS 1X
5. Repeat step 2-4
6. Discard carefully all DPBS
7. Prepare cells for the next procedure

4.8 Transfection with EZH2-specific small interfering RNAs

Purified $CD19^+$ B cells from 3 CLL cases with high EZH2 mRNA levels as determined by RT-qPCR were transfected with 70nM of 5 FlexiTube siRNAswith different sequences directed against human EZH2 (Qiagen), using the Amaxa Human B Cell Nucleofector Kit (Lonza).The $CD19^+$ B cells of each case were also transfected with the appropriate negative control (40 nM, AllStars Negative Control siRNA; Qiagen). Transfections were performed using the Amaxa Nucleofector device with the U-015 program (Lonza). Transfection efficiency was measured with the Block-iT Alexa Fluor Red Fluorescent Oligo (Invitrogen). CLL cells were

collected and processed for immunoblotting and apoptosis analysis with flow cytometry at indicated time points.

Procedure:

1. Prewarm appropriate volume of culture media (RPMI complete) to 37^{o}C
2. Defreeze cells at 37^{o}C
3. Transfer cells in 10ml warm medium
4. Centrifuge for 5 min at 2000 rpm
5. Discard supernatant
6. Count the number of cells and determine cell density
7. Centrifuge the required number of cells 5 x 10^6 cells per sample
8. Add medium to a final concentration 3 x 10^6 cells/ml
9. Incubate at 37^{o}C for 1 hr
10. Prepare 24-well plates by filling them with 2 ml of supplemented culture media and pre-incubate/equilibrate plates in a humidified 37^{o}C/5% CO_2 incubator for 1 hr
11. Centrifuge for 5 min at 2000 rpm
12. Discard supernatant
13. Resuspend the cell pellet carefully in 100µl of Human B Cell Nucleofector solution (RT) per sample
14. Add in new eppendorfs the appropriate concentration of siRNA for each sample
15. Add 100 µl of cell suspension each time
16. Transfer cell/siRNA suspension into certified cuvette (sample must cover the bottom of the cuvette without air bubbles)
17. Close the cuvette with the cap
18. Select the appropriate Nucleofector Program for B cells (U-015) for Nucleofector Device
19. Insert the cuvette with cell/siRNA suspension into the Nucleofector cuvette

4.9 Flow Cytometry studies

For all experiments data was acquired on a BD FACSCalibur flow cytometer (BD Bioscience, San Jose, CA). Data analysis was performed using the Flow Jo Kaluza Analysis Software (Tree Star, Ashland, OR).

4.9.1 Determination of CLL cell viability

Cells were collected, washed and stained, for apoptosis markers using the Annexin V-FITC Apoptosis Detection kit (Immunostep) by double staining with fluorescein isothiocyanate–conjugated Annexin V and propidium iodide, according to the manufacturer's instructions.

Procedure:

1. Harvest 1 x 10^6 cells after the desired method for the apoptosis induction and wash them twice with DPBS 1X
2. Resuspend cells in 1X Annexin-binding buffer
3. Add 5 µl of Annexin V-FITC and 5 µl PI to each 100 µl of the solution
4. Gently vortex the cells and incubate for 15 min at RT in the dark
5. Add 400 µl of 1X Annexin-binding buffer to each tube
6. Analyze by flow cytometry within 1 hr

For the determination of cell viability with flow cytometry, staining with 7-Aminoactinomycin D (7-AAD) was also used. 7-AAD stains the non-viable cells and is a membrane impermeant dye that is generally excluded from viable cells. It binds to double stranded DNA by intercalating between base pairs in GC-rich regions.

Procedure:

1. Wash 1 x 10^6 cells with DPBS 1X
2. Add 0.5ml DPBS 1X to the cells
3. Add 5 µl 7-AAD
4. Cells are resuspended in the mixture by vortex
5. Analyze by flow cytometer or procced to another protocol assay

In some cases, cell viability was also assessed through flow cytometric assays Fixable Viability Stain 660 (FVS 660) (BD Biosciences). The FVS 660 dye is useful for discriminating viable from non-viable cells. This dye reacts with and covalently binds to cell-surface and intracellular amines. Permeable plasma cell membranes, such as those present in necrotic cells, allow for the intracellular diffusion of the dye and covalent binding to higher overall concentrations of amines than in non-permeable live cells. Therefore, necrotic cells are labeled with 10-20 fold higher intensity fluorescence compared to viable cells. The labeled cells can be fixed with formaldehyde and subsequently permeabilized in order to proceed to intracellular staining for the desired target.

For FVS 660 staining

Procedure:

1. 1 ml of 1/4000 diluted FVS 660 dye in DPBS 1X is added to 1 x 10^6 cells
2. Cells are resuspended in the mixture by vortex
3. Incubation for 10 min in the dark
4. Centrifuge for 5 min at 2000 rpm
5. Discard supernatant
6. Analyze by flow cytometer or procced to another protocol assay for flow cytometry

4.9.2 Determination of intracellular calcium flux

To test the functionality of BcR signaling, we analyzed calcium mobilization after BcR engagement *in vitro* with flow cytometry using the fluorogenic probe Fluo-3 AM (Invitrogen). Cases that were able to increase intracellular Ca^{2+} upon BcR cross-linking with anti-IgM were classified as responders (calcium fluxes >5% cutoff for positivity).

Intracellular calcium flux was measured by using the fluorogenic probe Fluo-3 AM (Invitrogen).

Procedure:

1. 10^7 cells/mLwere incubated with 4μM Fluo3-AM and 0.02% (v/v) of Pluronic F-127 (Sigma-Aldrich) for 30 min at 37°C
2. Wash cells and resuspend at 5 x 10^6 cells/mL at RT

3. Cells (250 ul) were warmed to 37°C for 5 min before the acquisition of background fluorescence (ie, of unstimulated cells), followed by addition of anti-IgM and data acquisition for a further 5 min

4.9.3 Determination of cell viability and H3K27me3 levels

For concomitant analysis of H3K27me3 levels and viability by flow cytometry, cells were stained withthe conjugated antibodies, Alexa Fluor® 488 Rabbit H3K27me3 and Alexa Fluor®488 Rabbit IgG XP® Isotype Control (Cell Signaling) and FVS 660.

Procedure:

1. Wash cells with DPBS X1
2. Staining with FVS 660 (as described above)
3. Wash cells with DPBS X1
4. Fix cells with formaldehyde of a final concentration of 4%, for 10 min at 37^{o}C
5. Incubation on ice for one minute
6. Wash cells with DPBS X1
7. Add methanol and incubate on ice for 30 min
8. Wash cells twicewith incubation buffer containing 0.5% BSA in DPBS
9. Add 10 µl of each antibody (Alexa Fluor® 488 Rabbit H3K27me3 and Alexa Fluor®488 Rabbit IgG XP® Isotype Control) and incubate in RT for 1h
10. Wash cells with incubation buffer
11. Add 0.5ml DPBS 1X into each tube
12. Analyze samplesby flow cytometer

4.10 Ex vivo studies in Tcl1 leukemic cells

Eμ-TCL1 transgenic mice were kindly provided by Dr. J. Byrd (Ohio State University, Columbus, OH) on a C3H/B6 background and back-crossed for >10 generations to C57BL/6 mice were supplied by Charles River Laboratories. Mice were maintained in a specific pathogen-free animal facility and treated in accordance with European Union and approval of the San Raffaele Scientific Institute Institutional Ethical Committee.

Peripheral blood (PB) of Eμ-TCL1 transgenic mice was collected monthly from the submandibular vein and checked for the presence of leukemic cells. Mice were sacrificed when the percentage of $CD5^+/CD19^+$ double positive population reached 90% of total cells in the PB and the spleen was collected.

4.10.1 Purification of *Tcl1* leukemias and normal B cells

After the lysis of erythrocytes, the single-cell suspension obtained from the spleen of *Tcl1* mice was analyzed by flow cytometry for the purity of $CD5^+/CD19^+$or cryopreserved for the *ex vivo* experiments.

Cells were measured on a CANTO (BD Pharmingen) flow cytometer and data were analyzed using FCS Express 6 Flow Cytometry (De Novo Software). *Tcl1* leukemia cells were usually not purified, because they represented more than 90% of the splenocytes of leukemic animal and only *Tcl1* cells with >90% purity were used for the experiments.

Normal B cells were isolated from single-cell suspensions of splenocytes of WT mice by negative selection with the EasySep™ Mouse B Cell Isolation Kit (Stemcell technologies) according to the manufacturer's instructions. The purity of B cells was > 95% for $CD19^+$ cells as revealed by flow cytometry.

4.10.2 Determination of proliferation by measuring Ki-67 expression in Tcl1 leukemias

Ki-67 expression was assessed byflow-cytometry in order to determine the percentages of proliferating splenic B cells from *Tcl1* mice. For this assay, we used the FITC Mouse Anti-Human Ki-67 Set (BD Biosciences), following the manufacturer's instructions. In case of parallel assessment of cell viability, the FVS 660 staining procedure was applied first followed by the protocol below.

Procedure:

1. Cells were washed with 1ml DPBS X1
2. Fix cells with 70% ethanol overnight at -20^{o}C
3. Wash cells twice with PBS containing 1% FBS
4. Split each sample in two FACS tubes (control & Ki67)
5. Transfer 100 μl cell suspension into each fresh tube

6. Add 10 µl of each antibody (FITC Mouse Anti-Human Ki-67 and FITC Mouse Isotypic control) into the respective tubes above and mix gently
7. Incubate the tubes at RT for 30 min in the dark
8. Wash with PBS containing 1% FBS
9. Add 0.5 ml of PBS containing 1% FBS into each tube
10. Analyze samples by flow cytometer

4.10.3 Treatment of Tcl1 leukemias with EZH2 inhibitors and/or Ibrutinib

EZH2 inhibitors, GSK343 (10 µM) and GSK126 (10 µM), and/ or Ibrutinib (5 µM) were applied to *Tcl1* splenic B cells cultured *ex vivo* in a concentration of 10 x 10^6 cells with RPMI 1640 supplemented with 10% FBS, 100 U/mL penicillin, 0.1 mg/mL streptomycin, 2mM L-glutamine, and 1mM sodium pyruvate (Invitrogen). Cell viability and/or Ki-67 expression were analyzed after 1-2 days in culture by flow cytometry.

4.11 Statistical analysis

Descriptive statistics for quantitative variables included statistical measures like mean and SD. Significance of bivariate relationships between factors and variables normally distributed was assessed with the use of Student's t-test. In cases where the underlying distribution was not normal, the Mann-Whitney test was performed. Correlation analysis was performed using the Spearman correlation coefficient.

Classification of CLL cases into $EZH2^{high}$ and $EZH2^{low}$ subgroups based on EZH2 mRNA relative expression (2^-ΔCt) was determined by ROC curve analysis. U-CLL cases were used as control group and the cut-off value was chosen in order to ensure high specificity and sensitivity. This threshold was set at 1.087 and confirmed by applying the Youden Index test. This threshold led to U-CLL cases being assigned into the $EZH2^{low}$ group, and M-CLL cases into the $EZH2^{high}$ group, respectively. For all comparisons, a significance level of $p < 0.05$ was set.

All statistical analyses were performed with the use of the GraphPad Prism 5 software (La Jolla).

5 Study group

Blood samples were collected from patients with CLL monitored at the Hematology Department and HCT Unit of the G. Papanikolaou Hospital, Thessaloniki, Greece; and the Onco-Hematology Department of the San Raffaele Hospital, Milan, Italy. Patients provided informed consent for the collection of blood samples, according to all recommended national and international ethical and legal frames. The study was approved by the local ethics review committee of the participating institutions. Basic demographic, clinical and biological data for the patient cohort are given in **Table 13**. Further details about the experiment design for the patient cohort are given in **Table 14**.

Table 13: Overview of the analyzed CLL cohort.

Parameter	Number of cases
Gender	
Male	124
Female	65
IGHV gene somatic hypermutation status	
Mutated	90
Unmutated	95
ND	4
Binet stage at diagnosis	
A	150
B	27
C	8
Not available	4
CD38 expression	
Positive	43
Negative	126
Not determined	20

Table 14: Number of cases in each type of analysis.

Analysis	Number of cases
EZH2 mRNA expression	131
EZH2 protein expression	45
Transfection with siRNAs for EZH2	3
Responsive to BcR stimulation	10
Unresponsive to BcR stimulation	3
BcR stimulation for EZH2 mRNA levels	10
TLR9 or CD40 stimulation for EZH2 mRNA levels	6
TLR9/CD40 stimulation for EZH2 mRNA levels	6
TLR9 and/or CD40 stim for EZH2 protein expression	6
Viability after TLR9 stimulation	6
H3K27me3 after TLR9 stimulation	6
In vivo Ibrutinib studies	9
Ibrutinib treatment in EZH2 high/low cases	13
GSK343	6
EPZ6438	6
GSK126	8
IB/GSK343	12
IB/GSK126	10
IDE/GSK343	8
GSK126 treatment in relapse cases	6
GSK343 treatment in relapse cases	5
Resistance to Ibrutinib	3
Resistance to Idelalisib	3

6 Results

6.1 EZH2 overexpression is linked with clinical aggressiveness in CLL

EZH2 overexpression has been reported in many types of cancer and associated with poor prognosis. A recent study from our group implicated for the first time EZH2 in the pathophysiology of CLL. In more detail, we found that EZH2 was highly expressed in a subgroup of patients (subset #1), characterized by a stereotyped BcR with unmutated immunoglobulin heavy variable genes (U-CLL) and an aggressive disease course. Here we investigated the expression and functionality of EZH2 in CLL at both mRNA and protein levels and how it is linked to disease progression.

6.1.1 EZH2 gene expression in CLL

We analyzed *EZH2* mRNA expression by RT-qPCR in a cohort of 131 CLL cases of whom 75 (57.3%) and 56 (42.7%) concerned M-CLL and U-CLL, respectively.U-CLL cases were found to express significantly higher EZH2 mRNA levels compared to M-CLL cases (fold difference, FD>2, p<0.0001) (**Figure 13**).

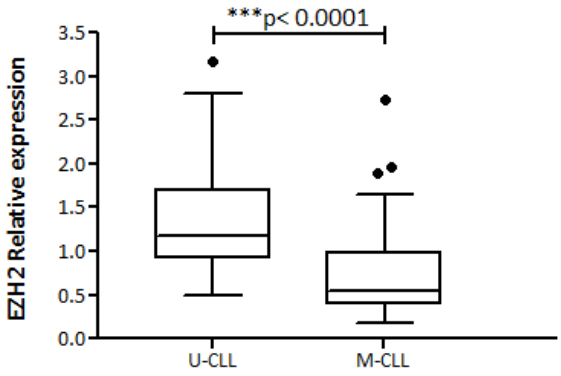

Figure 13: EZH2 mRNA is overexpressed in U-CLL. *U-CLL cases (n=56) express higher EZH2 mRNA levels compared to M-CLL cases (n=75). The Tukey whisker plots show EZH2 relative expression. ***p<0.0001*

6.1.2 EZH2 overexpression is associated with disease progression in CLL

Analysis of serial samples obtained over a period spanning 2-7 years from 6 progressive U-CLL cases, revealed that *EZH2* mRNA levels significantly increased at disease progression (FD=1.6, $p<0.05$) and relapse (FD=2, $p<0.05$) compared to diagnosis, consistent with the notion that disease aggressiveness is correlated with high *EZH2* levels (**Figure 14A, B**). Similar results were also observed at the protein level (**Figure 14C**).

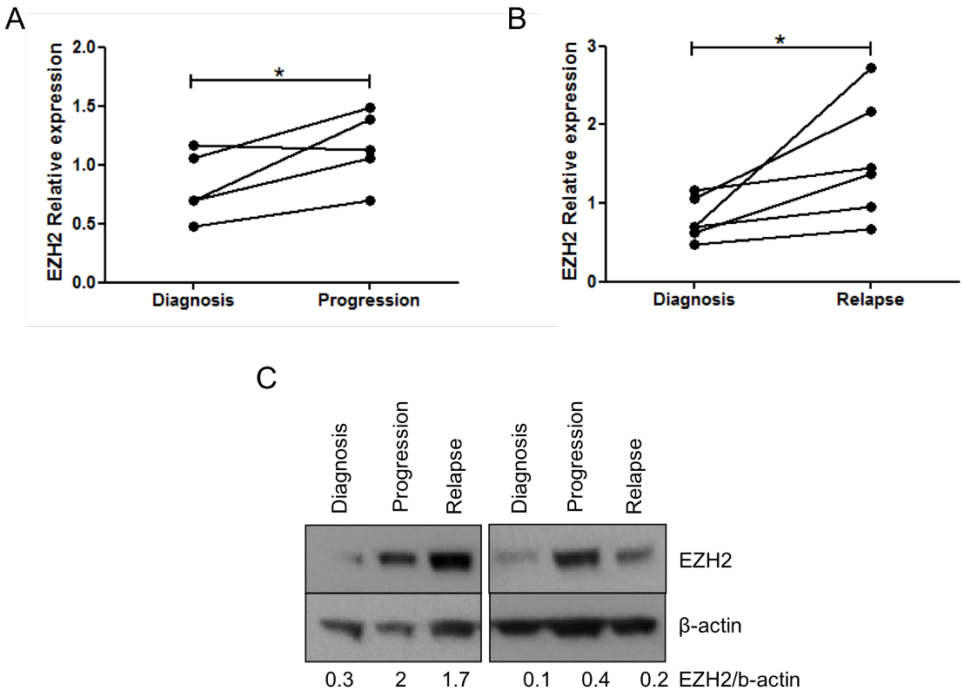

***Figure 14**: **EZH2 expression increases with disease progression**. Analysis of serial samples obtained over a period spanning 2-7 years. In the graph two connected points represent EZH2 relative expression at the two different time points **A**. diagnosis versus progression (n = 5) **B**. diagnosis vs relapse (n = 6) **C**. Western blotting analysis for EZH2 protein expression in serial samples obtained from 2 progressive U-CLL cases. The samples were obtained at diagnosis, at progression and at relapse. *p<0.05*

6.1.3 EZH2 protein expression in CLL

Next, we investigated EZH2 protein expression in U-CLL and M-CLL using western blotting and found significantly ($p<0.0001$) higher protein levels in U-CLL (n=20) versus M-CLL (n=25) (**Figure 15A, B**).

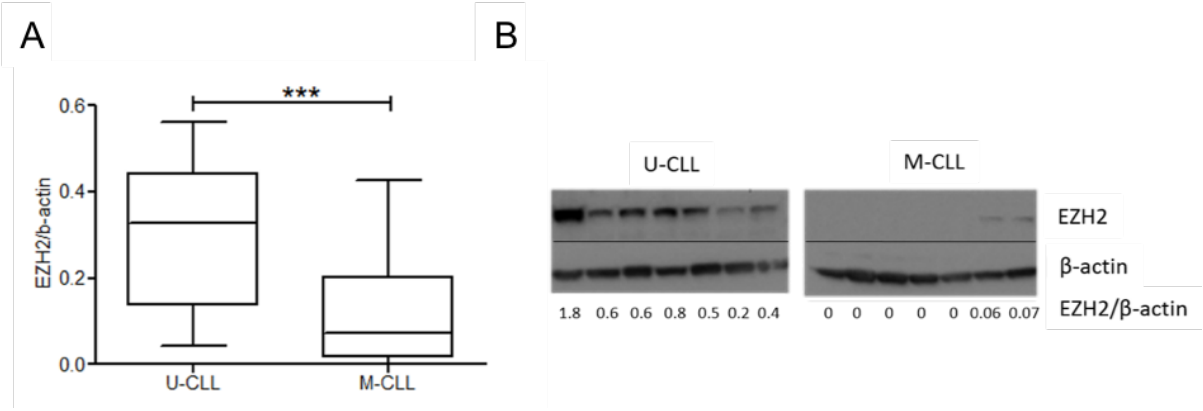

***Figure 15**: Significantly higher EZH2 protein levels in U-CLL versus M-CLL. **A**. The Tukey whisker plots show EZH2 protein levels normalized to ϐ-actin **B**. western blotting for EZH2 protein levels for 7 M-CLL and 7U-CLL representative cases. ***p < 0.0001.*

6.1.4 EZH2 mRNA and protein correlation in CLL

Statistical analysis revealed a significant ($r=0.4$, $p<0.005$) correlation between *EZH2* mRNA and protein levels (**Figure 16**).

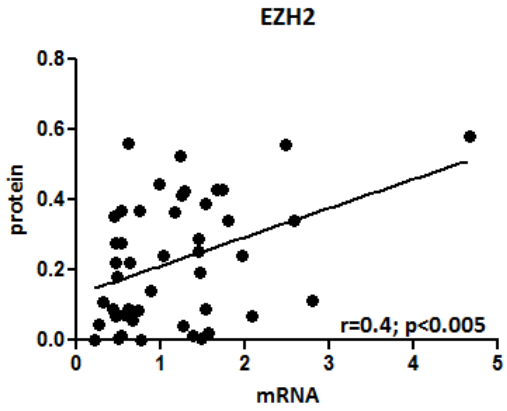

***Figure 16**: Correlation of EZH2 mRNA and protein levels. The x axis depicts EZH2 relative expression, while the y axis depicts EZH2 protein levels normalized to ϐ-actin.*

6.1.5 EZH2 expression induces H3K27me3 trimethylation and confers CLL cells a survival advantage

Despite the fact that U-CLL cases generally expressed higher EZH2 levels compared to M-CLL ones (**Figure 17**), outliers were noted, since occasional M-CLL cases showed high EZH2 expression levels. For this reason, in order to explore the functional impact of differential EZH2 expression in CLL, all CLL cases were classified into $EZH2^{high}$ and $EZH2^{low}$ subgroups based on EZH2 mRNA levelsusing ROC curve and Youden index statistical tests.

First, we assessed EZH2 functionality by measuring H3K27me3 using Western blotting in $EZH2^{high}$ (n=19) and $EZH2^{low}$(n=34)cases (**Figure 17A)**. We found that $EZH2^{high}$ cases displayed significantly higher H3K27me3 levels compared to $EZH2^{low}$ cases ($p<0.05$) (**Figure 17A, B**).

Next, in order to study the effect of EZH2 expression on CLL cell viability, we studied CLL cell apoptosis after 9 days in culture in 6 $EZH2^{high}$ and 9 $EZH2^{low}$ cases. We found that EZH2 levels correlated with cell viability, since cells from $EZH2^{high}$ cases displayed significantly higher viability ($p < 0.0001$) compared to $EZH2^{low}$ cases (**Figure 17C**).

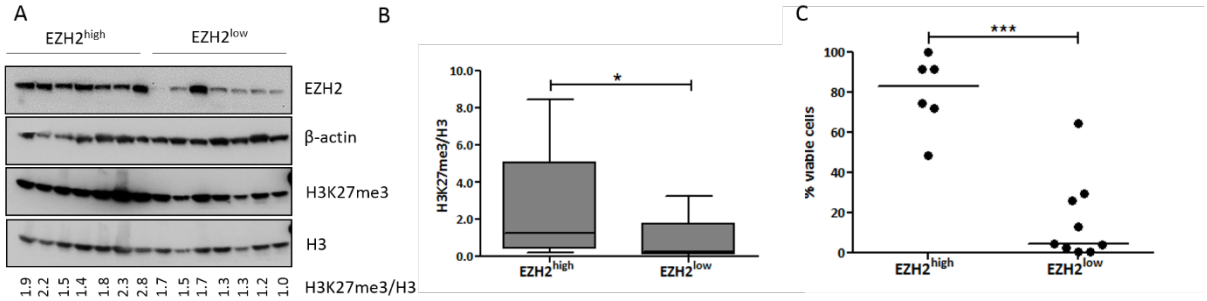

***Figure 17**: **EZH2 expression induces trimethylation of H3K27 in CLL cells**. Analysis of H3K27me3 using western blotting in **A.** 7 $EZH2^{high}$ and 7 $EZH2^{low}$ representative cases and **B.** all cases analyzed (19 $EZH2^{high}$ versus 34 $EZH2^{low}$ cases). The Tukey whisker plots depict the levels of H3K27me3 normalized to histone H3 levels. **C**. CLL cell viability analysis using annexin V/PI staining in $CD19^{+}$ CLL cells after 9 days in culture for 6 $EZH2^{high}$ and 9 $EZH2^{low}$ cases. The x axis shows the percentage of viable cells normalized to day 0. The black line corresponds to the median value. $*p < 0.05$, $***p < 0.0001$*

6.2 Impact of EZH2 silencing in CLL cells

Based on the above results implicating EZH2 as a pro-survival factor in CLL, we proceeded with exploring whether the difference in cell viability could be attributed to differential EZH2 levels by tampering with EZH2 expression in CLL cells from 3 $EZH2^{high}$ cases using EZH2-specific siRNAs. Cells were harvested at several time points (Days 5, 7 and 9) and significant downregulation of EZH2was documented using flow cytometry (**Figure 18**), followed by a more modest downregulation of H3K27me3 levels, determined by western blotting (**Figure 19**). Moreover, CLL cell viability was also reduced after treatment with EZH2-specific siRNAs compared to the control cells in all cases analyzed as assessed using flow cytometry (Annexin V/PI staining) (**Figure 20**).

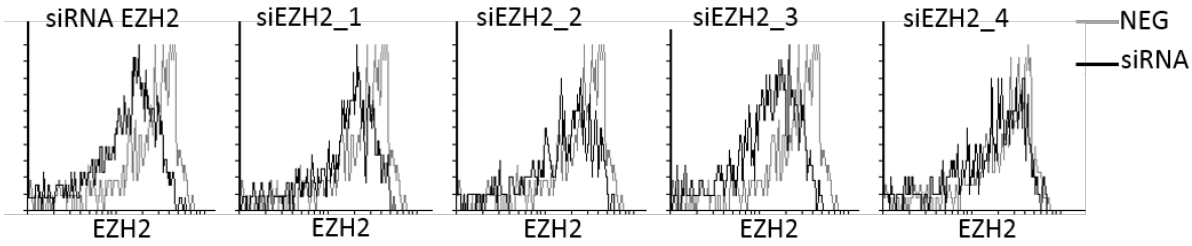

***Figure 18**: **EZH2 downregulation after treatment with specific siRNAs**. Levels of EZH2 expression (black lines), in one representative case, as measured by flow cytometry after transfection with the negative control (grey lines) or siRNAs against EZH2. siRNA-EZH2 refers to the initial siRNA used for all experiments. The other siRNAs represent the four clones that used for validation*

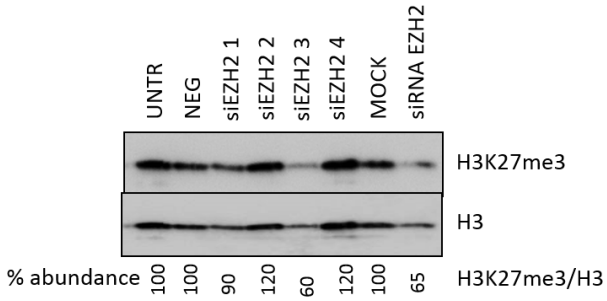

***Figure 19**: **Downregulation of trimethylation of H3K27 after treatment with EZH2-specific siRNAs**. H3K27me3 levels normalized to total H3 after EZH2 knock-down using different siRNAs in one representative case.*

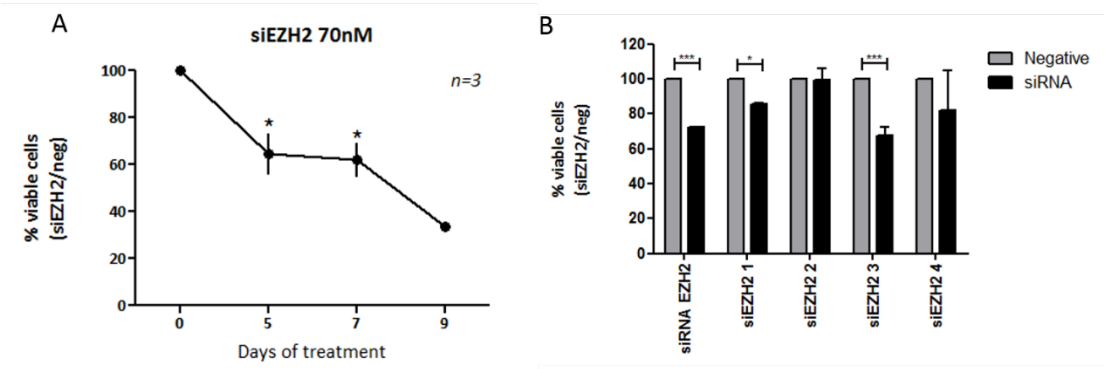

***Figure 20: EZH2 downregulation with siRNAs leads to apoptosis.A**. Cell viability analysis at different time points after treatment of primary cells from 3 cases with siRNA for EZH2. The x axis shows the percentage of viable cells normalized to the negative control. **B**. Cell viability analysis at day 5, after treatment of primary cells with all siRNAs used in the study for EZH2. The x axis shows the percentage of viable cells normalized to the negative control *p < 0.05, ***p < 0.0001.*

6.3 Pharmacological inhibition of EZH2 catalytic activity promotes CLL cell apoptosis

Prompted by these findings, we sought to obtain more supportive evidence for the anti-apoptotic role of EZH2 in CLL using two EZH2 pharmacological inhibitors, namely GSK343 and EPZ6438. First, in order to determine the effective concentrations of these inhibitors, we treated 5 $EZH2^{high}$ cases with different concentrations of GSK343 and EPZ6438, and measured CLL cell viabilityat different time points (Days 5, 7, 9, 13), which resulted in concentration-dependent reductions in CLL cell viability (**Figure 21A, B**). Moreover, in three $EZH2^{high}$ cases we treated cells with different concentrations of GSK343 and EPZ6438, which induced concentration-dependent reduction in global levels of H3K27m3 (**Figure 21C, D**).

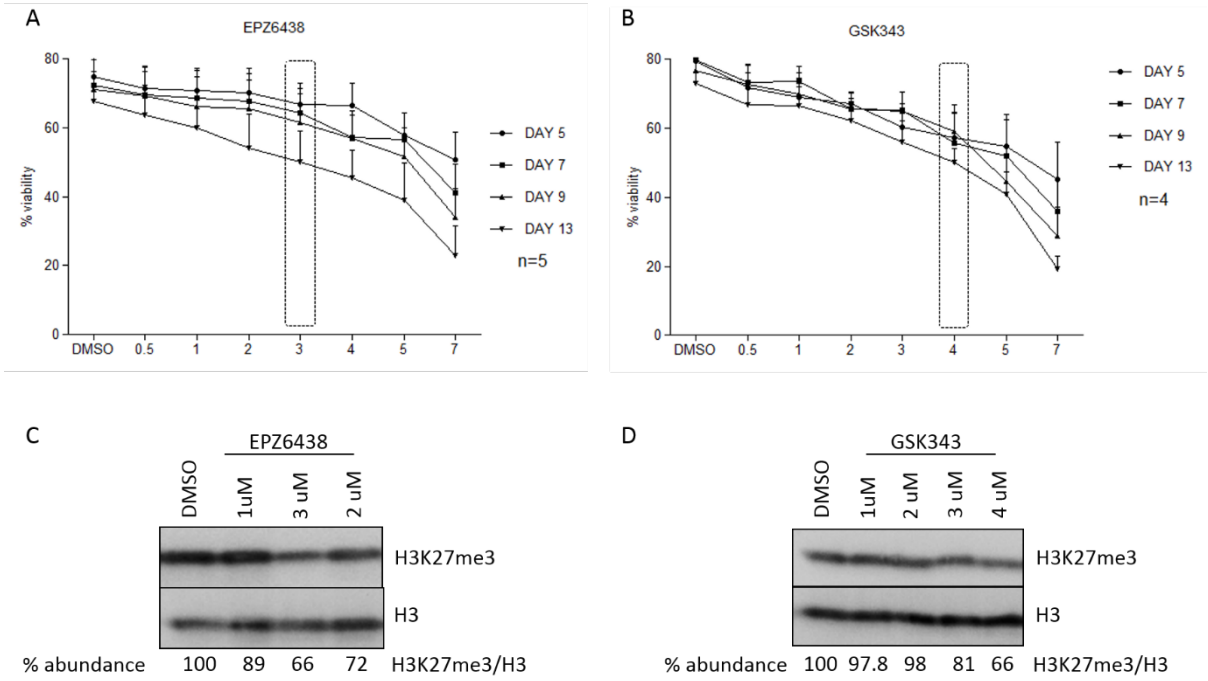

***Figure 21**: Mean percentage of cell viability of CLL cells from 5 cases treated with different concentrations of both **A.** EPZ6438 and **B.** GSK343 inhibitors, for different time points. Western blotting for H3K27me3 levels after inhibition with different concentrations of **C.** EPZ6438 and **D.** GSK343 for one representative case.*

Next, similar experiments were performed in order to determine the concentration that more effectively downregulates EZH2 activity, by usinganother EZH2 inhibitor, namely GSK126. To this end, we incubated $CD19^{+}$ cells from 3CLL cases with increasing concentrations of GSK126 (0.5, 1, 3, 5 and 10 μM)and measured CLL cell viability and H3K27me3 levels after 3 and 6 days in culture, which resulted in concentration-dependent reductions in both analyses (**Figure 22A, B**).

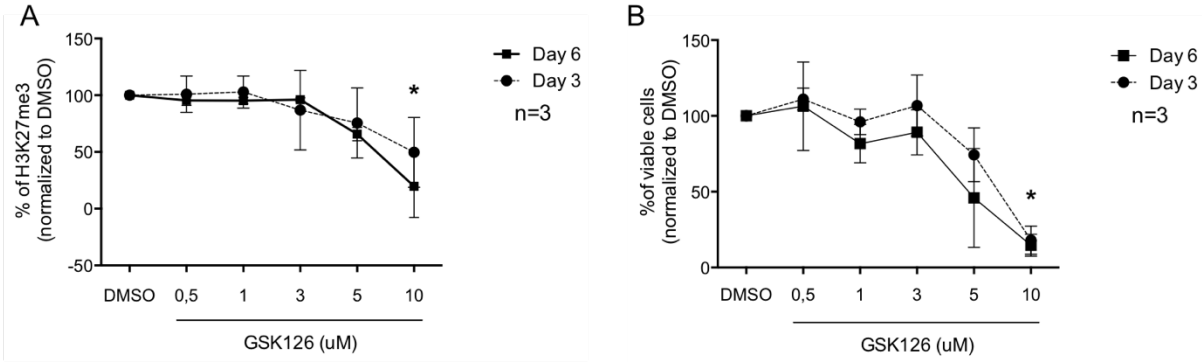

***Figure 22**: **Pharmacological inhibition of EZH2 catalytic activity with GSK126**. **A, B.** Mean percentage of H3K27me3 levels **A.** and cell viability **B.** of CLL cells from 3 cases treated with*

*increasing concentrations (0.5, 1, 3, 5 and 10μM) of the pharmacological inhibitor of EZH2, GSK126 or control cells (DMSO-treated), after 3 and 6 days in culture.*p < 0.05*

Based on this analysis, we chose the first concentration which reduced H3K27me3 levels and induced statistically significant difference in CLL cell viability. For EPZ6438, we chose 3 μM as the effective dose and treated 6 additional EZH2^{high} cases for a total of 10 days, documenting a time-dependent reduction of H3K27me3 levels starting from day 2 (**Figure 23A**). Similarly, treatment of the same cases with 4μM GSK343 induced reduction of H3K27me3 levels, albeit at later timepoints starting from day 6; **Figure 23B**).

***Figure 23**: **Pharmacological inhibition of EZH2 catalytic activity. A.** Western blotting analysis of H3K27me3 levels in one representative case after treatment with EPZ6438 for different time points. **B.** Western blotting analysis of H3K27me3 levels in one representative case after treatment with GSK343 for different time points.*

We also assessed the effects of these inhibitors on cell apoptosis after incubation of the same 6 EZH2^{high} cases with EPZ6438 (3 μM) and GSK343 (4μM) in different time points (0, 5, 7, 9 and 13 days) and found decreased cell viability after 5 days of exposure to either inhibitor compared to the control cells (DMSO-treated) (**Figure 24A, B**). Both inhibitors decreased CLL cell viability in a time-dependent manner, suggesting that the histone trimethylation catalytic activity of EZH2 is vital for CLL cell survival.

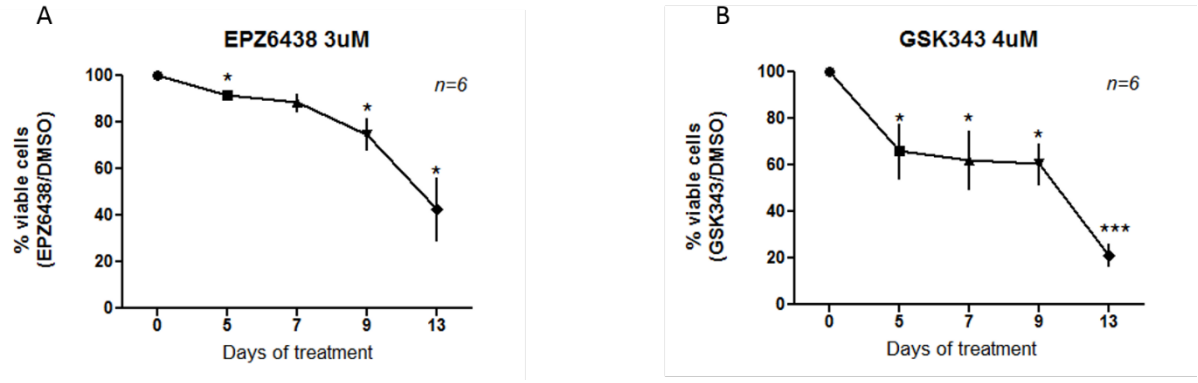

***Figure 24**: **Pharmacological inhibition of EZH2 catalytic activityA.** and **B.** Effects of incubation with EPZ6438 and GSK343 for 13 days on CLL cell viability as measured by annexin V/PI staining using flow cytometry. For both graphs, the x axis shows the percentage of viable cells normalized to control cells that were treated with DMSO. *p < 0.05, ***p < 0.0001.*

Applying the same treatment to 3 EZH2^{low} cases revealed that cell viability is more dependent on EZH2 function in EZH2^{high} vs EZH2^{low} cases (**Figure 25A, B**), since no time-dependent decrease in viability levels of CLL cells was observed in the latter group.

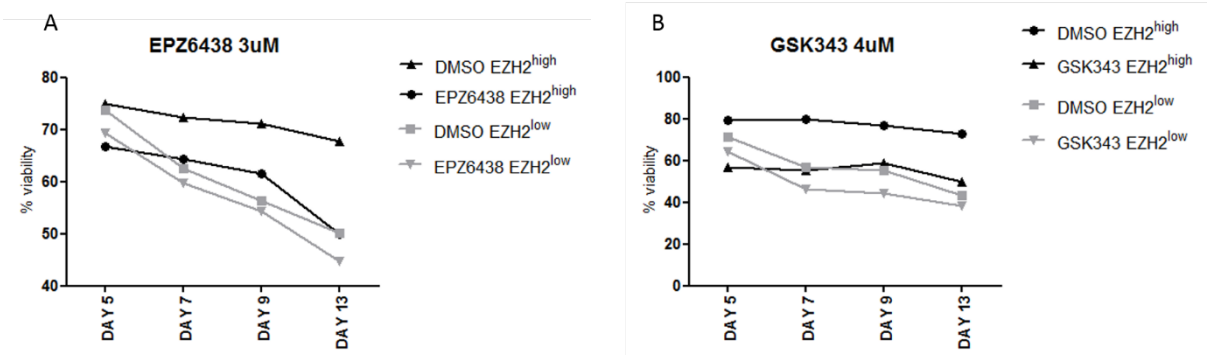

***Figure 25**: Mean percentage of viable cells in 5 EZH2^{high}(black lines) and 3 EZH2^{low} cases (grey lines). **A.** The cells were treated with either DMSO as control or with 3uM EPZ6438. **B.** The cells were treated with either DMSO as control or with 4uM GSK343.*

Concerning GSK126, we proceeded by treating 8 CLL cases with 10 μM of this inhibitor and after 3 and 6 days measured viability levels and H3K27me3 levels. Our previous findings with EPZ6438 and GSK343 were also confirmed with GSK126, since decreased viability and H3K27me3 levels were observed in cells treated with the inhibitor compared to the control cells (DMSO-treated) (**Figure 26A, B**).

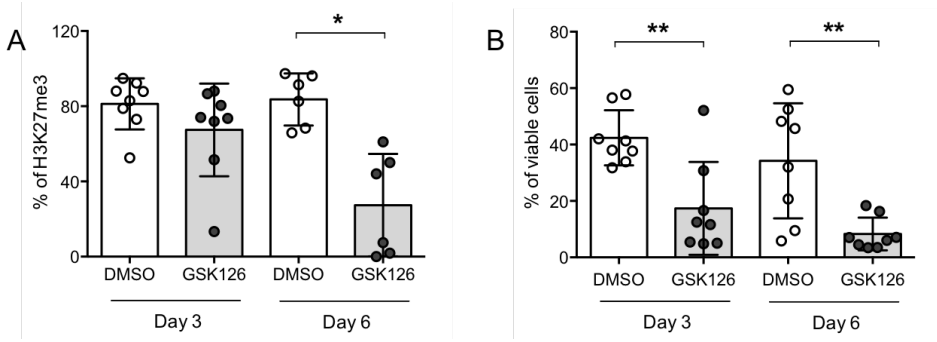

***Figure 26**: **Pharmacological inhibition of EZH2 catalytic activity with GSK126 A.** and **B.** Effects of treatment with 10 μM GSK126 on CLL cells from 8 cases after 3 and 6 days. In the graphs the scatter plot shows the percentage of H3K27me3 levels **A.** or viable cells **B.** and the bars correspond to the mean values. *p < 0.05, **p < 0.01.*

6.4 Microenvironmental stimuli modulate EZH2 expression and function ex vivo

Besides deregulated cell-intrinsic mechanisms, cell-extrinsic mechanisms are also critical for the development and progression of CLL[30]. These mainly pertain to microenvironmental interactions of CLL cells with various bystander cells and chemical stimuli in the tumor milieu that are mediated by various receptors e.g. the B cell receptor (BcR), Toll like receptors (TLRs), CD40, cytokine receptors and complement receptors, amongst others[61–63]. Considering the significant role of external triggering in promoting CLL cell survival and proliferation as well as the emerging role of EZH2 in these processes, here we explored potential links between microenvironmental stimuli and EZH2 expression and function.

6.4.1 Ability to respond to BcR stimulation

First, in order to explore the impact of BcR stimulation on EZH2 expression, we assessed a group of 13 CLL cases with the aim of selecting those able to respond to activation with anti-IgM in vitro and excluding the anergic cases. We analyzed calcium mobilization by flow cytometry and phosphorylation of PLCγ2 by immunoblotting, as direct signs of B cell activation through the BcR. Ten out of 13 cases (9 U-CLL and 1 M-CLL) were able to increase intracellular Ca^{2+}>5%(**Figure 27**) and/or p-PLCγ2 levels (**Figure 28A, B**) upon BcR stimulation with anti-IgM for 10 minutes compared to unstimulated cells [fold change (FC)=1.7, p<0.05, n=5]. These BcR-responsive cases were subjected to subsequent analysis.

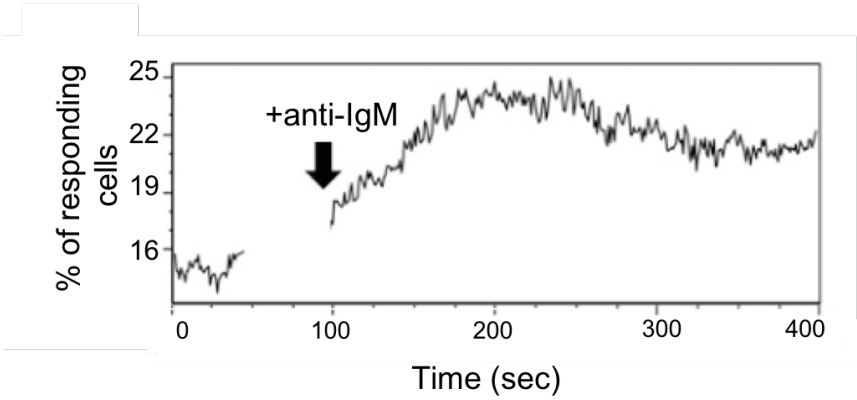

Figure 27: One representative responsive case, where leukemic cells were labeled with the calcium-sensitive dye Fluo-3, AM and analyzed by flow cytometry before and after BcR stimulation with anti-IgM.

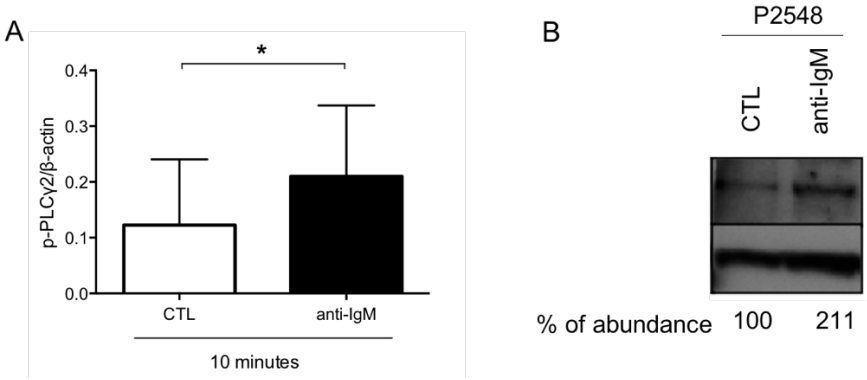

Figure 28: **A**. Each bar depicts the mean values with SD of p-PLCγ2 normalized to β-actin for 5 CLL cases that were stimulated or not with anti-IgM for 10 min. **B.** Western blotting analysis of p-PLCγ2 of one representative case. *p<0.05

6.4.2 BcR stimulation and EZH2 expression

First, we investigated the kinetics of *EZH2* mRNA expression after BcR stimulation in order to define the time-point that *EZH2* expression is more effectively upregulated. We cultured $CD19^+$ B cells from 3 CLL cases in the absence or the presence of anti-IgM for 12 and 48 hours and *EZH2* gene expression was upregulated (FC=1.8) after 12 hours; the observed effect was dampened at 48 hours (**Figure 29**).

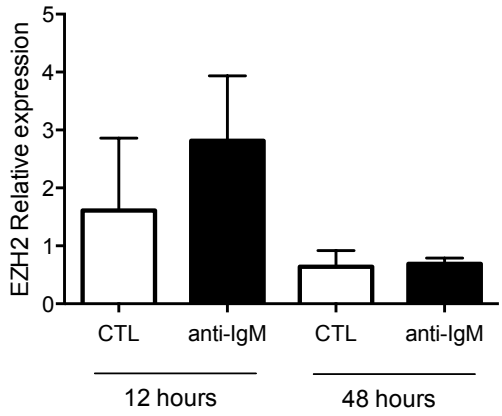

Figure 29*:The bars show the mean values with SD of EZH2 mRNA levels from 3 CLL cases stimulated or not through the BcR for 12 and 48 hours.*

Thus, we focused our attention on the 12 hours time-point. BcR activation was found to variably affect EZH2 mRNA expression in CLL (n=10) since half of the examined cases (5/10) upregulated (FC=1.7, $p<0.05$) while the remaining half downregulated (FC=1.4, $p<0.01$) EZH2 mRNA levels after 12 hours in culture (**Figure 30**).

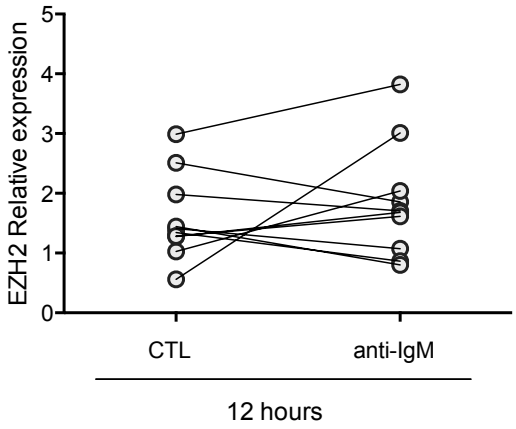

Figure 30*: **Impact ofBcR stimulation on EZH2 mRNA levels**. EZH2 mRNA analysis of 10 CLL cases after stimulation through the BcR for 12 hours. In the graph two connected points represent EZH2 relative expression in two different conditions for each patient, in the presence or absence (control) of anti-IgM.*

6.4.3 CD40 and/or TLR9 stimulation and EZH2 expression

Next, we investigated the potential impact of CD40 and TLR9 signaling on *EZH2* expression in primary CLL cells. First, we performed a kinetics analysis of *EZH2* mRNA levels after CD40/TLR9 co-stimulation in order to define the time-point that is more effectively upregulated. We cultured $CD19^+$ B cells from 1 CLL case in the absence or presence of CpG/CD40L for 6, 9, 12 and 24 hours and*EZH2* gene expression was upregulated more (FC=4.2) after 12 hours (**Figure 31**).

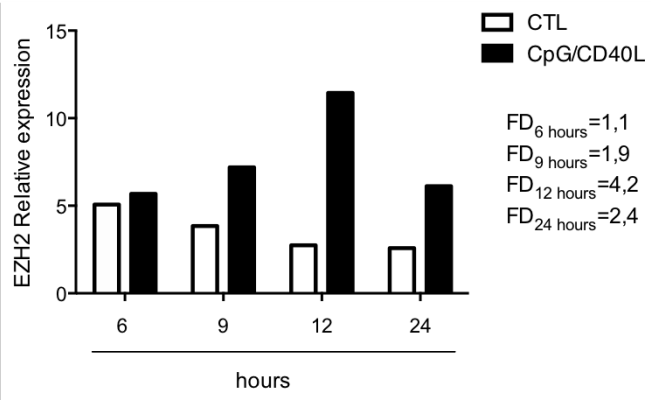

Figure 31*:The bars show the relative expression of EZH2 from 1 CLL case stimulated or not through the CD40/TLR9 for 6, 9, 12 and 24 hours.*

We proceeded with the 12 hours time-point of stimulation to the next experiments. EZH2 mRNA expression analysis after stimulation through CD40 with soluble CD40L (sCD40L) did not reveal significant changes, while stimulation of TLR9 with CpG or co-stimulation with CpG/CD40L for 12 hours caused pronounced and consistent upregulation of EZH2 mRNA levels compared to unstimulated cells (n=6) (FC=1.2, FC=8.9, $p<0.05$ and FC=10.5, $p<0.05$, respectively) (**Figure 32**).

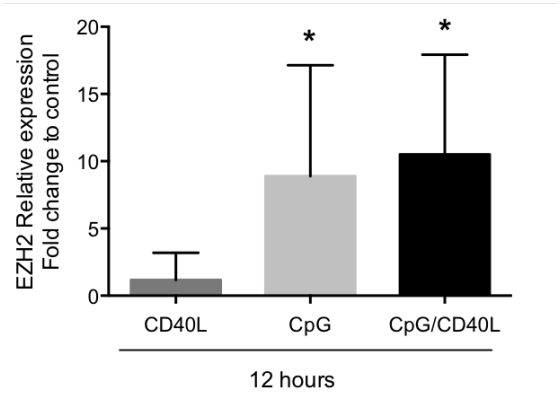

***Figure 32**: **Impact of TLR9 and/or CD40stimulationon EZH2 mRNA expression.** Each bar in the graph shows the mean values of FC of EZH2 relative expression in cells stimulated with CD40L and/or CpG normalized to unstimulated-control cells. Asterisks indicate significant differences compared to the unstimulated control. *p<0.05*

A similar pattern of response was observed at the protein level in cells treated with CD40L, CpG and CpG/CD40L for 24 hours, where EZH2 protein was significantly upregulated as revealed by Western blot analysis, in particular when stimulated through the TLR9 (FC=1.9, p<0.01; FC=4.6, p<0.01 and FC=4.3, p<0.05, respectively; n=6) (**Figure 33A, B**).

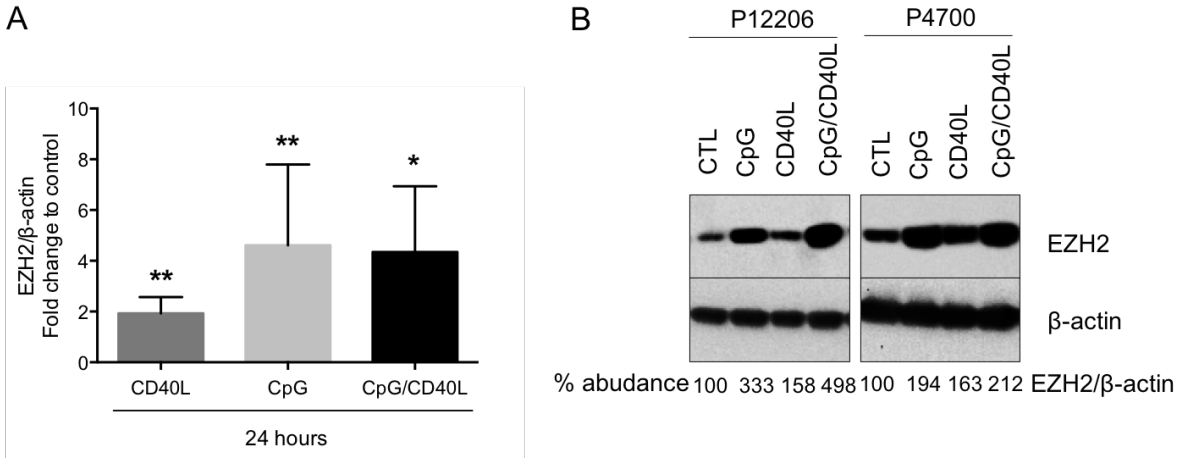

***Figure 33**: **Impact of TLR9 and/or CD40 stimulationon EZH2 protein expression. A.** Each bar in the graph shows the mean values of FC of EZH2 protein expression in cells stimulated with CD40L and/or CpG normalized to unstimulated-control cells. Asterisks indicate significant differences compared to the unstimulated control **B.** Immunoblotting analysis of EZH2 protein expression and β-actin of two representative cases.*p<0.05, **p<0.01*

Since the effects on EZH2 expression were greater after external triggering by CpG through TLR9, we then focused our attention on CpG stimulation and tested its effect on H3K27me3 levels and CLL cell viability. In cultures of primary CLL cells stimulated with CpG for 3 days, EZH2 induction was accompanied by a significant increase in both H3K27me3 levels (FC=1.2, p<0.05, n=6) andcell viability (FC=2.1, p<0.01, n=6) (**Figure 34A, B).**

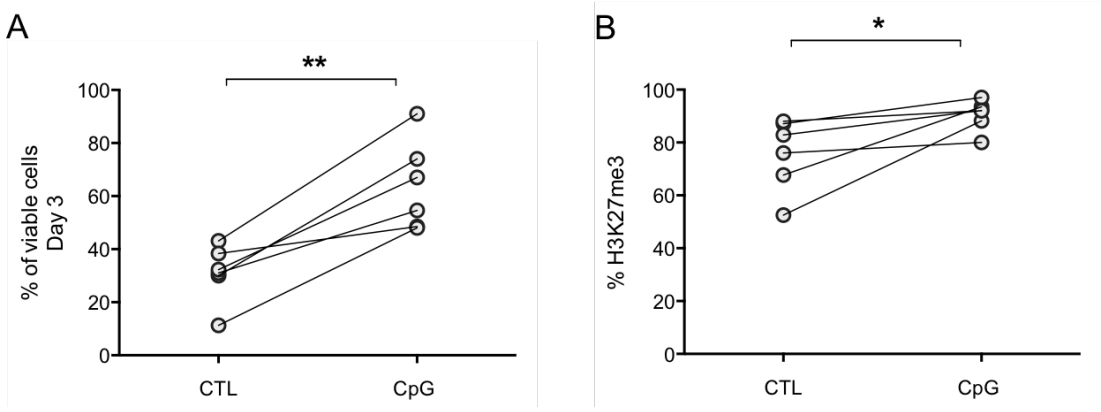

***Figure 34**: **Impact of TLR9 stimulationon EZH2 function in CLL cells. A.** CLL cell viability analysis and **B.** H3K27me3 levels at day 3 after TLR9 stimulation, using flow cytometry. In the graph connected points represent the percentage of viable cells or H3K27me3 levels in two conditions unstimulated-control (CTL) and the cells stimulated with CpG. *p<0.05, **p<0.01*

6.5 Ibrutinib affects EZH2 expression and function both in vivo and ex vivo

Prompted by these findings, we then investigated whether in vivo B cell signaling inhibition might also modulate EZH2 expression and H3K27me3 levels. To this end, we performed longitudinal profiling of a group of 9 CLL patients under Ibrutinib (IB) treatment. In each case, we analyzed samples before treatment initiation and at +1, +6 and >+6 months under treatment. At +1 month we observed a significant decrease in EZH2 protein (FC=3, p<0.001; n=9) and a trend to decreased H3K27me3 levels (FC=1.4, p=0.07; n=6) compared to the pre-treatment samples. This effect was no longer evident at later time points, when both EZH2 and H3K27me3 expression in the residual CLL cells rebounded to baseline levels or even higher (**Figure 35A-D**).

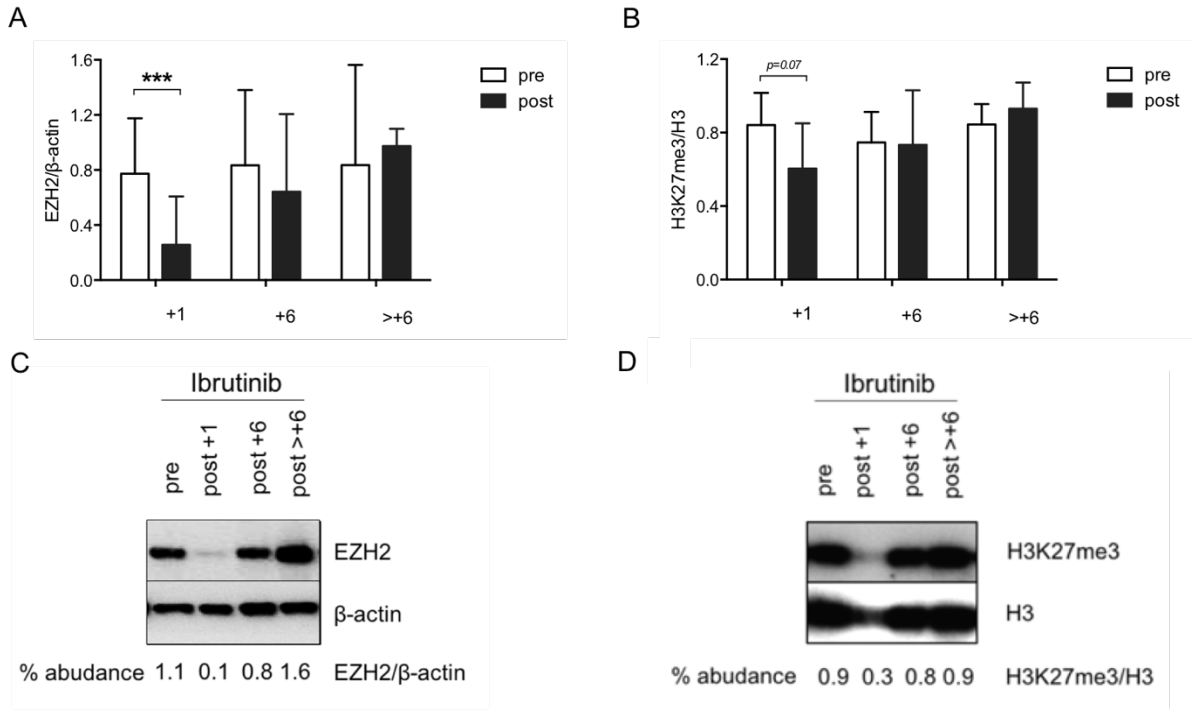

***Figure 35**: **Altered EZH2 protein expression and function after in vivo treatment with ibrutinib**. CD19⁺cells from patients before initiation of treatment with ibrutinib and at +1, +6 and >+6 months under treatment were lysed for analysis of: **A**. EZH2 protein expression; and, **B.** H3K27me3 levels using western blotting. Each bar in the graph represents the mean values with SD of EZH2/β-actin protein expression and H3K27me3/H3 levels. **C., D.**Immunoblotting analysis of EZH2,β-actin levels and H3K27me3 , total H3 for one representative case. ***p<0.001*

Next, we analyzed EZH2 protein expression after *ex vivo* IB treatment in 3 CLL cases and found that IB induced a dose-dependent downregulation of EZH2 protein (**Figure 36A**), accompanied by a concommitant dose-dependent reduction in cell viability (**Figure 36B**); based on these results, we chose 5 μM as the effective concentration for IB to be used in our experiments.

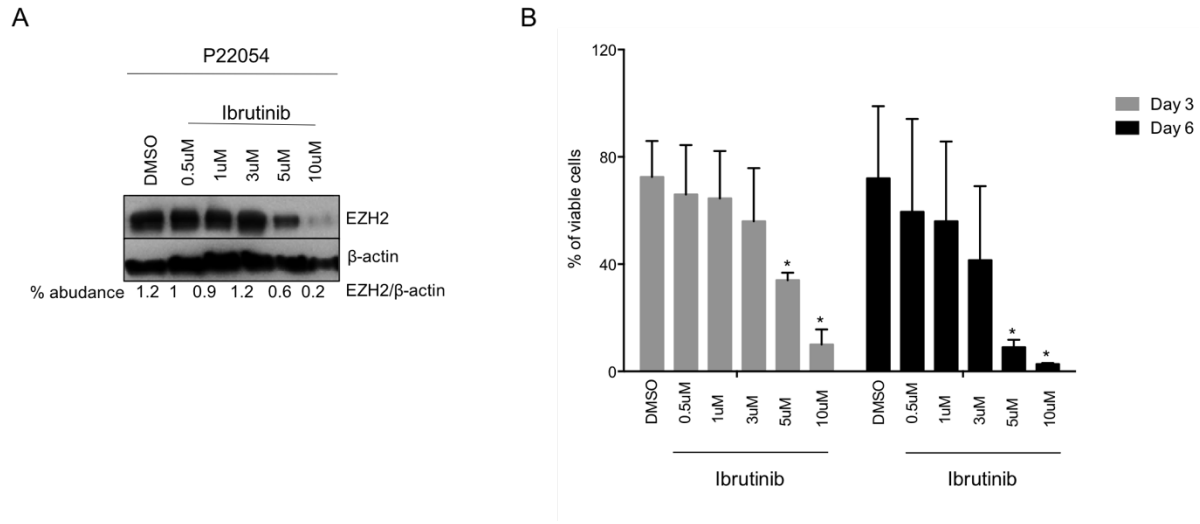

***Figure 36**: **Altered EZH2 protein expression and function after ex vivo treatment withibrutinib. A.** Western blotting analysis for EZH2 protein expression after treatment with increasing concentrations of ibrutinib in one representative case. **B.** The bars in the graph show the mean values with SD of the percentage of viable cells from three cases, treated with increasing concentrations of Ibrutinib normalized to control cells (DMSO-treated) after 3 and 6 days in culture.*p<0.05*

Following, we focused our attention in cases with divergent EZH2 expression andassessed the effect of *ex vivo* treatment with IB on CLL cell viability, particularly in 7 $EZH2^{high}$ vs 6 $EZH2^{low}$ cases [the cut-off used for this classification was based on EZH2 mRNA relative expression (2^-ΔCt=1.087) as described before[173]]. $EZH2^{high}$ cases showed decreased viability levels in cells treated with IB compared to control cells (DMSO-treated) (FD=1.9, p<0.01) after 3 days in culture; in contrast, no difference in viability was detected in $EZH2^{low}$ cases (**Figure 37**).

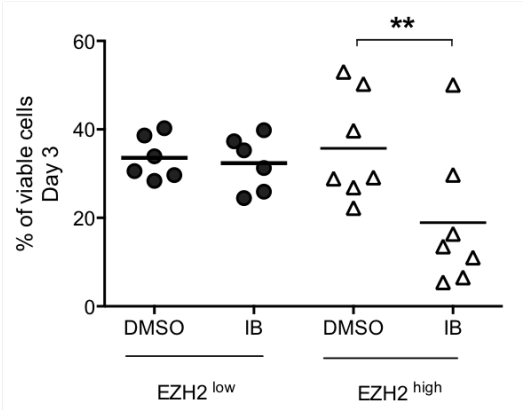

***Figure 37**: CLL cells from 7 $EZH2^{high}$ and 6 $EZH2^{low}$ cases were incubated with 5 μM IB and after 3 days in culture cell viability was measured using flow cytometry. The graph shows a scatter plot and*

*the black line corresponds to the mean value of the percentage of viable cells treated with ibrutinib or DMSO (control) in the EZH2^{high} and EZH2^{low} cases. **p<0.01*

6.6 Combined ex vivo treatment with B cell signaling and EZH2 inhibitors in primary CLL cells is more effective than individual single treatment

We have previously reported that the GSK343 EZH2 inhibitor induces down-regulation of H3K27me3 levels associated with increased cell apoptosis[173]. Similar effects were also obtained for GSK126, a different EZH2 inhibitor, as mentioned above. These two agents were then assessed for potential synergism with signaling inhibitors i.e IB and idelalisib (IDE) in primary CLL cells ex vivo.

First, in order to induce EZH2 expression and function, negatively selected CLL cells were pre-stimulated by CpG for 24 hours and then exposed to either single inhibitors i.e. IB, IDE, GSK343, GSK126 or combinations thereof. Flow cytometry analysis (**Figure 39**) after 3 days in culture revealed significantly ($p<0.05$) lower cell viability in CLL cells exposed to single treatments compared to CpG stimulated cells that received no treatment and served as controls ($FC>1.4$, $p<0.05$ for all single drug comparisons) (**Figure 38A, C and E**). Of note, however, combined inhibition had a significantly ($p<0.05$) more profound effect in decreasing cell viability compared to single inhibition with IB or IDE. Concordant results were obtained in these settings regarding H3K27me3 levels (**Figure 38B, D and F**).

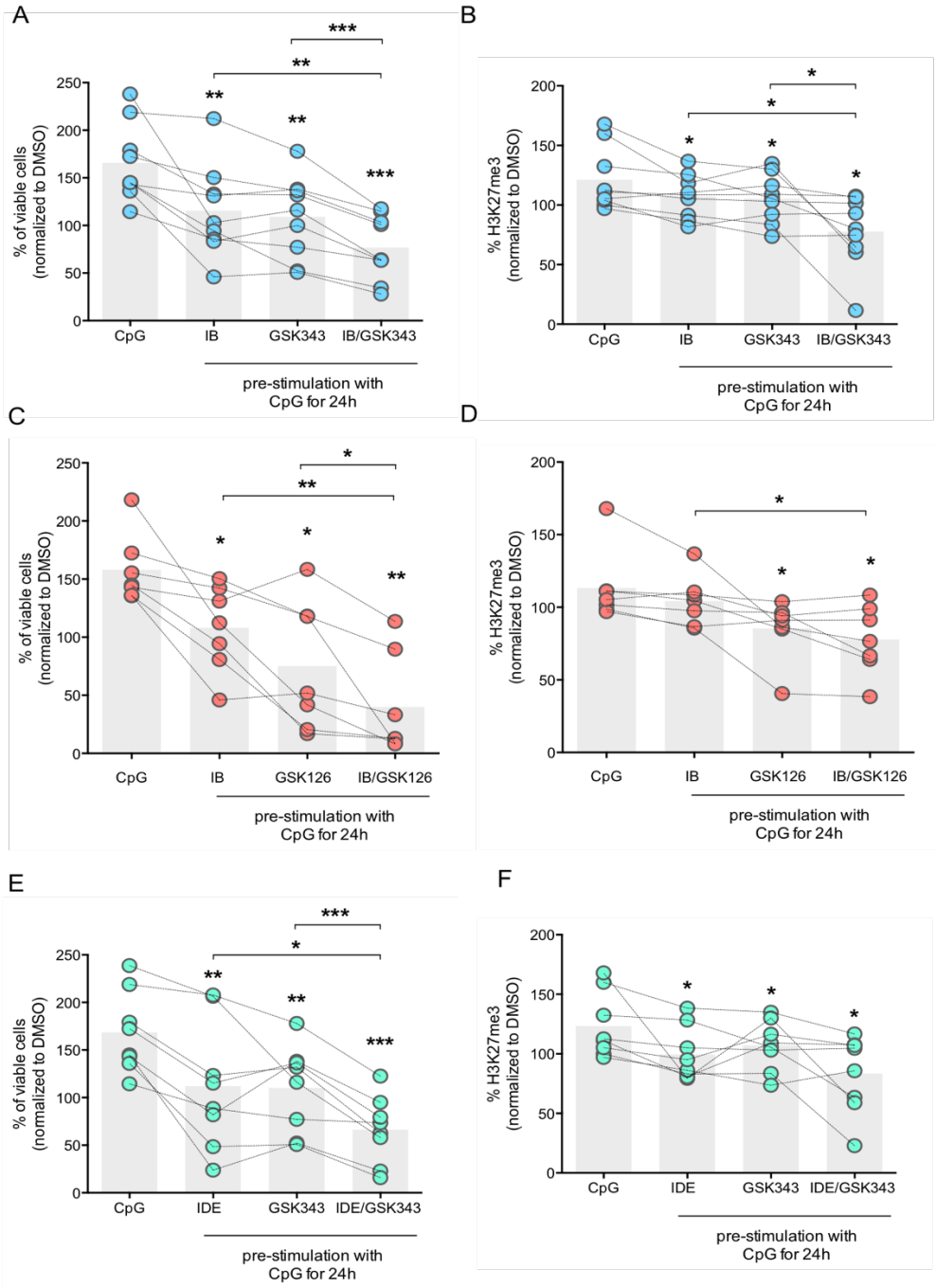

***Figure 38**: **Combination of signaling and EZH2 inhibitors in primary CLL cells**. Effects of incubation with CpG for 24 hours following single or combined treatment of 5 µM IB or 10 µM IDE with EZH2 inhibitors, 10 µM GSK343 or 10 µM GSK126 for 3 days on CLL cell viability A, C, E, and H3K27me3 levels B, D, F, using flow cytometry. In the graphs connected points represent the percentage of viable cells or H3K27me3 levels for each case in all conditions described, normalized to control cells (DMSO-treated). The bars in the graphs show the mean values. Asterisks above bars indicate significant differences compared to CpG-treated cells. *p < 0.05, **p < 0.01, ***p<0.001*

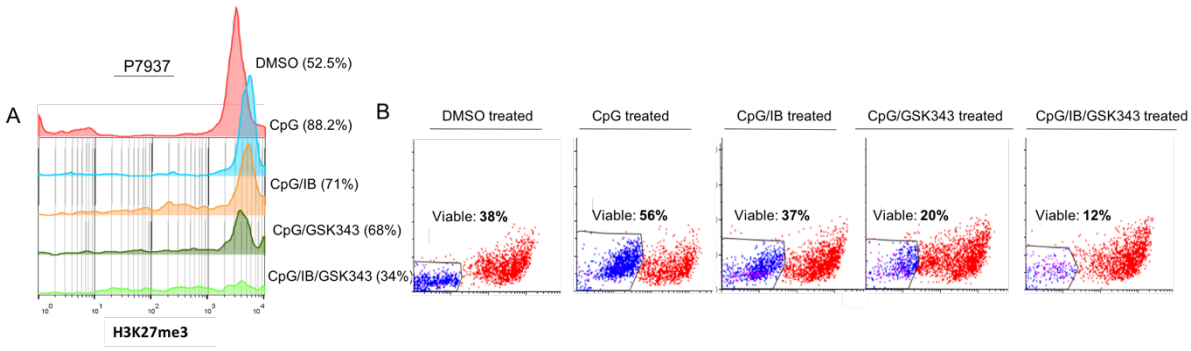

***Figure 39**: **Combination of signaling and EZH2 inhibitors in primary CLL cells.A**. Single parameter histogram showing H3K27me3 levels for one representative case after the indicated treatments for 3 days. **B.** Dot plot representing CLL cells stained with fixable viability dye (FVS) for one representative case. The negative fraction of cells for FVS represent the percentage of viable cells.*

Next, we performed similar experiments in cases with low EZH2 levels and unresponsive to TLR9 stimulation (n=3). No significant differences were observed between single versus combined inhibition on either CLL cell viability or H3K27me3 levels (**Figure 40**), indicating that the synergism identified above is context-dependent rather than generic i.e. it is likely linked to a particular functional status shaped by immune activation and the resultant EZH2 induction.

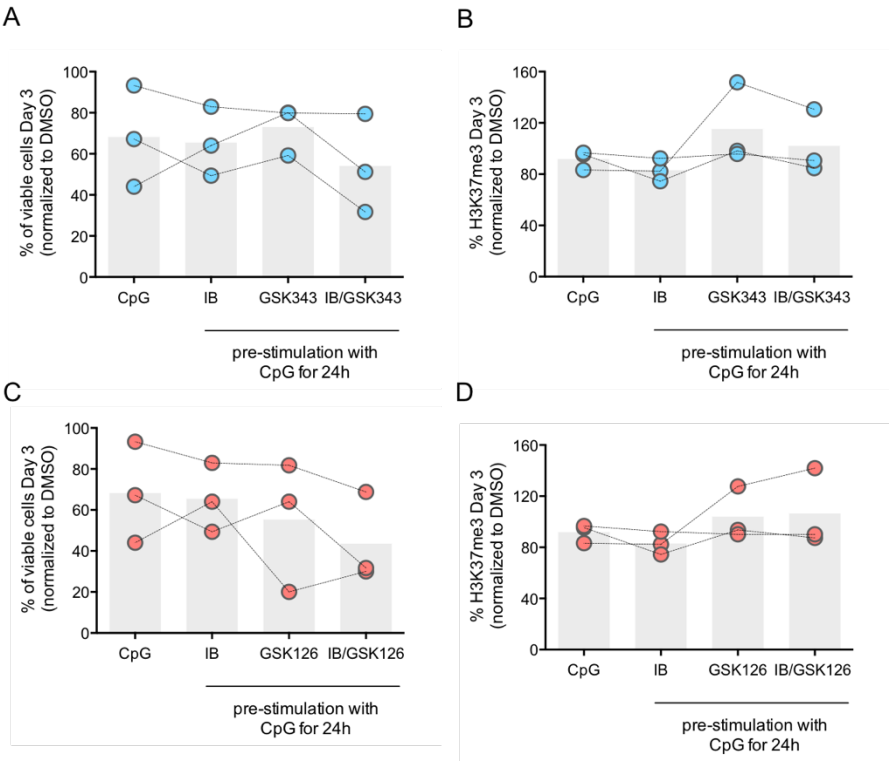

Figure 40: Combination of signaling and EZH2 inhibitors in EZH2^{low}cases. A, B,C, D. *Effects of incubation with CpG for 24 hours following single or combined treatment of 5uM IB with EZH2 inhibitors, 10uM GSK343 or 10uM GSK126 for 3 days on CLL cell viability* ***A,C.*** *and on levels of H3K27me3* ***B, D.*** *using flow cytometry. In the graphs connected points represent the percentage of viable cellsor H3K27me3 levelsin all conditions described, normalized to control cells (DMSO-treated). The bars in the graphs show the mean values with SD of viable cells or the H3K27me3 levels normalized to control cells (DMSO-treated).*

6.7 Combined ex vivo treatment with B cell signaling and EZH2 inhibitors in TCL1-tg murine splenic B cells is more effective than individual single treatment

6.7.1 EZH2 protein expression in *Tcl1* splenic mouse B cells

We also sought for additional evidence about the synergism of EZH2 inhibitors with B cell signaling inhibitors by *ex vivo* studies in the *Tcl1* transgenic mouse model of CLL. First, we compared EZH2 protein levels in *Tcl1* splenic B cells, wild-type mice and CLL cases. We observed significantly (FC=4.6, $p<0.05$) higher EZH2 protein expression in splenic B cells from *Tcl1* leukemic mice (n=3) versus wild-type mice (n=2) (**Figure 41**), similar to the expression of EZH2 in primary human CLL cells.

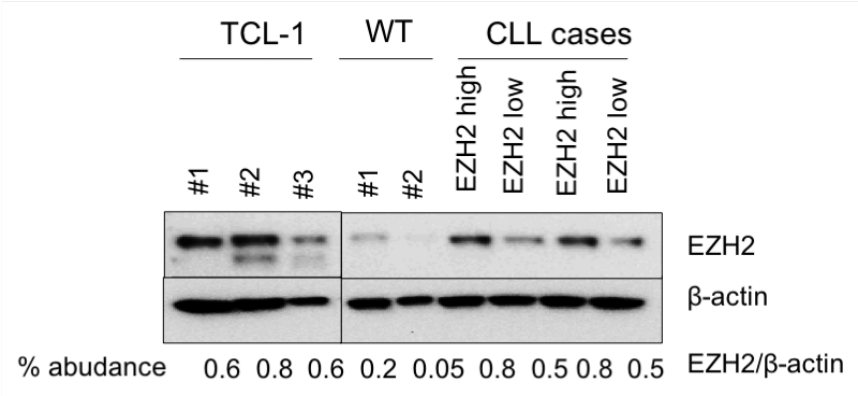

***Figure 41**: **Studies in Tcl1 splenic mouse B cells ex vivo**. Immunoblotting of EZH2 protein and β-actin expression of 3 Tcl1 tg-mice, 2 wild type mice and 4 CLL cases.*

6.7.2 Proliferation rates in *Tcl1* splenic mouse B cells

Next, we assessed the proliferation rates of *Tcl1* splenic mouse B cells by determining Ki-67 expression using flow cytometry; high Ki-67 expression was noted in all samples examined (**Figure 42**).

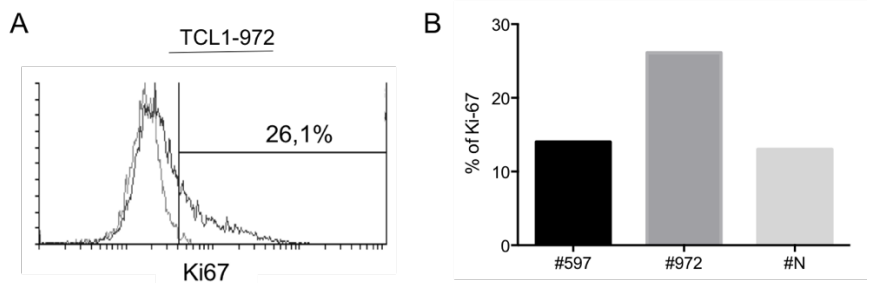

***Figure 42: A.** Flow cytometry analysis of Tcl1 splenic B cells proliferation using Ki-67 staining in one representative case. Overlay histogram for Ki-67 expression in Tcl1 B cells (black histogram); grey histogram: isotypic control. **B.** Each bar represents the Ki-67 expression of the 3 investigated Tcl1 mice.*

6.7.3 EZH2 inhibition in *Tcl1* splenic mouse B cells

On these grounds we investigated the effects of EZH2 inhibition in this system by *ex vivo* treatment with GSK126 and GSK343 for 1 and 2 days. Especially noteworthy was the fact that EZH2 inhibition resulted in reduction in both the number of Ki-67 positive cells (**Figure 43A**) and cell viability compared to DMSO-treated (control) cells (**Figure 43B**), after 2 days in culture.

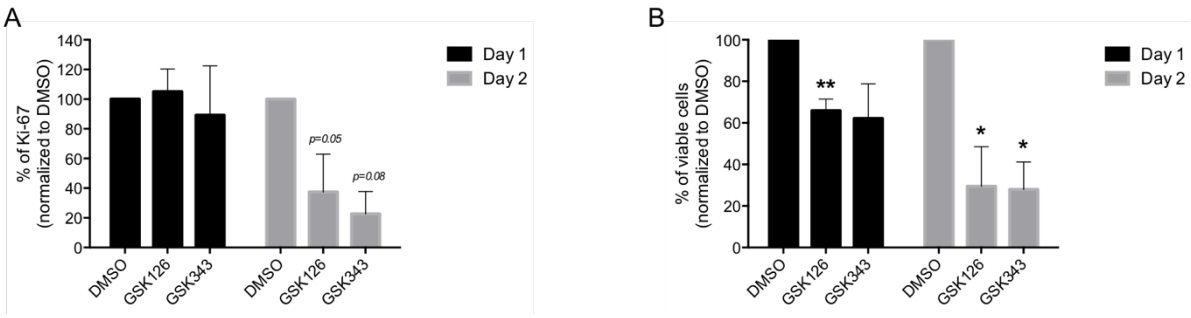

***Figure 43**: **Studies in Tcl1 splenic mouse B cells ex vivo**. Effects of Tcl1 splenic B cells incubation with EZH2 inhibitors 10 μM GSK126 or 10 μMGSK343 for one and two days on **A.**proliferation and **B.**cell viability, as measured by flow cytometry.*p < 0.05, **p < 0.01.*

6.7.4 Single and combined inhibition of EZH2 and B cell signaling in *Tcl1* splenic mouse B cells

We incubated *Tcl1* splenic B cells for 2 days with single (IB or IDE or GSK126 or GSK343) or combined B cell signaling and EZH2 inhibitors and found (i) significantly (p<0.05) lower cell viability for IB combinations with GSK126 or GSK343 (**Figure 44A**); and, a similar trend, though not reaching statistical significance, for IDE combinations with EZH2 inhibitors (**Figure 44B**), overall supporting synergism between B cell signaling and EZH2 inhibitors also in this mouse model of CLL.

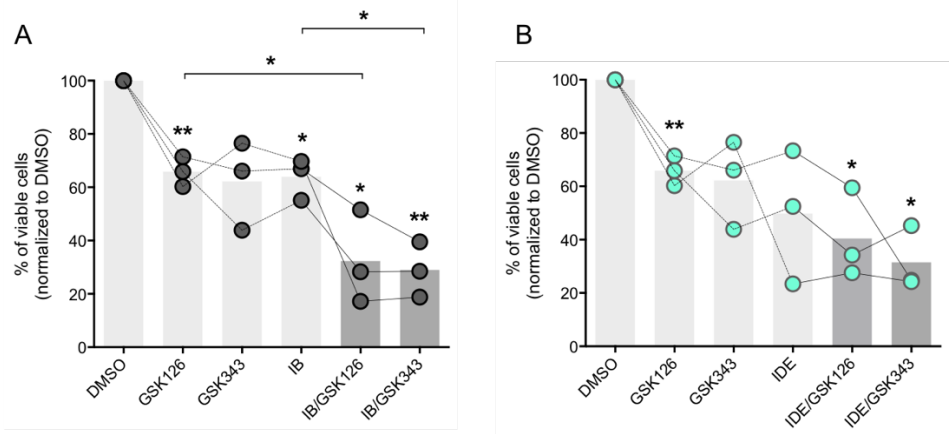

***Figure 44: Studies in Tcl1 splenic B cells ex vivo.** Effects of single or combined treatment of Tcl1 splenic B cells with **A.** 5 μM IB,10 μMGSK126, 10 μM GSK343 and **B.** 10 μM IDE,10 μMGSK126, 10 μM GSK343for two days on cell viability, as measured by flow cytometry. In the graphs connected points represent the percentage of viable cells for each case in all conditions described, normalized to control cells (DMSO-treated). The bars show the mean values. Asterisks above bars indicate significant differences compared to DMSO-treated (control) cells *p < 0.05, **p < 0.01*

6.8 EZH2 inhibitors exert a pro-apoptotic effect in CLL cells from patients with suboptimal responses to B cell signaling inhibitors

We investigated the potential impact of EZH2 inhibition on CLL cell viability and H3K27me3 levels in primary cells from CLL cases resistant to ibrutinib (IB, n=4) or idelalisib (IDE, n=2). Samples were collected at the time of lack of response. $CD19^+$ cells from these cases were *ex vivo* treated with EZH2 inhibitors (GSK126, GSK343) for 3 days leading to a statistically significant decrease in H3K27me3 levels (FC=1.1, $p<0.05$; n=6 and FC=1.3, $p<0.05$; n=5) (**Figure 59A, C)** and CLL cell viability (FD=2.4, $p<0.05$; n=6 and FC=1.6, $p<0.05$; n=5) (**Figure 45B, D**).

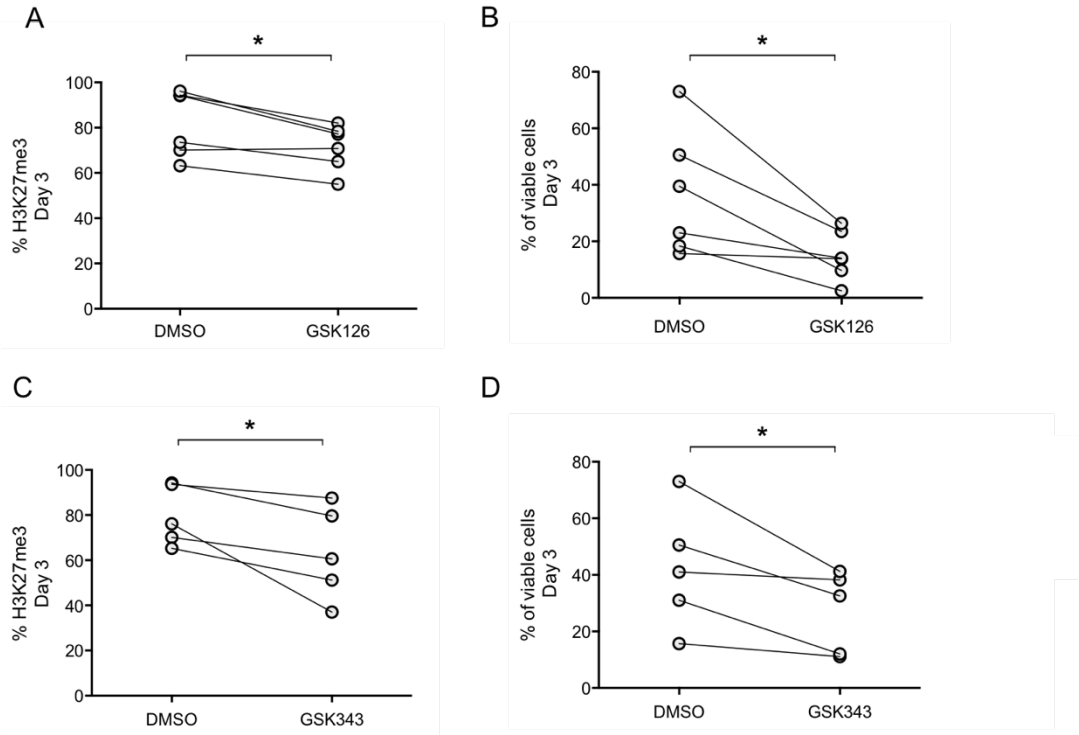

***Figure 45**: **Ex vivo pharmacological inhibition of EZH2 catalytic activity in cases resistant to treatment with immune signaling inhibitors.** Effects of incubation with EZH2 inhibitors, 10 µM GSK343 or 10 µM GSK126 for 3 days on levels of **A, C.** H3K27me3 and on **B, D.** CLL cell viability using flow cytometry. In the graphs connected points represent the percentage of H3K27me3 or viable cells treated with GSK343 or GSK126 or DMSO-treated control cells. * $p < 0.05$*

7 Discussion

EZH2 is the core enzymatic subunit of PRC2, a complex that methylates lysine 27 of histone H3 (H3K27) to promote transcriptional silencing[174,175]. Several studies show that EZH2 deregulation, by either overexpression or mutations, is frequently associated with poor prognosis in B cell malignancies[176,177].

In this study, we summarize the spectrum of EZH2 and H3K27 perturbations found in CLL and propose potent therapeutic approaches tailored to clinically aggressive cases based on our novel findings about the role of EZH2 in CLL.

We first provided evidence supporting the oncogenic role of EZH2 in CLL by showing that EZH2 is overexpressed in a stereotyped CLL subset #1, a paradigmatic aggressive subgroup of CLL cases displaying a distinctive immune signaling profile[164,166]. Prompted by these initial observations, we here performed a detailed molecular and functional analysis of EZH2 in a large series of CLL cases in order to better characterize its role in CLL pathophysiology. The findings of the present study highlight EZH2 as an important novel player in the puzzle of clinical aggressiveness in CLL. EZH2 mRNA and protein expression levels were found to be significantly higher in U-CLL compared to M-CLL and, moreover, their increased levels were correlated to disease progression. Consequently, it can be argued that EZH2 expression is not a uniform mechanism of aggressiveness in CLL but rather that it contributes specifically to the inferior prognosis of U-CLL[173].

In order to obtain insight into the potential functional impact of EZH2 in CLL, we subdivided CLL cases based on the mRNA expression levels into $EZH2^{high}$ and $EZH2^{low}$ subgroups and found that the former displayed higher H3K27me3 levels, supporting an association between EZH2 expression and enzymatic activity: indeed, high levels of EZH2 correlated with higher viability of CLL cells compared to $EZH2^{low}$ cases. Next, we tampered EZH2 by transfecting CLL cells of $EZH2^{high}$ cases with siRNAs specific for EZH2 and observed significant downregulation of EZH2, accompanied also by down-modulation of H3K27me3 levels and induction of CLL cell apoptosis, prompting us to argue that EZH2 is implicated in the anti-apoptotic phenotype of U-CLL clones.

Several mechanisms may be implicated in defective regulation of EZH2 expression. The EZH2 transcript is known to be regulated by several miRNAs[178], amongst which miR-101

targets the 3'UTR of EZH2 mRNA and promotes its degradation[179]. Along these lines, we presented a rationale for epigenetic regulation of EZH2 expression in CLL through a negative regulatory feedback loop controlled by miR-101. More specifically, we provided for the first time evidence that overexpression of EZH2 in clinical aggressive cases of CLL is a result of downregulation of miR-101[164].

Additionally, upregulation of EZH2 may be caused by immune triggering, since signaling pathway activation induced by external triggering is critical for the survival and proliferation of the malignant B cells in CLL, a characteristic highly relevant to U-CLL cases that are more responsive[23,62,87]. Indeed, it has been reported that CLL cell stimulation with the CD40 ligand, which strongly induces the alternative NF-κB pathway, also induces EZH2 expression, leading to suppression of a subset of p53 target genes previously associated with the senescent cell phenotype, including *DEK* and *RacGAP1*[84]. Furthermore, in another study c-Rel was found to be a critical activator of EZH2 transcription in activated primary murine B and T cells, and also in human leukemia and multiple myeloma cell lines[180]. On these grounds, it can be argued that the interplay between immune signaling and microRNAs may be the major mechanism underlying EZH2 overexpression in U-CLL, opening new directions for future research.

With this in mind and also considering the seminal pro-survival signals emanating from the CLL microenvironment, we also investigated whether links may exist between extrinsic triggering and EZH2 status in CLL.Our findings indicate that activation of immune receptors in CLL B cells, more particularly the BcR, TLR9 and/or CD40, induces EZH2 expression and functionality as evidenced by elevated H3K27me3 levels. Moreover, this is accompanied by a significant increase in CLL cell viability, thus implicating EZH2 in the microenvironmentally-induced anti-apoptotic response which is known to involve NF-κB signaling with resultant upregulation of anti-apoptotic proteins, including BCL2 and MCL1[63,84,89]. Future studies are warranted for deciphering the underlying molecular mechanisms and processes, especially regarding the possibility that EZH2 induction mediates a transcriptional rewiring, affecting, amongst others, critical players in survival and apoptotic pathways.

In recent years, selective EZH2 inhibitors have been tested with promising results in preclinical/clinical studies in various cancers, including B cell malignancies[181,182].Testing

such inhibitors (EPZ6438, GSK126 and GSK343) on primary CLL cells, we obtained additional decisive support for a role of EZH2 in the apoptosis resistance exhibited by CLL cells with high EZH2 expression, whereby EZH2 inhibition led to reduced H3K27me3 levels and induction of apoptosis. This recalls what has previously been reported in the WSU-DLCL2DLBCL cell line, where pharmacological inhibition of EZH2 causes cell cycle arrest in the G1 phase and then cell apoptosis, accompanied by reduction of H3K27me3 levels and upregulation of EZH2 target genes[157]. Consequently, pharmacological inhibition of EZH2 may represent a potential novel therapeutic approach for a subgroup of CLL patients, an enticing idea that is readily achievable, since EZH2 pharmacological inhibitors are currently in clinical trials for other types of cancer.

Since CLL cells receive survival signals from the microenvironment through various receptors, most notably the BcR, it appeared necessary to provide additional treatment approaches with agents that target crucial components in the BcR signaling pathway. Inhibitors of immune signaling are commonly used in the therapy of CLL with great efficacy[183]. The BTK inhibitor, Ibrutinib, represents one of the most significant treatment options available in the clinical activity against CLL, while it demonstrated high response rates and prolonged progression-free survival (PFS)[12,59,184].

With this in mind, we addressed whether EZH2 might be modulated by immune signaling inhibitors, particularly Ibrutinib. The herein reported results indicate that *ex vivo* Ibrutinib treatment promotes CLL cell apoptosis in $EZH2^{high}$ clones, while having a significantly less important effect on $EZH2^{low}$ clones, further highlighting the links between immune signaling and EZH2 expression and its anti-apoptotic role. *In vivo*, at +1 month under Ibrutinib treatment EZH2 expression drops; interestingly, however, at later timepoints residual CLL cells express EZH2 at levels similar to baseline if not higher. These results indicate that EZH2 expression likely contributes to disease persistence under monotherapy with Ibrutinib, justifying the hypothesis that targeting both BTK and EZH2 might prove a potentially beneficial treatment strategy for CLL.This is not only conceptually appealing but also feasible, considering that EZH2 inhibitors are already in clinical trials for other types of aggressive malignancies.

Despite the significant efficacy and tolerability of BcR signaling inhibitors, even in heavily treated patients, responses are often suboptimal, alluding to a characteristic resistance[56–

[58] and indicating that novel combination strategies are required. Several recent studies explored the synergistic effects of blocking components that participate in the interacting network responsible for the survival signals in the microenvironment of CLL cells[185,186]. The available data support that drug combinations are essential in order to obtain durable and complete responses and overcome drug resistance[186,187]. This conclusion is also born out by our *ex vivo* studies revealingthat targeting both EZH2 and immune signaling processes in cases competent for signaling leads to a significant decrease in leukemic cell viability and H3K27me3 levels as compared to isolated inhibition. This further emphasizes the value of targeting distinct albeit inter-connected mechanisms and pathways contributing pro-survival and drug escape signals to the CLL clone.

To further validate our results, we performed additional experiments in splenic B cells from the *Tcl1* leukemic mice, which is the most common mouse model in CLL. TCL1 leukemias seem to display higher EZH2 expression than wild type mice and also increased proliferation rates compared to human CLL cells. Of note, *ex vivo* treatment of such cells with EZH2 pharmacological inhibitors resulted in a significant decrease in cell proliferation and also viability levels. Finally, we confirmed the above described synergism of EZH2 and signaling inhibitors in primary CLL cells also in splenic B cells from the *Tcl1* leukemic mice. These results are in line with a recent study where agents inhibiting B cell activation (BTK inhibitors, SYK inhibitors, Glucocorticoid receptor agonists-GRAGs) showed a strong synergistic relationship with EZH2 inhibitors in DLBCL cell lines with wild-type EZH2[188].

In conclusion, EZH2 is overexpressed in CLL cases with aggressive clinical course, is associated with disease progression and confers a survival advantage to the malignant cells. Consequently, pharmacological inhibition of EZH2 may represent a potential novel therapeutic approach for a subgroup of CLL patients, an enticing idea that is readily achievable, since EZH2 pharmacological inhibitors are currently in clinical trials for other types of cancer, including B cell malignancies. Moreover, we show that EZH2 expression is regulated by signals emanating from CLL microenvironment and present for the first time evidence that the combined inhibition of EZH2 and immune signaling is more effective than immune signaling inhibition alone in both primary CLL cells and splenic B cells from the *Tcl1* leukemic mice. Finally, we show that EZH2 inhibitors are effective in primary CLL cells from

cases with suboptimal response to immune signaling inhibitors, further highlighting that EZH2 might represent a rational choice for combinational treatment of CLL, capable of improving the efficacy/quality of responses to signaling inhibitors.

8 Περίληψη

8.1 Η υπερέκφραση της μεθυλοτρανσφεράσης των ιστονών EZH2 στη Χρόνια Λεμφοκυτταρική λευχαιμία παρέχει προστασία από απόπτωση και συνδέεται με κλινική επιθετικότητα

Η μεθυλοτρανσφεράση των ιστονών EZH2 είναιη καταλυτική υπομονάδα του κατασταλτικού συμπλόκου Polycomb 2 (PolycombRepressorComplex 2, PRC2) μέσω του οποίου καταλύει την τριμεθυλίωση της ιστόνης H3 στο κατάλοιπο λυσίνη 27 (H3K27me3) επάγοντας αποσιώπηση γονιδίων. Η EZH2 υπερεκφράζεται σε πλειάδα κακοηθειών, μεταξύ άλλων και κακοήθειες του λεμφικού ιστού και γενικά συσχετίζεται με δυσμενή πρόγνωση. Σε προκαταρκτική μελέτη μας δείξαμε για πρώτη φορά ότι η EZH2 εκφράζεται στη χρόνια λεμφοκυτταρική λευχαιμία (ΧΛΛ), ιδίως σε περιπτώσεις που ανήκουν στο υποσύνολο #1, ομάδα ασθενών οι οποίοι χαρακτηρίζονται από δυσμενή κλινική πορεία. Στην παρούσα μελέτη επεκτείναμε την ανάλυση της έκφρασης της EZH2 σε καλά χαρακτηρισμένη ομάδα 131 ασθενών με ΧΛΛ και διερευνήσαμε το λειτουργικό αντίκτυπό της στη συμπεριφορά των λευχαιμικών κλώνων. Η μελέτη περιλάμβανε: (i) ποσοτικοποίηση των mRNA μεταγράφων της EZH2, (ii) προσδιορισμό της έκφρασης της EZH2 σε επίπεδο πρωτεΐνης, (iii) μέτρηση επιπέδωντου δείκτη λειτουργίας της EZH2, H3K27me3, (iv) ανάλυση βιωσιμότητας ΧΛΛ κυττάρων με κυτταρομετρία ροής, (v) διαμόλυνση των ΧΛΛ κυττάρων με siRNA ειδικό για την EZH2 και τέλος, (vi) εφαρμογή φαρμακολογικών αναστολέων της EZH2 σε κύτταρα ΧΛΛ. Τεκμηριώνουμε ότι η υπερέκφραση της EZH2 αποτελεί βασικό χαρακτηριστικό των κλινικά επιθετικών περιπτώσεων ΧΛΛ που φέρουν κυρίως αμετάλλακτα γονίδια IGHV, επηρεάζοντας τα επίπεδα της H3K27me3 στα λευχαιμικά κύτταρα και προσδίδοντάς τους έτσι πλεονέκτημα επιβίωσης και προστασία από απόπτωση. Στη συνέχεια, για να αποδείξουμε ότι η EZH2 ευθύνεται για την αυξημένη βιωσιμότητα των κυττάρων,καταστείλαμε την έκφραση της EZH2 με ειδικά siRNAs σε περιπτώσεις με ‘’υψηλή EZH2’’και διαπιστώσαμε ότι μείωση της έκφρασης της EZH2 επιφέρει επίσης μείωση των αντίστοιχων επιπέδων της H3K27me3, καθώς και επαγωγή απόπτωσης των κυττάρων της ΧΛΛ. Επιπλέον, δείξαμε ότι αυξημένη έκφραση της EZH2 συσχετίζεται με ταχύτερη πρόοδο νόσου. Επίσης, παρουσιάζουμε προκλινικά δεδομένα που δείχνουν ότι η αναστολή της καταλυτικής ενεργότητας της EZH2 με ειδικούς φαρμακολογικούς αναστολείς, όπως οι EPZ6438, GSK343 και GSK126, προάγει

απόπτωση των κυττάρων της ΧΛΛ, καθώς και μείωση των επίπεδων της H3K27me3, αναδεικνύοντας ένα νέο πιθανό θεραπευτικό στόχο για ασθενείς με επιθετική νόσο.

8.2 Συνεργική δράση των αναστολέων της άνοσης σηματοδότησης και της μεθυλοτρανσφεράσης των ιστονών EZH2 στη Χρόνια Λεμφοκυτταρική λευχαιμία: θεραπευτικές προεκτάσεις

Η EZH2 υπερεκφράζεται σε κλινικά επιθετικές περιπτώσεις με ΧΛΛ και επάγει αυξημένη επιβίωση και προστασία από απόπτωση στα λευχαιμικά κύτταρα. Τα Β κύτταρα της ΧΛΛ λαμβάνουν σήματα επιβίωσης από το μικροπεριβάλλον μέσω πολλαπλών υποδοχέων, όπως ο Β κυτταρικός υποδοχέας (BKY), οι υποδοχείς τύπου Toll (TLR) και ο CD40. Με βάση τα παραπάνω, στην παρούσα μελέτη εξετάσαμε εάν ερεθίσματα από το μικροπεριβάλλον μπορούν να επηρεάσουν την έκφραση της EZH2 και κατ' επέκταση τη βιωσιμότητα των κυττάρων της ΧΛΛ. Η ομάδα μελέτης καθορίστηκε με βάση την ικανότητα απάντησης στη διέγερση του BKY: έτσι, επιλέχθηκαν για ανάλυση μόνο περιπτώσεις που απαντούσαν στην ενεργοποίηση του BKY. Διαπιστώσαμε ότι ερεθίσματα του μικροπεριβάλλοντος μέσω του TLR9 και/ή CD40, αλλά ιδίως η διέγερση μέσω του υποδοχέα TLR9, οδηγεί σε αυξημένη έκφραση της EZH2 και ενισχύει την επιβίωση του λευχαιμικού κλώνου. Σε αυτό το πλαίσιο, εξετάσαμε την επίδραση των αναστολέων της άνοσης σηματοδότησης στην έκφραση της EZH2 στα ΧΛΛ κύτταρα καθώς και την πιθανή συνεργική δράση τους με αναστολείς της EZH2. Αρχικά, μελετήσαμε εάν η θεραπεία με Ibrutinib μπορεί να επηρεάσει την έκφραση της EZH2 και τα επίπεδα της H3K27me3 *invivo*. Η ομάδα μελέτης περιλάμβανε ασθενείς με ΧΛΛ οι οποίοι έλαβαν Ibrutinib ως μονοθεραπεία. Ανάλυση με ανοσοαποτύπωση western ανέδειξε μείωση των επιπέδων της πρωτεϊνικής έκφρασης της EZH2 καθώς και των επιπέδων της H3K27me3 μετά από 1 μήνα θεραπείας συγκριτικά με το αντίστοιχο δείγμα πριν τη θεραπεία, ενισχύοντας τα προηγούμενα ευρήματά μας που συνδέουν τη σηματοδότηση των Β κυττάρων με την έκφραση και λειτουργία της EZH2. Στη συνέχεια, ελέγξαμε με κυτταρομετρία ροής την επίδραση του Ibrutinib στη βιωσιμότητα των κυττάρων *ex vivo* σε περιπτώσεις ασθενών ΧΛΛ με υψηλά και χαμηλά επίπεδα EZH2 και διαπιστώσαμε ότι το Ibrutinib οδηγεί σε απόπτωση των ΧΛΛ κυττάρων μόνο στις περιπτώσεις με υψηλά επίπεδα EZH2. Σε μια διαφορετική ομάδα ασθενών με ΧΛΛ οι

οποίοι είχαν ελεγχθεί και βρεθεί να απαντούν σε διέγερση μέσω του TLR9 εξετάσαμε την πιθανή συνεργική δράση μεταξύ των αναστολέων της άνοσης σηματοδότησης Ibrutinib (IB) και Idelalisib (IDE) και των αναστολέων της EZH2 (GSK343, GSK126). Μετά από διέγερση με CpG (ειδικός προσδέτης για τον TLR9) επί 24 ώρες, ώστε να αυξηθεί η έκφραση της EZH2, ακολούθησε μεμονωμένη επώαση με κάθε αναστολέα (IB, IDE, GSK343, GSK126) και συνδυαστική εφαρμογή των αναστολέων (IB/GSK343, IDE/GSK343, IB/GSK126). Μετά από 3 ημέρες καλλιέργειας αναλύθηκαν με κυτταρομετρία ροής τα επίπεδα βιωσιμότητας και H3K27me3. Η μεμονωμένη αναστολή με IB, IDE, GSK343 και GSK126 οδήγησε σε απόπτωση των ΧΛΛ κυττάρων σε σχέση με ΧΛΛ κύτταρα χωρίς έκθεση σε αναστολείς (FD≥ 1.4), ενώ η συνδυαστική αναστολή με IB/GSK343, IDE/GSK343 και IB/GSK126 ήταν πολύ πιο αποτελεσματική, εφόσον οδήγησε σε ακόμα μεγαλύτερη μείωση της βιωσιμότητας και των επιπέδων της H3K27me3 σε σύγκριση με τη μεμονωμένη αναστολή (FD≥1.5, $p<0.05$). Στη συνέχεια απομονώσαμε Β σπληνοκύτταρα από *Tcl1* λευχαιμικά ποντίκια (το καλύτερα μελετημένο μοντέλο ποντικού στη ΧΛΛ) όπου παρατηρήσαμε αυξημένη έκφραση EZH2 σε σχέση με κύτταρα από ποντίκια μάρτυρες (Wild Type, WT), καθώς επίσης αυξημένα επίπεδα πολλαπλασιασμού συγκριτικά με τα κύτταρα της ΧΛΛ. Τα προηγούμενα ευρήματα σχετικά με τη συνεργική δράση των αναστολέων άνοσης σηματοδότησης και της EZH2 επιβεβαιώθηκαν επίσης στα Β σπληνοκύτταρα από *Tcl1* λευχαιμικά ποντίκια, με εμφανή μείωση επιπέδων πολλαπλασιασμού και βιωσιμότητας μετά από συνδυαστική δράση των αναστολέων συγκριτικά με τη μεμονωμένη επώαση. Τέλος, δείξαμε ότι η εφαρμογή φαρμακολογικών αναστολέων της EZH2 (GSK343 και GSK126) επάγει απόπτωση και μείωση στα επίπεδα H3K27me3 σε κύτταρα από περιπτώσεις ΧΛΛ που εμφάνισαν ανθεκτικότητα ή μειωμένη απόκριση στη θεραπεία με αναστολείς σηματοδότησης (IB ή IDE), παρέχοντας έτσι νέα δεδομένα για το σχεδιασμό και την παρακολούθηση των ασθενών με εξατομικευμένες θεραπευτικές στρατηγικές προσεγγίσεις.

Συμπερασματικά, παρουσιάζουμε για πρώτη φορά ισχυρές *ex vivo* ενδείξεις ότι ο συνδυασμός φαρμακολογικών αναστολέων της άνοσης σηματοδότησης και αναστολέων της EZH2 έχει συνεργική δράση στη ΧΛΛ, υποδεικνύοντας μια εναλλακτική θεραπευτική στρατηγική για κλινικά επιθετικές περιπτώσεις ΧΛΛ.

11 Abstract

11.1 The histone methyltransferase EZH2 as a novel prosurvival factor in clinically aggressive chronic lymphocytic leukemia

The histone methyltransferase EZH2 induces gene repression through trimethylation of histone H3 at lysine 27 (H3K27me3). EZH2 overexpression has been reported in many types of cancer and associated with poor prognosis. Chronic lymphocytic leukemia (CLL) is the most common leukemia in the Western world, characterized by the progressive accumulation of small, mature B lymphocytes in blood, bone marrow and lymphatic tissues. CLL is a very heterogeneous malignancy at both clinical and biological levels. In our previous study we demonstrated that EZH2 is highly expressed in a subgroup of patients (subset #1), characterized by a stereotyped B cell receptor (BcR) with unmutated immunoglobulin heavy variable genes (U-CLL) and an aggressive disease course.Here we investigated in a larger cohort of patients the expression and functionality of EZH2 in CLL. Aggressive cases with unmutated IGHV genes (U-CLL) displayed significantly higher EZH2 expression compared to indolent CLL cases with mutated IGHV genes (M-CLL), both in mRNA and protein levels; furthermore, in U-CLL EZH2 expression was upregulated with disease progression. $EZH2^{high}$ cases displayed high H3K27me3 levels and increased viability suggesting that EZH2 is functional and likely confers a survival advantage to CLL cells. This argument was further supported by siRNA-mediated downmodulation of EZH2 which resulted in increased apoptosis and reduced H3K27me3 levels in $EZH2^{high}$ cases. Treatment of primary CLL cells with EZH2 inhibitors, namely EPZ6438, GSK343 and GSK126 induced downregulation of H3K27me3 levels leading to increased cell apoptosis.

In conclusion, EZH2 is overexpressed in adverse-prognosis CLL and associated with increased cell survival. Pharmacologic inhibition of EZH2 catalytic activity promotes apoptosis, highlighting EZH2 as a novel potential therapeutic target for specific subgroups of patients with CLL.

11.2 Inhibition of EZH2 and immune signaling exerts synergistic anti-tumor effects in ChronicLymphocytic Leukemia

Multiple lines of evidence highlight the role of external drive in CLL pathogenesis and suggest that microenvironmental stimuli received from the CLL cells through their immune receptors (e.g. BcR, TLRs, CD40, cytokine receptors and complement receptors) play an important role in the survival and proliferation of CLL cells *in vivo.* Here, we explored if EZH2 expression and function could be affected by microenvironmental triggering and whether synergism may exist between EZH2 and signaling inhibitors. The study group included cases responsive to BcR stimulation. *Ex vivo* stimulation of primary CLL cells from these cases through the BcR, CD40 and, especially, TLR9 led to EZH2 upregulation, accompanied by elevated H3K27me3 levels and significant increase in cell viability, suggesting that EZH2 expression likely contributes to the anti-apoptotic phenotype induced by microenvironmental signals. *Ex vivo* exposure to Ibrutinib exerted a significantly higher pro-apoptotic effect in CLL cells from $EZH2^{high}$ versus $EZH2^{low}$ cases, further highlighting links between microenvironmental triggering and EZH2 expression and functionality. Next, we investigated whether signaling inhibition might also modulate EZH2 expression and functionality *in vivo* by longitudinal profiling of CLL patients under Ibrutinib treatment. EZH2 protein levels and H3K27me3 declined at +1 month under treatment. However, at later time points they returned to levels similar to the pre-treatment sample, suggesting that EZH2 expression and functionality may characterize persisting cells, retained after prolonged treatment. *Ex vivo* treatment of primary CLL cells and splenic B cells from *Tcl1* leukemic mice (the most common murine model in CLL) by combined EZH2 and signaling inhibitors (Ibrutinib, Idelasisib) was more effective in promoting apoptosis than single inhibition. Finally, *ex vivo* exposure to EZH2 inhibitorsinduced apoptosis in primary CLL cells from cases with suboptimal response to signaling inhibitors, further highlighting that targeting both processes might represent a novel therapeutic strategy for CLL.

12 References

1. Janeway C, Travers P, Walport M, Shlomchik M. The immune system in health and disease. *Immunobiology*. 2005;
2. Janeway C a, Medzhitov R. Innate immune recognition. *Annu. Rev. Immunol.* 2002;20(2):197–216.
3. Iwasaki A, Medzhitov R. Regulation of adaptive immunity by the innate immune system. *Science (80-.).* 2010;327(5963):291–295.
4. Goldsby RA et al. Immunology. *Book*. 2007;
5. Hsu DC. JANEWAY'S IMMUNOBIOLOGY, 7TH EDITION. *Shock*. 2008;29:770.
6. Abul K. Abbas et al. Basic Immunology.
7. Chiorazzi N, Rai KR, Ferrarini M. Chronic lymphocytic leukemia. *N. Engl. J. Med.* 2005;352(8):804–815.
8. Moreau EJ, Matutes E, A'Hern RP, et al. Improvement of the chronic lymphocytic leukemia scoring system with the monoclonal antibody SN8 (CD79b). *Am. J. Clin. Pathol.* 1997;108(4):378–382.
9. Ginaldi L, De Martinis M, Matutes E, et al. Levels of expression of CD19 and CD20 in chronic B cell leukaemias. *J. Clin. Pathol.* 1998;51:364–369.
10. Sant M, Allemani C, Tereanu C, et al. Incidence of hematological malignancies in Europe by morphological subtype: results of the HAEMACARE project. *Blood*. 2010;116(19):blood-2010-05-282632.
11. National Cancer Institute SSB. Cancer Incidence – Surveillance, Epidemiology, and End Results (SEER) Registries Research Data. *Surveillance, Epidemiol. End Results Progr. (http//www.seer.cancer.gov).* 2007;
12. Kipps TJ, Stevenson FK, Wu CJ, et al. Chronic lymphocytic leukaemia. *Nat. Rev. Dis. Prim.* 2017;3:17008.
13. Slager SL, Benavente Y, Blair A, et al. Medical history, lifestyle, family history, and occupational risk factors for chronic lymphocytic leukemia/small lymphocytic lymphoma: The InterLymph non-Hodgkin lymphoma subtypes project. *J. Natl. Cancer Inst. - Monogr.* 2014;(48):41–51.
14. Cerhan JR, Slager SL. Familial predisposition and genetic risk factors for lymphoma. *Blood*. 2015;126(20):2265–2273.
15. Lichtenstein P, Holm N V., Verkasalo PK, et al. Environmental and Heritable Factors in the Causation of Cancer ? Analyses of Cohorts of Twins from Sweden, Denmark, and Finland. *N. Engl. J. Med.* 2000;343(2):78–85.
16. Marcucci F, Mele A. Hepatitis viruses and non-Hodgkin lymphoma: epidemiology, mechanisms of tumorigenesis, and therapeutic opportunities. *Blood*. 2011;117(6):.
17. Scarfò L, Ferreri AJM, Ghia P. Chronic lymphocytic leukaemia. *Crit. Rev. Oncol.* 2016;104:169–182.
18. Vardi A, Agathangelidis A, Sutton L-A, et al. Immunogenetic Studies of Chronic Lymphocytic Leukemia: Revelations and Speculations about Ontogeny and Clinical Evolution Immunogenetic Analysis in Chronic Lymphocytic Leukemia: Early Evidence of Immunoglobulin Repertoire Restriction.
19. Stamatopoulos K, Belessi C, Hadzidimitriou A, et al. Immunoglobulin light chain repertoire in chronic lymphocytic leukemia.
20. Oscier DG, Thompsett A, Zhu D, Stevenson FK. Differential rates of somatic hypermutation in V(H) genes among subsets of chronic lymphocytic leukemia defined by chromosomal abnormalities. *Blood*. 1997;89(11):4153–60.

21. Damle RN, Batliwalla FM, Ghiotto F, et al. Telomere length and telomerase activity delineate distinctive replicative features of the B-CLL subgroups defined by immunoglobulin V gene mutations. *Blood*. 2004;103(2):375–382.
22. Chiorazzi N, Ferrarini M. Cellular origin(s) of chronic lymphocytic leukemia: Cautionary notes and additional considerations and possibilities. *Blood*. 2011;117(6):1781–1791.
23. Lanham S, Hamblin T, Oscier D, et al. Differential signaling via surface IgM is associated with VH gene mutational status and CD38 expression in chronic lymphocytic leukemia. *Blood*. 2003;101(3):1087–1093.
24. Deaglio S, Vaisitti T, Aydin S, et al. CD38 and ZAP-70 are functionally linked and mark CLL cells with high migratory potential. *Blood*. 2007;110(12):4012–4021.
25. Deaglio S, Vaisitti T, Bergui L, et al. CD38 and CD100 lead a network of surface receptors relaying positive signals for B-CLL growth and survival. *Blood*. 2005;105(8):3042–3050.
26. Kil LP, Yuvaraj S, Langerak AW, Hendriks RW. The role of B cell receptor stimulation in CLL pathogenesis. *Curr. Pharm. Des.* 2012;18(23):3335–3355.
27. Ghia P, Guida G, Stella S, et al. The pattern of CD38 expression defines a distinct subset of chronic lymphocytic leukemia (CLL) patients at risk of disease progression. *Blood*. 2003;101(4):1262–1269.
28. Chen L, Huynh L, Apgar J, et al. ZAP-70 enhances IgM signaling independent of its kinase activity in chronic lymphocytic leukemia. *Blood*. 2008;111(5):2685–2692.
29. Wiestner A. ZAP-70 expression identifies a chronic lymphocytic leukemia subtype with unmutated immunoglobulin genes, inferior clinical outcome, and distinct gene expression profile. *Blood*. 2003;101(>12):4944–4951.
30. Sutton LA, Rosenquist R. The complex interplay between cell-intrinsic and cell-extrinsic factors driving the evolution of chronic lymphocytic leukemia. *Semin. Cancer Biol.* 2015;34:22–35.
31. Gaidano G, Foà R, Dalla-favera R. Review series Molecular pathogenesis of chronic lymphocytic leukemia. *J. Clin. Invest.* 2012;122(10):3432–3438.
32. Hallek M. Chronic lymphocytic leukemia: 2015 Update on diagnosis, risk stratification, and treatment. *Am. J. Hematol.* 2015;90(5):446–60.
33. Rossi D, Gaidano G. Richter syndrome: Molecular insights and clinical perspectives. *Hematol. Oncol.* 2009;27(1):1–10.
34. Fangazio M, De Paoli L, Rossi D, Gaidano G. Predictive markers and driving factors behind Richter syndrome development. *Expert Rev. Anticancer Ther.* 2011;11(3):433–442.
35. Döhner H, Stilgenbauer S, Benner A, et al. Genomic aberrations and survival in chronic lymphocytic leukemia. *N. Engl. J. Med.* 2000;343(26):1910–1916.
36. Stevenson FKF, Krysov S, Davies AJ, Steele AJ, Packham G. B-cell receptor signaling in chronic lymphocytic leukemia. *Blood*. 2011;118(16):4313–4320.
37. Hallek M, Cheson BD, Catovsky D, et al. Guidelines for diagnosis, indications for treatment, response assessment and supportive management of chronic lymphocytic leukemia. *Blood*. 2018;blood-2017-09-806398.
38. Jain N, O'Brien S. Initial treatment of CLL: Integrating biology and functional status. *Blood*. 2015;126(4):463–470.
39. Byrd JC, Brown JR, O'Brien S, et al. Ibrutinib versus Ofatumumab in Previously

Treated Chronic Lymphoid Leukemia. *N. Engl. J. Med.* 2014;371(3):213–223.
40. Burger JA, Tedeschi A, Barr PM, et al. Ibrutinib as Initial Therapy for Patients with Chronic Lymphocytic Leukemia. *N. Engl. J. Med.* 2015;373(25):2425–2437.
41. Byrd JC, Harrington B, O'Brien S, et al. Acalabrutinib (ACP-196) in Relapsed Chronic Lymphocytic Leukemia. *N. Engl. J. Med.* 2016;374(4):323–332.
42. Furman RR, Sharman JP, Coutre SE, et al. Idelalisib and Rituximab in Relapsed Chronic Lymphocytic Leukemia. *N. Engl. J. Med.* 2014;370(11):997–1007.
43. Moore VDG, Brown JR, Certo M, et al. Chronic lymphocytic leukemia requires BCL2 to sequester prodeath BIM, explaining sensitivity to BCL2 antagonist ABT-737. *J. Clin. Invest.* 2007;117(1):112–121.
44. Roberts AW, Davids MS, Pagel JM, et al. Targeting BCL2 with Venetoclax in Relapsed Chronic Lymphocytic Leukemia. *N. Engl. J. Med.* 2016;374(4):311–322.
45. Honigberg LA, Smith AM, Sirisawad M, et al. The Bruton tyrosine kinase inhibitor PCI-32765 blocks B-cell activation and is efficacious in models of autoimmune disease and B-cell malignancy. *Proc. Natl. Acad. Sci.* 2010;107(29):13075–13080.
46. Cai Q, Westin J, Fu K, et al. Accelerated therapeutic progress in diffuse large B cell lymphoma. *Ann. Hematol.* 2014;93(4):541–556.
47. Alinari L, Christian B, Baiocchi R a. Novel targeted therapies for mantle cell lymphoma. *Oncotarget*. 2012;3(2):203–211.
48. Harrison C. Trial watch: BTK inhibitor shows positive results in B cell malignancies. *Nat. Rev. Drug Discov.* 2012;11(2):96–97.
49. Byrd JC, Furman RR, Coutre SE, et al. Targeting BTK with Ibrutinib in Relapsed Chronic Lymphocytic Leukemia. *N. Engl. J. Med.* 2013;369(1):32–42.
50. Herman SEM, Gordon AL, Hertlein E, et al. Bruton tyrosine kinase represents a promising therapeutic target for treatment of chronic lymphocytic leukemia and is effectively targeted by PCI-32765. *Blood*. 2011;117(23):6287–6296.
51. Ponader S, Chen SS, Buggy JJ, et al. The Bruton tyrosine kinase inhibitor PCI-32765 thwarts chronic lymphocytic leukemia cell survival and tissue homing in vitro and in vivo. *Blood*. 2012;119(5):1182–1189.
52. Dubovsky JA, Beckwith KA, Natarajan G, et al. Ibrutinib is an irreversible molecular inhibitor of ITK driving a Th1-selective pressure in T lymphocytes. *Blood*. 2013;122(15):2539–2549.
53. Sahu N, Venegas AM, Jankovic D, et al. Selective expression rather than specific function of Txk and Itk regulate Th1 and Th2 responses. *J Immunol*. 2008;181(9):6125–6131.
54. Okkenhaug K, Vanhaesebroeck B. PI3K in lymphocyte development, differentiation and activation. *Nat. Rev. Immunol.* 2003;3(4):317–330.
55. Hoellenriegel J, Meadows SA, Sivina M, et al. The phosphoinositide 3'-kinase delta inhibitor, CAL-101, inhibits B-cell receptor signaling and chemokine networks in chronic lymphocytic leukemia. *Blood*. 2011;118(13):3603–3612.
56. Ghia P. Ibrutinib: Better combined with other drugs? *Lancet Oncol.* 2014;15(10):1043–1044.
57. Ayed AO, Parikh SA. Management of patients with chronic lymphocytic leukemia at high risk of relapse on ibrutinib therapy. *Leuk. Lymphoma*. 2017;0(0):1–10.
58. Nair KS, Cheson B. The role of idelalisib in the treatment of relapsed and refractory chronic lymphocytic leukemia. *Ther. Adv. Hematol.* 2016;7(2):69–84.

59. Hallek M. Chronic lymphocytic leukemia: 2017 update on diagnosis, risk stratification, and treatment. *Am. J. Hematol.* 2017;92(9):946–965.
60. Sutton LA, Rosenquist R. The complex interplay between cell-intrinsic and cell-extrinsic factors driving the evolution of chronic lymphocytic leukemia. *Semin. Cancer Biol.* 2015;34:22–35.
61. Ghia P, Chiorazzi N, Stamatopoulos K. Microenvironmental influences in chronic lymphocytic leukaemia: The role of antigen stimulation. *J. Intern. Med.* 2008;264(6):549–562.
62. Chatzouli M, Ntoufa S, Papakonstantinou N, et al. Heterogeneous Functional Effects of Concomitant B Cell Receptor and TLR Stimulation in Chronic Lymphocytic Leukemia with Mutated versus Unmutated Ig Genes. *J. Immunol.* 2014;192(10):4518–4524.
63. Scielzo C, Apollonio B, Scarfò L, et al. The functional in vitro response to CD40 ligation reflects a different clinical outcome in patients with chronic lymphocytic leukemia. *Leukemia*. 2011;25(11):1760–1767.
64. Ntoufa S, Vardi A. Distinct Innate Immunity Pathways to Activation and Tolerance in Subgroups of Chronic Lymphocytic Leukemia with Distinct Immunoglobulin Receptors. *Mol. Med.* 2012;18(9):1.
65. Burger JA, Chiorazzi N. B cell receptor signaling in chronic lymphocytic leukemia. *Trends Immunol.* 2013;34(12):592–601.
66. Efremov DG, Gobessi S, Longo PG. Signaling pathways activated by antigen-receptor engagement in chronic lymphocytic leukemia B-cells. *Autoimmun. Rev.* 2007;7(2):102–108.
67. Muzio M, Scielzo C, Bertilaccio MTS, et al. Expression and function of toll like receptors in chronic lymphocytic leukaemia cells. *Br. J. Haematol.* 2009;144(4):507–516.
68. ten Hacken E, Scielzo C, Bertilaccio MTS, et al. Targeting the LYN/HS1 signaling axis in chronic lymphocytic leukemia. *Blood*. 2013;121(12):.
69. Ten Hacken E, Burger J a. Microenvironment interactions and B-cell receptor signaling in Chronic Lymphocytic Leukemia: Implications for disease pathogenesis and treatment. *Biochim. Biophys. Acta*. 2015;1863(3):401–413.
70. Muzio M, Apollonio B, Scielzo C, et al. Constitutive activation of distinct BCR-signaling pathways in a subset of CLL patients: a molecular signature of anergy. *Blood*. 2008;112(1):188–195.
71. Semichon M, Merle-Béral H, Lang V, Bismuth G. Normal Syk protein level but abnormal tyrosine phosphorylation in B-CLL cells. *Leukemia*. 1997;11(11):1921–8.
72. Chen L, Widhopf G, Huynh L, et al. Expression of ZAP-70 is associated with increased B-cell receptor signaling in chronic lymphocytic leukemia. *Blood*. 2002;100(13):4609–4614.
73. Petlickovski A, Laurenti L, Li X, et al. Sustained signaling through the B-cell receptor induces Mcl-1 and promotes survival of chronic lymphocytic leukemia B cells. *Blood*. 2005;105(12):4820–4827.
74. Healy JI, Dolmetsch RE, Timmerman L a, et al. Different nuclear signals are activated by the B cell receptor during positive versus negative signaling. *Immunity*. 1997;6(4):419–428.
75. Wong SC, Chew WK, Tan JEL, et al. Peritoneal CD5+ B-1 cells have signaling

properties similar to tolerant B cells. *J. Biol. Chem.* 2002;277(34):30707–30715.
76. Bishop GA, Hostager BS. The CD40-CD154 interaction in B cell-T cell liaisons. *Cytokine Growth Factor Rev.* 2003;14(3–4):297–309.
77. Lee BO, Moyron-Quiroz J, Rangel-Moreno J, et al. CD40, but not CD154, expression on B cells is necessary for optimal primary B cell responses. *J. Immunol.* 2003;171(11):5707–5717.
78. Schattner EJ, Mascarenhas J, Reyfman I, et al. Chronic lymphocytic leukemia B cells can express CD40 ligand and demonstrate T-cell type costimulatory capacity. *Blood*. 1998;91(8):2689–2697.
79. Banchereau J, Bazan F, Blanchard D, et al. The CD40 Antigen and its Ligand. *Annu. Rev. Immunol.* 1994;12(1):881–926.
80. Von Bergwelt-Baildon MS, Vonderheide RH, Maecker B, et al. Human primary and memory cytotoxic T lymphocyte responses are efficiently induced by means of CD40-activated B cells as antigen-presenting cells: Potential for clinical application. *Blood*. 2002;99(9):3319–3325.
81. Essen D Van, Kikutani H, Gray D. CD40 ligand-transduced co-stimulation of T cells in the development of helper function. *Nature*. 1995;378(6557):620–623.
82. Ranheim E a, Kipps TJ. Activated T cells induce expression of B7/BB1 on normal or leukemic B cells through a CD40-dependent signal. *J. Exp. Med.* 1993;177(4):925–935.
83. Gricks CS, Zahrieh D, Zauls AJ, et al. Differential regulation of gene expression following CD40 activation of leukemic compared to healthy B cells. *Blood*. 2004;104(13):4002–4009.
84. Iannetti A, Ledoux AC, Tudhope SJ, et al. Regulation of p53 and Rb Links the Alternative NF-κB Pathway to EZH2 Expression and Cell Senescence. *PLoS Genet.* 2014;10(9):.
85. Rožková D, Novotná L, Pytlík R, et al. Toll-like receptors on B-CLL cells: Expression and functional consequences of their stimulation. *Int. J. Cancer*. 2010;126(5):1132–1143.
86. Arvaniti E, Ntoufa S, Papakonstantinou N, et al. Toll-like receptor signaling pathway in chronic lymphocytic leukemia: distinct gene expression profiles of potential pathogenic significance in specific subsets of patients. *Haematologica*. 2011;96(11):1644–1652.
87. Ntoufa S, Vardi A, Papakonstantinou N, et al. Distinct innate immunity pathways to activation and tolerance in subgroups of chronic lymphocytic leukemia with distinct immunoglobulin receptors. *Mol. Med.* 2012;18:1281–91.
88. Jahrsdorfer B, Mühlenhoff L, Blackwell SE, et al. B-cell lymphomas differ in their responsiveness to CpG oligodeoxynucleotides. *Clin. Cancer Res.* 2005;11(4):1490–1499.
89. Longo PG, Laurenti L, Gobessi S, et al. The Akt signaling pathway determines the different proliferative capacity of chronic lymphocytic leukemia B-cells from patients with progressive and stable disease. *Leukemia*. 2007;21(1):110–120.
90. Fabbri G, Dalla-Favera R. The molecular pathogenesis of chronic lymphocytic leukaemia. *Nat. Rev. Cancer*. 2016;16(3):145–162.
91. Balatti V, Pekarky Y, Croce CM. Role of microRNA in chronic lymphocytic leukemia onset and progression. *J. Hematol. Oncol.* 2015;8(1):12.

92. Martín-Subero JI, López-Otín C, Campo E. Genetic and epigenetic basis of chronic lymphocytic leukemia. *Curr. Opin. Hematol.* 2013;20(4):362–8.
93. Döhner H, Stilgenbauer S, Benner A, et al. Genomic Aberrations and Survival in Chronic Lymphocytic Leukemia. *N. Engl. J. Med.* 2000;343(26):1910–1916.
94. Strati P, Abruzzo L V., Wierda WG, et al. Second Cancers and Richter Transformation Are the Leading Causes of Death in Patients With Trisomy 12 Chronic Lymphocytic Leukemia. *Clin. Lymphoma Myeloma Leuk.* 2015;15(7):420–427.
95. Del Giudice I, Rossi D, Chiaretti S, et al. NOTCH1 mutations in +12 chronic lymphocytic leukemia (CLL) confer an unfavorable prognosis, induce a distinctive transcriptional profiling and refine the intermediate prognosis of +12 CLL. *Haematologica*. 2012;97(3):437–41.
96. Klein U, Lia M, Crespo M, et al. The DLEU2/miR-15a/16-1 cluster controls B cell proliferation and its deletion leads to chronic lymphocytic leukemia. *Cancer Cell*. 2010;17(1):28–40.
97. Hammarsund M, Corcoran MM, Wilson W, et al. Characterization of a novel B-CLL candidate gene--DLEU7--located in the 13q14 tumor suppressor locus. *FEBS Lett.* 2004;556(1–3):75–80.
98. Shiloh Y, Ziv Y. The ATM protein kinase: regulating the cellular response to genotoxic stress, and more. *Nat. Rev. Mol. Cell Biol.* 2013;14(4):197–210.
99. Skowronska A, Parker A, Ahmed G, et al. Biallelic *ATM* Inactivation Significantly Reduces Survival in Patients Treated on the United Kingdom Leukemia Research Fund Chronic Lymphocytic Leukemia 4 Trial. *J. Clin. Oncol.* 2012;30(36):4524–4532.
100. Stankovic T, Skowronska A. The role of *ATM* mutations and 11q deletions in disease progression in chronic lymphocytic leukemia. *Leuk. Lymphoma*. 2014;55(6):1227–1239.
101. Stilgenbauer S, Schnaiter A, Paschka P, et al. Gene mutations and treatment outcome in chronic lymphocytic leukemia: Results from the CLL8 trial. *Blood*. 2014;123(21):3247–3254.
102. Baliakas P, Hadzidimitriou a, Sutton L, et al. Recurrent mutations refine prognosis in chronic lymphocytic leukemia. *Leukemia*. 2014;(April):1–8.
103. Cortese D, Sutton LA, Cahill N, et al. On the way towards a “CLL prognostic index”: Focus on TP53, BIRC3, SF3B1, NOTCH1 and MYD88 in a population-based cohort. *Leukemia*. 2014;28(3):710–713.
104. Rossi D, Rasi S, Spina V, et al. Integrated mutational and cytogenetic analysis identifies new prognostic subgroups in chronic lymphocytic leukemia. *Blood*. 2013;121(8):1403–1412.
105. Rossi D, Rasi S, Fabbri G, et al. Mutations of NOTCH1 are an independent predictor of survival in chronic lymphocytic leukemia. *Blood*. 2012;119(2):521–529.
106. Pospisilova S, Gonzalez D, Malcikova J, et al. ERIC recommendations on TP53 mutation analysis in chronic lymphocytic leukemia. *Leukemia*. 2012;26(7):1458–1461.
107. Rossi D, Cerri M, Deambrogi C, et al. The Prognostic Value of TP53 Mutations in Chronic Lymphocytic Leukemia Is Independent of Del17p13: Implications for Overall Survival and Chemorefractoriness. *Clin. Cancer Res.* 2009;15(3):995–1004.
108. Zenz T, Krober A, Scherer K, et al. Monoallelic TP53 inactivation is associated with

poor prognosis in chronic lymphocytic leukemia: results from a detailed genetic characterization with long-term follow-up. *Blood*. 2008;112(8):3322–3329.
109. Puente XS, Beà S, Valdés-Mas R, et al. Non-coding recurrent mutations in chronic lymphocytic leukaemia. *Nature*. 2015;526(7574):519–524.
110. Di Ianni M, Baldoni S, Rosati E, et al. A new genetic lesion in B-CLL: a *NOTCH1* PEST domain mutation. *Br. J. Haematol.* 2009;146(6):689–691.
111. Arruga F, Gizdic B, Serra S, et al. Functional impact of NOTCH1 mutations in chronic lymphocytic leukemia. *Leukemia*. 2014;28(5):1060–70.
112. Riches JC, O'Donovan CJ, Kingdon SJ, et al. Trisomy 12 chronic lymphocytic leukemia cells exhibit upregulation of integrin signaling that is modulated by NOTCH1 mutations. *Blood*. 2014;123(26):.
113. Kopan R, Ilagan MXG. The Canonical Notch Signaling Pathway: Unfolding the Activation Mechanism. *Cell*. 2009;137(2):216–233.
114. Puente XS, Pinyol M, Quesada V, et al. Whole-genome sequencing identifies recurrent mutations in chronic lymphocytic leukaemia. *Nature*. 2011;475(7354):101–105.
115. Shin C, Manley JL. Cell signalling and the control of pre-mRNA splicing. *Nat. Rev. Mol. Cell Biol.* 2004;5(9):727–738.
116. Quesada V, Conde L, Villamor N, et al. Exome sequencing identifies recurrent mutations of the splicing factor SF3B1 gene in chronic lymphocytic leukemia. *Nat. Genet.* 2011;44(1):47–52.
117. te Raa GD, Derks IAM, Navrkalova V, et al. The impact of SF3B1 mutations in CLL on the DNA-damage response. *Leukemia*. 2015;29(5):1133–1142.
118. Wang L, Lawrence MS, Wan Y, et al. *SF3B1* and Other Novel Cancer Genes in Chronic Lymphocytic Leukemia. *N. Engl. J. Med.* 2011;365(26):2497–2506.
119. Rossi D, Bruscaggin A, Spina V, et al. Mutations of the SF3B1 splicing factor in chronic lymphocytic leukemia: association with progression and fludarabine-refractoriness. *Blood*. 2011;118(26):6904–8.
120. Jaenisch R, Bird A. Epigenetic regulation of gene expression: How the genome integrates intrinsic and environmental signals. *Nat. Genet.* 2003;33(3S):245–254.
121. Moore LD, Le T, Fan G. DNA methylation and its basic function. *Neuropsychopharmacology*. 2013;38(1):23–38.
122. Portela A, Esteller M. Epigenetic modifications and human disease. *Nat. Biotechnol.* 2010;28(10):1057–1068.
123. Krol J, Loedige I, Filipowicz W. The widespread regulation of microRNA biogenesis, function and decay. *Nat. Rev. Genet.* 2010;11(9):597–610.
124. Huntzinger E, Izaurralde E. Gene silencing by microRNAs: Contributions of translational repression and mRNA decay. *Nat. Rev. Genet.* 2011;12(2):99–110.
125. Calin GA, Ferracin M, Cimmino A, et al. A MicroRNA Signature Associated with Prognosis and Progression in Chronic Lymphocytic Leukemia. *N. Engl. J. Med.* 2005;353(17):1793–1801.
126. Fabbri M, Bottoni A, Shimizu M, et al. Association of a MicroRNA/TP53 Feedback Circuitry With Pathogenesis and Outcome of B-Cell Chronic Lymphocytic Leukemia. *JAMA J. Am. Med. Assoc.* 2011;305(1):59–67.
127. Balatti V, Rizzotto L, Miller C, et al. *TCL1* targeting *miR-3676* is codeleted with tumor protein p53 in chronic lymphocytic leukemia. *Proc. Natl. Acad. Sci.*

2015;112(7):2169–2174.
128. Bichi R, Shinton SA, Martin ES, et al. Human chronic lymphocytic leukemia modeled in mouse by targeted TCL1 expression. *Proc. Natl. Acad. Sci.* 2002;99(10):6955–6960.
129. Cui B, Chen L, Zhang S, et al. Micro RNA-155 influences B-cell receptor signaling and associates with aggressive disease in chronic lymphocytic leukemia. *Blood*. 2014;124(4):546–554.
130. Kulis M, Heath S, Bibikova M, et al. Epigenomic analysis detects widespread gene-body DNA hypomethylation in chronic lymphocytic leukemia. *Nat. Genet.* 2012;44(11):1236–1242.
131. Oakes CC, Claus R, Gu L, et al. Evolution of DNA methylation is linked to genetic aberrations in chronic lymphocytic leukemia. *Cancer Discov.* 2014;4(3):348–361.
132. Landau DA, Clement K, Ziller MJ, et al. Locally Disordered Methylation Forms the Basis of Intratumor Methylome Variation in Chronic Lymphocytic Leukemia. *Cancer Cell*. 2014;26(6):813–825.
133. Cahill N, Bergh A-C, Kanduri M, et al. 450K-array analysis of chronic lymphocytic leukemia cells reveals global DNA methylation to be relatively stable over time and similar in resting and proliferative compartments. *Leukemia*. 2013;27(1):150–158.
134. Oakes CC, Seifert M, Assenov Y, et al. DNA methylation dynamics during B cell maturation underlie a continuum of disease phenotypes in chronic lymphocytic leukemia. *Nat. Genet.* 2016;48(3):253–264.
135. Viré E, Brenner C, Deplus R, et al. The Polycomb group protein EZH2 directly controls DNA methylation. *Nature*. 2006;439(7078):871–874.
136. Yamagishi M, Uchimaru K. Targeting EZH2 in cancer therapy. *Curr. Opin. Oncol.* 2017;29(5):375–381.
137. Cao R, Wang L, Wang H, et al. Role of histone H3 lysine 27 methylation in polycomb-group silencing. *Science (80-.).* 2002;298(5595):1039–1043.
138. Wang H, Wang L, Erdjument-Bromage H, et al. Role of histone H2A ubiquitination in Polycomb silencing. *Nature*. 2004;431(7010):873–878.
139. Varambally S, Dhanasekaran SM, Zhou M, et al. The polycomb group protein EZH2 is involved in progression of prostate cancer. *Nature*. 2002;419(6907):624–629.
140. Yu J, Yu J, Rhodes DR, et al. A polycomb repression signature in metastatic prostate cancer predicts cancer outcome. *Cancer Res.* 2007;67(22):10657–10663.
141. Woods BA, Levine RL. The role of mutations in epigenetic regulators in myeloid malignancies. *Immunol. Rev.* 2015;263(1):22–35.
142. Saramäki OR, Tammela TLJ, Martikainen PM, Vessella RL, Visakorpi T. The gene for polycomb group protein enhancer of zeste homolog 2 (EZH2) is amplified in late-stage prostate cancer. *Genes Chromosom. Cancer*. 2006;45(7):639–645.
143. Fujii S, Tokita K, Wada N, et al. MEK-ERK pathway regulates EZH2 overexpression in association with aggressive breast cancer subtypes. *Oncogene*. 2011;30(39):4118–28.
144. Coe BP, Thu KL, Aviel-Ronen S, et al. Genomic Deregulation of the E2F/Rb Pathway Leads to Activation of the Oncogene EZH2 in Small Cell Lung Cancer. *PLoS One*. 2013;8(8):.
145. Hou P, Liu D, Dong J, Xing M. The BRAFV600E causes widespread alterations in gene methylation in the genome of melanoma cells. *Cell Cycle*. 2012;11(2):286–

295.
146. Esposito F, Tornincasa M, Pallante P, et al. Down-regulation of the miR-25 and miR-30d contributes to the development of anaplastic thyroid carcinoma targeting the polycomb protein EZH2. *J. Clin. Endocrinol. Metab.* 2012;97(5):.
147. Huang SD, Yuan Y, Zhuang CW, et al. MicroRNA-98 and microRNA-214 post-transcriptionally regulate enhancer of zeste homolog 2 and inhibit migration and invasion in human esophageal squamous cell carcinoma. *Mol. Cancer*. 2012;11:.
148. Visser HPJ, Gunster MJ, Kluin-Nelemans HC, et al. The Polycomb group protein EZH2 is upregulated in proliferating, cultured human mantle cell lymphoma. *Br. J. Haematol.* 2001;112(4):950–958.
149. Morin RD, Johnson NA, Severson TM, et al. Somatic mutations altering EZH2 (Tyr641) in follicular and diffuse large B-cell lymphomas of germinal-center origin. *Nat. Genet.* 2010;42(2):181–185.
150. Lund K, Adams PD, Copland M. EZH2 in normal and malignant hematopoiesis. *Leukemia*. 2014;28(1):44–49.
151. Kaur M, Cole MD. MYC acts via the PTEN tumor suppressor to elicit autoregulation and genome-wide gene repression by activation of the Ezh2 methyltransferase. *Cancer Res.* 2013;73(2):695–705.
152. Zhang X, Zhao X, Fiskus W, et al. Coordinated Silencing of MYC-Mediated miR-29 by HDAC3 and EZH2 as a Therapeutic Target of Histone Modification in Aggressive B-Cell Lymphomas. *Cancer Cell*. 2012;22(4):506–523.
153. Chou RH, Yu YL, Hung MC. The roles of EZH2 in cell lineage commitment. *Am. J. Transl. Res.* 2011;3(3):243–250.
154. Su IH, Basavaraj A, Krutchinsky AN, et al. Ezh2 controls B cell development through histone H3 methylation and Igh rearrangement. *Nat. Immunol.* 2003;4(2):124–131.
155. van Galen JC, Dukers DF, Giroth C, et al. Distinct expression patterns of polycomb oncoproteins and their binding partners during the germinal center reaction. *Eur. J. Immunol.* 2004;34(7):1870–1881.
156. Knutson SK, Warholic NM, Wigle TJ, et al. Durable tumor regression in genetically altered malignant rhabdoid tumors by inhibition of methyltransferase EZH2. *Proc. Natl. Acad. Sci.* 2013;110(19):7922–7927.
157. Knutson SK, Kawano S, Minoshima Y, et al. Selective Inhibition of EZH2 by EPZ-6438 Leads to Potent Antitumor Activity in EZH2-Mutant Non-Hodgkin Lymphoma. *Mol. Cancer Ther.* 2014;13(4):842–854.
158. Italiano A, Soria JC, Toulmonde M, et al. Tazemetostat, an EZH2 inhibitor, in relapsed or refractory B-cell non-Hodgkin lymphoma and advanced solid tumours: a first-in-human, open-label, phase 1 study. *Lancet Oncol.* 2018;
159. Béguelin W, Popovic R, Teater M, et al. EZH2 Is Required for Germinal Center Formation and Somatic EZH2 Mutations Promote Lymphoid Transformation. *Cancer Cell*. 2013;23(5):677–692.
160. Schubert HL, Blumenthal RM, Cheng X. Many paths to methyltransfer: A chronicle of convergence. *Trends Biochem. Sci.* 2003;28(6):329–335.
161. McCabe MT, Ott HM, Ganji G, et al. EZH2 inhibition as a therapeutic strategy for lymphoma with EZH2-activating mutations. *Nature*. 2012;492(7427):108–112.
162. Chen YT, Zhu F, Lin WR, et al. The novel EZH2 inhibitor, GSK126, suppresses cell migration and angiogenesis via down-regulating VEGF-A. *Cancer Chemother.*

Pharmacol. 2016;77(4):757–765.
163. Zeng D, Liu M, Pan J. Blocking EZH2 methylation transferase activity by GSK126 decreases stem cell-like myeloma cells. *Oncotarget*. 2017;8(2):3396–3411.
164. Papakonstantinou N, Ntoufa S, Chartomatsidou E, et al. Differential microRNA profiles and their functional implications in different immunogenetic subsets of chronic lymphocytic leukemia. *Mol. Med.* 2013;19(c):115–23.
165. Stamatopoulos K, Belessi C, Moreno C, et al. Over 20% of patients with chronic lymphocytic leukemia carry stereotyped receptors: Pathogenetic implications and clinical correlations. *Blood*. 2007;109(1):259–270.
166. Baliakas P, Hadzidimitriou A, Sutton LA, et al. Clinical effect of stereotyped B-cell receptor immunoglobulins in chronic lymphocytic leukaemia: A retrospective multicentre study. *Lancet Haematol.* 2014;1(2):e74–e84.
167. Rabello D do A, Lucena-Araujo AR, Alves-Silva JCR, et al. Overexpression of EZH2 associates with a poor prognosis in chronic lymphocytic leukemia. *Blood Cells, Mol. Dis.* 2015;54(1):97–102.
168. Kopparapu PK, Bhoi S, Mansouri L, et al. Epigenetic silencing of miR-26A1 in chronic lymphocytic leukemia and mantle cell lymphoma: Impact on EZH2 expression. *Epigenetics*. 2016;11(5):335–343.
169. Virgilio L, Narducci MG, Isobe M, et al. Identification of the TCL1 gene involved in T-cell malignancies. *Proc. Natl. Acad. Sci. U. S. A.* 1994;
170. Herling M, Patel KA, Weit N, et al. High TCL1 levels are a marker of B-cell receptor pathway responsiveness and adverse outcome in chronic lymphocytic leukemia. *Blood*. 2009;
171. Browning RL, Geyer SM, Johnson AJ, et al. Expression of TCL-1 as a potential prognostic factor for treatment outcome in B-cell chronic lymphocytic leukemia. *Leuk. Res.* 2007;
172. Suljagic M, Longo PG, Bennardo S, et al. The Syk inhibitor fostamatinib disodium (R788) inhibits tumor growth in the Eμ-TCL1 transgenic mouse model of CLL by blocking antigen-dependent B-cell receptor signaling. *Blood*. 2010;116(23):4894–4905.
173. Papakonstantinou N, Ntoufa S, Chartomatsidou E, et al. The histone methyltransferase EZH2 as a novel prosurvival factor in clinically aggressive chronic lymphocytic leukemia. *Oncotarget*. 2016;7(24):35946–35959.
174. Margueron R, Reinberg D. The Polycomb complex PRC2 and its mark in life. *Nature*. 2011;469(7330):343–349.
175. Di Croce L, Helin K. Transcriptional regulation by Polycomb group proteins. *Nat. Publ. Gr.* 2013;20(10):1–4.
176. Hu G, Gupta SK, Troska TP, Nair A, Gupta M. Long non-coding RNA profile in mantle cell lymphoma identifies a functional lncRNA ROR1-AS1 associated with EZH2/PRC2 complex. *Oncotarget*. 2017;
177. Liu Y, Yu K, Li M, et al. EZH2 overexpression in primary gastrointestinal diffuse large B-cell lymphoma and its association with the clinicopathological features. *Hum. Pathol.* 2017;64:213–221.
178. Yamaguchi H, Hung MC. Regulation and role of EZH2 in cancer. *Cancer Res. Treat.* 2014;46(3):209–222.
179. Varambally S, Cao Q, Mani RS, et al. Genomic loss of microRNA-101 leads to

overexpression of histone methyltransferase EZH2 in cancer. *Science (80-.).* 2008;322(5908):1695–1699.
180. Neo WH, Lim JF, Grumont R, Gerondakis S, Su IH. C-rel regulates Ezh2 expression in activated lymphocytes and malignant lymphoid cells. *J. Biol. Chem.* 2014;289(46):31693–31707.
181. Yamagishi M, Uchimaru K. Targeting EZH2 in cancer therapy. *Curr. Opin. Oncol.* 2017;29(5):375–381.
182. Morera L, Lübbert M, Jung M. Targeting histone methyltransferases and demethylases in clinical trials for cancer therapy. *Clin. Epigenetics*. 2016;8(1):57.
183. Hallek M. Chronic lymphocytic leukemia: 2017 update on diagnosis, risk stratification, and treatment. *Am. J. Hematol.* 2017;92(9):946–965.
184. Cheng S, Ma J, Guo A, et al. BTK inhibition targets in vivo CLL proliferation through its effects on B-cell receptor signaling activity. *Leukemia*. 2014;28(3):649–657.
185. Burger JA, Keating MJ, Wierda WG, et al. Safety and activity of ibrutinib plus rituximab for patients with high-risk chronic lymphocytic leukaemia: A single-arm, phase 2 study. *Lancet Oncol.* 2014;15(10):1090–1099.
186. Jayappa KD, Portell CA, Gordon VL, et al. Microenvironmental agonists generate de novo phenotypic resistance to combined ibrutinib plus venetoclax in CLL and MCL. *Blood Adv.* 2017;1(14):933–946.
187. Zelenetz AD, Barrientos JC, Brown JR, et al. Idelalisib or placebo in combination with bendamustine and rituximab in patients with relapsed or refractory chronic lymphocytic leukaemia: interim results from a phase 3, randomised, double-blind, placebo-controlled trial. *Lancet Oncol.* 2017;18(3):297–311.
188. Brach D, Johnston-Blackwell D, Drew A, et al. EZH2 inhibition by tazemetostat results in altered dependency on B-cell activation signaling in DLBCL. *Mol. Cancer Ther.* 2017;molcanther.0840.2016.